NISTIR 6277

Draft Guidelines for Evaluating Liquefaction Resistance Using Shear Wave Velocity Measurements and Simplified Procedures

Building and Fire Research Laboratory
Gaithersburg, MD 20899

United States Department of Commerce
Technology Administration
National Institute of Standards and Technology

NISTIR 6277

Draft Guidelines for Evaluating Liquefaction Resistance Using Shear Wave Velocity Measurements and Simplified Procedures

Ronald D. Andrus,[1] Kenneth H. Stokoe, II,[2] and Riley M. Chung[3]

[1]Building and Fire Research Laboratory
National Institute of Standards and Technology
Gaithersburg, MD 20899

[2]Department of Civil Engineering
The University of Texas at Austin
Austin, TX 78712

[3]Consulting Engineering
Potomac, MD 20854
Formerly, National Institute of Standards and Technology
Gaithersburg, MD 20899

March 1999
Building and Fire Research Laboratory
National Institute of Standards and Technology
Gaithersburg, MD 20899

U.S. Department of Commerce
William M. Daley, *Secretary*

Technology Administration
Gary R. Bachula, *Under Secretary for Technology*

National Institute of Standards and Technology
Raymond G. Kammer, *Director*

ABSTRACT

Predicting the liquefaction resistance of soil is an important step in the engineering design of new and the retrofit of existing structures in earthquake-prone regions. The procedure currently used in the U.S. and throughout much of the world to predict liquefaction resistance is termed the simplified procedure. This simplified procedure was originally developed by H. B. Seed and I. M. Idriss in the late 1960s using blow count from the Standard Penetration Test. Small-strain, shear wave velocity measurements provide a promising alternative and/or supplement to the penetration-based approach. This report presents draft guidelines for evaluating liquefaction resistance using shear wave velocity measurements. These draft guidelines were written in cooperation with industry, researchers and practitioners, and evolved from workshops in 1996 and 1998. The guidelines outline the development of a recommended procedure, which follows the general format of the penetration-based simplified procedure. The proposed procedure has been validated through case history data from more than 20 earthquakes and 70 measurement sites in soils ranging from clean fine sand to sandy gravel with cobbles to profiles including silty clay layers. Liquefaction resistance curves were established by applying a modified relationship between shear wave velocity and cyclic stress ratio for constant average cyclic shear strain suggested by R. Dobry. These curves correctly predict moderate to high liquefaction potential for over 95 % of the liquefaction case histories, and are shown to be consistent with the penetration-based curves. To further validate the procedure, additional case histories are needed with all soil types that have and have not liquefied, particularly from deeper deposits (depth > 8 m) and from denser soils (shear wave velocity > 200 m/s) shaken by stronger ground motions (peak ground acceleration > 0.4 g). The guidelines serve as a resource document for a final recommended practice, and for practitioners and researchers involved in evaluating soil liquefaction resistance.

KEYWORDS: building technology; earthquakes; *in situ* measurements; seismic testing; shear wave velocity; soil liquefaction

ACKNOWLEDGMENTS

The authors gratefully acknowledge the contributions of the participants at two workshops. The first workshop was held on January 4-5, 1996, and was sponsored by the National Center for Earthquake Engineering Research (NCEER). The second workshop was held on August 14-15, 1998, and was sponsored by the Multidisciplinary Center for Earthquake Engineering Research (MCEER, formally NCEER) and the National Science Foundation (NSF). Workshop participants include:

T. Leslie Youd (Chair)	Brigham Young University
Izzat M. Idriss (Co-chair)	University of California at Davis
Ronald D. Andrus	National Institute of Standards and Technology
Ignacio Arango	Bechtel Corporation
John Barniech	Woodward-Clyde Consultants
Gonzalo Castro	GEI Consultants, Inc.
John T. Christian	Consulting Engineer
Ricardo Dobry	Rensselaer Polytechnic Institute
W. D. Liam Finn	University of British Columbia
Leslie F. Harder, Jr.	California Department of Water Resources
Mary Ellen Hynes	U.S. Army Corps of Engineers, WES
Kenji Ishihara	Science University of Tokyo
Joseph P. Koester	U.S. Army Corps of Engineers, WES
Sam S.C. Liao	Parsons Brinkerhoff
Faiz Makdisi	Geomatrix Consultants
William F. Marcuson, III	U.S. Army Corps of Engineers, WES
Geoffrey R. Martin	University of Southern California
James K. Mitchell	Virginia Tech
Yoshiharu Moriwaki	Woodward-Clyde Consultants
Maurice S. Power	Geomatrix Consultants
Peter K. Robertson	University of Alberta
Raymond B. Seed	University of California at Berkeley
Kenneth H. Stokoe, II	The University of Texas at Austin

Their comments and suggestions are much appreciated and have enhanced the quality of this report.

The authors thank the many people who provided project reports and other information presented in this report. Special thanks to Susumu Iai and Kohji Ichii of the Port and Harbour Research Institute, Osamu Matsuo of the Public Works Research Institute, Susumu Yasuda of the Tokyo Denki University, Mamoru Kanatani and Yukihisa Tanaka of the Central Research Institute for Electric Power Industry, Kohji Tokimatsu of the Tokyo Institute of Technology, Kenji Ishihara of the Science University of Tokyo, Fumio Tatsuoka of the University of Tokyo, and Takeji Kokusho of the Chuo University for the information graciously shared with the first author on Japanese liquefaction case histories and dynamic soil properties. Roman Hryciw of the University of Michigan provided information on the location of seismic cone penetration test sites and liquefaction effects on Treasure Island. Ross Boulanger of the University of California at Davis provided information on liquefaction case histories at Moss Landing. Michael Bennett of the United States Geological Survey shared first-hand knowledge of the field performance for some of the California case histories. David Sykora of Bing Yen & Associates, Inc., graciously shared his database of shear wave velocity measurements and SPT blow counts.

Richard Woods of the University of Michigan served as the outside reader for this report. Review comments were also received from Ricardo Dobry of the Rensselaer Polytechnic Institute, Mary Ellen Hynes of the U.S. Army Corps of Engineers, Izatt M. Idriss of the University of California at Davis, T. Leslie Youd of the Brigham Young University, and Robert Pyke, consulting engineer. Their comments and suggestions are sincerely appreciated.

Finally, the authors express their thanks to the staff at the National Institute of Standards and Technology. Harry Brooks, Rose Estes, Bonnie Gray and other library staff assisted with the collection of several references cited in this report. Fahim Sadek and Nicholas Carino of the Structures Division also reviewed this report, and provided many helpful suggestions.

TABLE OF CONTENTS

LIST OF TABLES

LIST OF FIGURES

Figure Page

Figure | Page

Figure

Page

Figure | Page

CHAPTER 1

INTRODUCTION

1.1 BACKGROUND

A major cause of damage from earthquakes is liquefaction-induced ground failure. For example, direct property loss caused by liquefaction during the 1989 Loma Prieta, California earthquake (moment magnitude, M_w = 7.0) was over $100 million (Holzer, 1998). Large indirect property loss by fire almost occurred in 1989 when liquefaction-induced ground deformation ruptured water mains that served the Marina District of San Francisco. Fortunately, the fire in the Marina District at Divisadero and Beach Streets was contained to the three-story apartment building where it ignited. It was also fortunate that the 1989 earthquake did not occur closer to the San Francisco Bay area. The cities of Kobe and Osaka, Japan were not so fortunate. The 1995 Hyogoken-Nanbu earthquake (M_w = 6.9) directly struck this metropolitan area, causing over $100 billion in property damage (Kimura, 1996). A significant portion of the damage in Kobe can be attributed to liquefaction-induced ground deformation. Predicting soil liquefaction resistance is an important step in the engineering design of new and the retrofit of existing structures in seismic-prone regions.

The procedure for predicting the liquefaction resistance of soils currently used in the United States and throughout much of the world is termed the *simplified procedure*. This simplified procedure was originally developed by Seed and Idriss (1971) using blow count from the Standard Penetration Test (SPT) correlated with a parameter representing the seismic loading on the soil, called *cyclic stress ratio*. Since 1971, the procedure has been revised and updated (Seed, 1979; Seed and Idriss, 1982; Seed et al., 1983; Seed et al., 1985). Correlations based on the Cone Penetration Test (CPT), the Becker Penetration Test (BPT), and shear wave velocity measurements have also been developed by various investigators. General reviews of the simplified procedure are contained in a report by the National Research Council (1985) and a workshop report edited by Youd and Idriss (1997).

Small-strain shear wave velocity, V_S, measurements provide a promising alternative and/or supplement to the penetration-based approach. The use of V_S as an index of liquefaction resistance is solidly based since both V_S and liquefaction resistance are influenced by many of the same factors (e.g., void ratio, state of stress, stress history, and geologic age).

The *in situ* V_S can be measured by several seismic tests including crosshole, downhole, seismic cone penetrometer (SCPT), suspension logger, and Spectral-Analysis-of-Surface-Waves (SASW). A review of these test methods is given in Woods (1994). ASTM D-4428M-91 provides a standard test method for crosshole seismic testing. Standard test methods do not exist for the other seismic tests.

Some advantages of using V_S are (Dobry et al., 1981; Seed et al., 1983; Stokoe et al., 1988a; Tokimatsu and Uchida, 1990): (1) Measurements are possible in soils that are hard to sample, such as gravelly soils where penetration tests may be unreliable. (2) Measurements can be performed on small laboratory specimens, allowing direct comparisons between laboratory and field behavior. (3) V_S is a basic mechanical property of soil materials, directly related to small-strain shear modulus, G_{max}, by:

$$G_{max} = \rho V_S^2 \tag{1.1}$$

where

ρ = the mass density of soil.

(4) G_{max}, or V_S, is in turn a required property in analytical procedures for estimating dynamic shearing strain in soil in earthquake site response and soil-structure interaction analyses. (5) V_S can be measured by the SASW test method at sites where borings may not be permitted, such as capped landfills, and at sites that extend for great distances where rapid evaluation is required, such as lifelines and large building complexes.

Three concerns when using V_S to evaluate liquefaction resistance are: (1) Measurements are made at small strains, whereas pore-water pressure buildup and liquefaction are medium- to high-strain phenomenon (Jamiolkowski and Lo Presti, 1990; Teachavorasinskun et al., 1994; Roy et al., 1996). This concern can be significant for cemented soils, since small-strain measurements are highly sensitive to weak interparticle bonding which is eliminated at medium and high strains. It can also be significant in silty soils above the water table where negative pore water pressures can increase V_S. (2) No samples are obtained for classification of soils and identification of non-liquefiable soft clayey soils. According to the so-called Chinese criteria, non-liquefiable clayey soils have clay contents (particles smaller than 5 μm) greater than 15 %, liquid limits greater than 35 %, or moisture contents less than 90 % of the liquid limit (Seed and Idriss, 1982). (3) Thin, low V_S strata may not be detected if the measurement interval is too large (USBR, 1989; Boulanger et al., 1997).

In general, borings should always be a part of the field investigation. Surface geophysical measurements and cone soundings are often conducted first to help select the best locations for borehole sampling and testing. Surface geophysical tests usually involve making measurements at several different locations, and provide general, or average, stratigraphy for sediments beneath the area tested. The ability of surface geophysical methods to resolve a layer at depth depends on the thickness, depth, and continuity of that layer, as well as the test and interpretation procedures employed. Cone soundings provide detailed stratigraphy at each test location for sediments that can be penetrated. The preferred practice when using V_S measurements to evaluate liquefaction resistance is to drill sufficient boreholes and conduct sufficient tests to detect and delineate thin liquefiable strata, to identify non-liquefiable clay-rich soils, to identify silty soils above the ground water table that might have lower values of V_S should the water table rise, and to detect liquefiable weakly cemented soils.

1.2 PURPOSE

This report presents draft guidelines for evaluating liquefaction resistance through shear wave velocity measurements. The draft guidelines incorporate suggestions from two workshops. The first workshop was held on January 4-5, 1996 in Salt Lake City, Utah, and was sponsored by the National Center for Earthquake Engineering Research (NCEER). The second workshop was held on August 14-15, 1998 also in Salt Lake City, and was sponsored by the Multidisiplinary Center for Earthquake Engineering Research (MCEER, formally NCEER) and the National Science Foundation (NSF). The guidelines outline the development of a recommended procedure based on the suggestions given at these two workshops, herein called the 1996 NCEER workshop and the 1998 MCEER workshop. The guidelines provide guidance on selecting site variables and correction factors that are consistent with the shear-wave-based procedure.

1.3 REPORT OVERVIEW

Following this introduction, Chapter 2 outlines the development of several proposed relationships between liquefaction resistance and V_S. Chapter 3 presents case history data and describes their general characteristics. Chapter 4 establishes the recommended liquefaction resistance evaluation curves from the case history data. Chapter 5 shows how the recommended evaluation curve is applied, as demonstrated by two case studies. And Chapter 6 summarizes the recommended procedure, as well as identifies issues that remain to be resolved.

To assist the reader, Appendix A provides a list of Symbols and Notation, and Appendix B provides a Glossary of Terms. Appendix C presents a summary of case history data used to develop the recommended curves.

CHAPTER 2

LIQUEFACTION RESISTANCE AND SHEAR WAVE VELOCITY

During the past two decades, several procedures for predicting liquefaction resistance based on V_S have been proposed. These procedures were developed from laboratory studies (Dobry et al., 1981; Dobry et al., 1982; de Alba et al., 1984; Hynes, 1988; Tokimatsu and Uchida, 1990; Tokimatsu et al., 1991a; Rashidian, 1995), analytical studies (Bierschwale and Stokoe, 1984; Stokoe et al., 1988c; Andrus, 1994), penetration-V_S correlations (Seed et al., 1983; Lodge, 1994; Kayabali, 1996; Rollins et al., 1998b), or field performance data and *in situ* V_S measurements (Robertson et al., 1992; Kayen et al., 1992; Andrus and Stokoe, 1997). Several of these procedures follow the general format of the simplified procedure, where V_S is corrected to a reference overburden stress and correlated with the cyclic stress, or resistance, ratio.

2.1 CYCLIC STRESS RATIO

The cyclic stress ratio, *CSR*, at a particular depth in a level soil deposit can be expressed as (Seed and Idriss, 1971):

$$CSR = \frac{\tau_{av}}{\sigma'_v} = 0.65\left(\frac{a_{max}}{g}\right)\left(\frac{\sigma_v}{\sigma'_v}\right)r_d \qquad (2.1)$$

where

τ_{av} = the average equivalent uniform shear stress generated by the earthquake assumed to be 0.65 of the maximum induced stress,
a_{max} = the peak horizontal ground surface acceleration,
σ'_v = the initial effective vertical (overburden) stress at the depth in question,
σ_v = the total overburden stress at the same depth,
g = the acceleration of gravity, and
r_d = a shear stress reduction coefficient to adjust for flexibility of the soil profile.

Equation 2.1 is based on Newton's second law where force is equal to mass times acceleration. The coefficient r_d is added because the soil column behaves as a deformable body rather than a rigid body.

2.1.1 Peak Horizontal Ground Surface Acceleration

Peak horizontal ground surface acceleration is a characteristic of the ground shaking intensity, and is defined as the peak value in a horizontal ground acceleration record that would occur at the site without the influence of excess pore-water pressures or liquefaction that might develop (Youd et al., 1997). Peak accelerations are commonly estimated using empirical attenuation relationships of a_{max}, as a function of earthquake magnitude, distance from the energy source, and local site conditions.

Regional or national seismic hazard maps (Frankel et al., 1996; Frankel et al., 1997; http://geohazards.cr.usgs.gov/eq/) are also often used to estimate peak accelerations. If peak acceleration is estimated from a map, the magnitude and distance information should be obtained from the deaggregated matrices used to develop the map. The value of a_{max} selected will depend on the target level of risk and compatibility of site conditions. For site conditions not compatible with available probabilistic maps or attenuation relationships, the value of a_{max} may be corrected based on dynamic site response analyses or site class coefficients given in the latest building codes.

2.1.2 Total and Effective Overburden Stresses

Required in the calculation of σ_v and σ'_v are densities of the various soil layers, as well as characteristics of the ground water. For non-critical projects involving hard-to-sample soils below the ground water table, densities are often estimated from typical values for soils with similar grain size and penetration or velocity characteristics. Fortunately, *CSR* is not very sensitive to density, and reasonable estimates of density yield reasonable results.

The values of σ'_v and *CSR* are sensitive to the ground water table depth. Other ground water characteristics that may be significant to liquefaction evaluations include seasonal and long-term water level variations, depth of and pressure in artesian zones, and whether the water table is perched or normal.

2.1.3 Stress Reduction Coefficient

2.1.3.1 Relationship by Seed and Idriss (1971)—Values of r_d are commonly estimated from the chart by Seed and Idriss (1971) shown in Fig. 2.1. This chart was determined analytically using a variety of earthquake motions and soil conditions. Average r_d

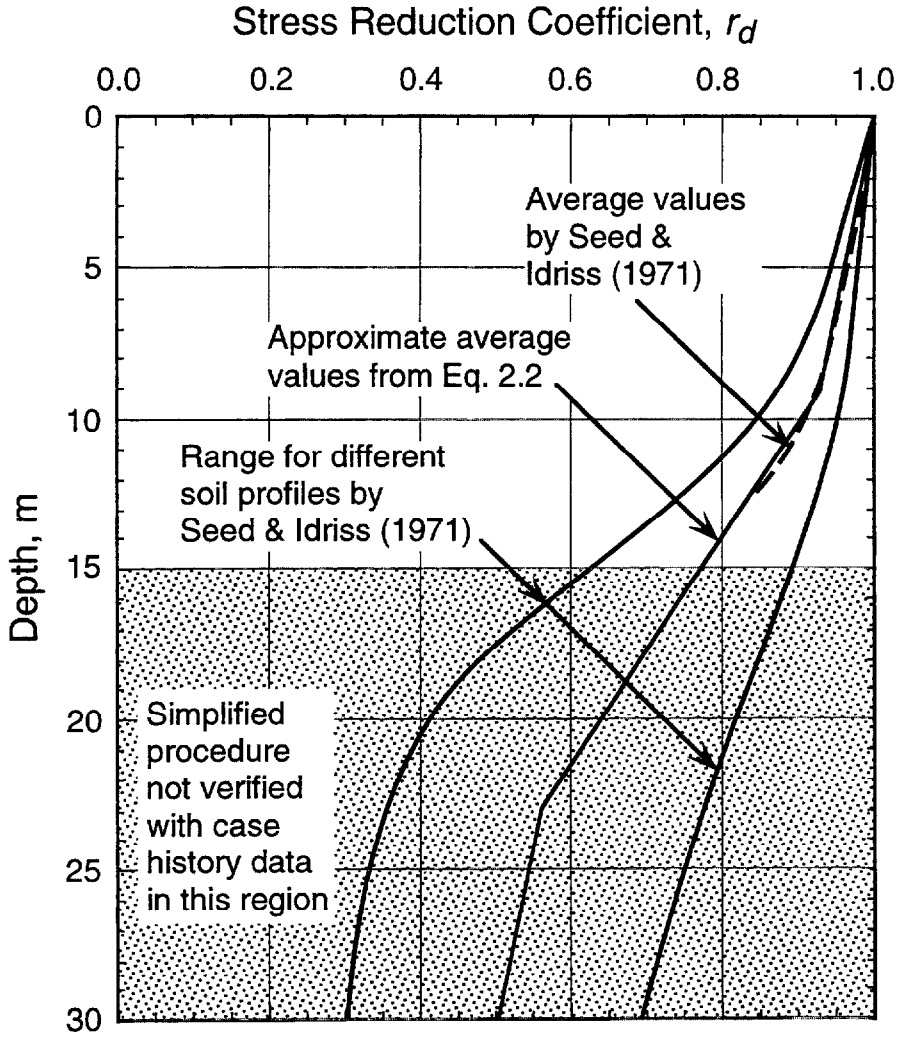

Fig. 2.1 - Relationship Between Stress Reduction Coefficient and Depth Developed by Seed and Idriss (1971) with Approximate Average Value Lines from Eq. 2.2. (after Youd et al., 1997)

values given in the chart can be estimated using the following functions (Liao and Whitman, 1986; Robertson and Wride, 1997):

$$r_d = 1.0 - 0.00765\, z \qquad \text{for } z \le 9.15 \text{ m} \qquad (2.2a)$$

$$r_d = 1.174 - 0.0267\, z \qquad \text{for } 9.15 \text{ m} < z \le 23 \text{ m} \qquad (2.2b)$$

$$r_d = 0.744 - 0.008\, z \qquad \text{for } 23 \text{ m} < z \le 30 \text{ m} \qquad (2.2c)$$

where

z = the depth below the ground surface in meters.

Figure 2.1 shows the average r_d values approximated by Eq. 2.2.

2.1.3.2 Revised Relationship Proposed by Idriss (1998; 1999)—Figure 2.2 presents revised average values of r_d proposed by Idriss (1998; 1999) for various earthquake magnitudes. The plotted curves are averages of many individual curves derived analytically by Golesorkhi (1989) under the supervision of the late Prof. H. B. Seed. They are defined by the following relationship (after Idriss, 1998; modified for depth in meters):

$$ln(r_d) = \alpha(z) + \beta(z)\, M_w \qquad (2.3)$$

where

$$\alpha(z) = -1.012 - 1.126\, sin\left(\frac{z}{11.7} + 5.133\right), \qquad (2.4)$$

$$\beta(z) = 0.106 + 0.118\, sin\left(\frac{z}{11.3} + 5.142\right), \qquad (2.5)$$

As shown in Fig. 2.2, the curve defined by Eq. 2.3 for M_w = 7.5 is almost identical to the average of the range published by Seed and Idriss (1971).

The scatter in the individual curves used to determined the average curves shown in Fig. 2.2, as well as Fig. 2.1, is rather large. For example, coefficients determined for a 30 m thick, loose sand deposit and magnitude 5.5 earthquakes exhibit standard deviations of about 0.1 at a depth of 5 m and 0.15 at a depth of 10 m. These standard deviation values would be larger if soil deposits of various thicknesses and densities are considered. Figure 2.2 provides an estimate of the effects of earthquake magnitude on r_d.

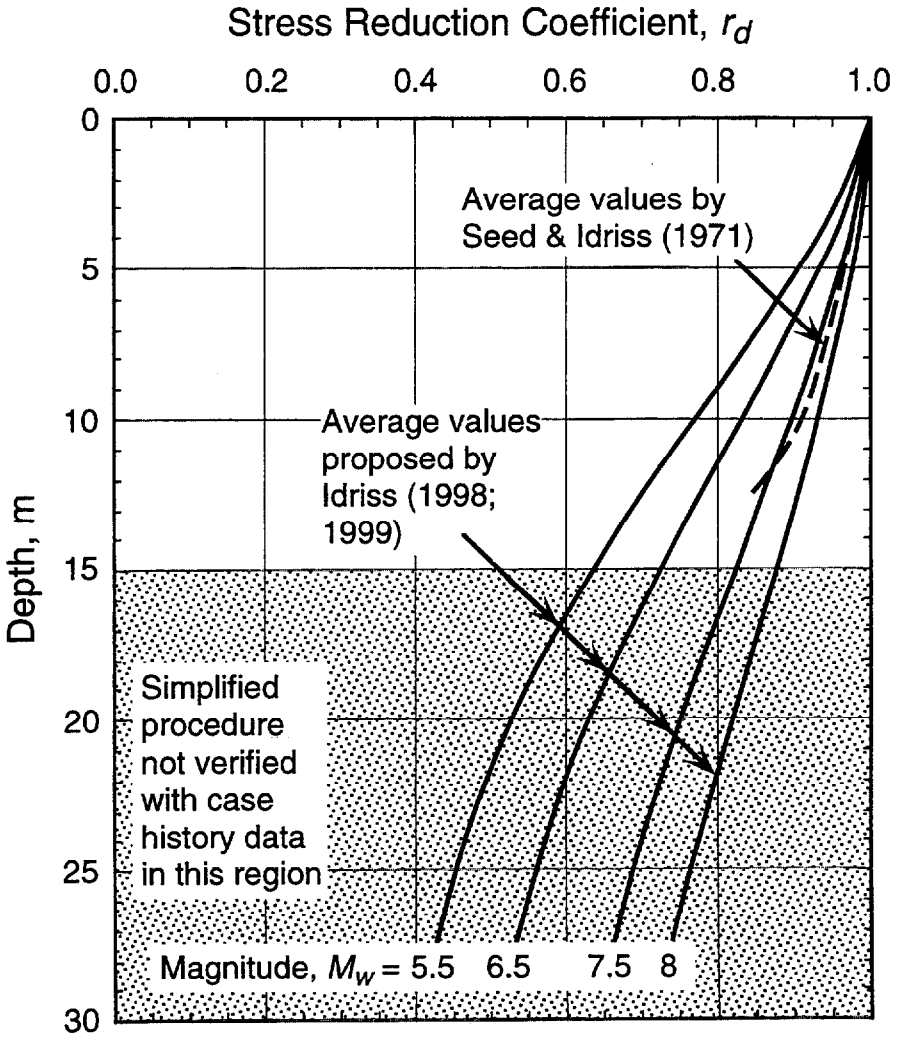

Fig. 2.2 - Relationship Between Average Stress Reduction Coefficient and Depth Proposed by Idriss (1998; 1999) with Average of Range Determined by Seed and Idriss (1971).

2.2 STRESS-CORRECTED SHEAR WAVE VELOCITY

As mentioned in Chapter 1, the *in situ* V_S can be measured by a number of methods. The accuracy of these methods can be sensitive to procedural details, soil conditions, and interpretation techniques.

One important factor influencing V_S is state of stress in soil (Hardin and Drnevich, 1972; Seed et al., 1986). Laboratory tests (Roesler, 1979; Yu and Richart, 1984; Stokoe et al., 1985; S. H. Lee, 1986; N. J. Lee, 1993) have shown that the velocity of a propagating shear wave depends equally on principal stresses in the direction of wave propagation, and the direction of particle motion. Thus, V_S measurements made with wave propagation or particle motion in the vertical direction can be generally related by the following empirical relationship (Stokoe et al., 1985):

$$V_S = A\ (\sigma'_v)^m (\sigma'_h)^m \tag{2.6}$$

where

A = a parameter that depends on the soil structure,
σ'_h = the initial effective horizontal stress at the depth in question, and
m = a stress exponent with a value of about 0.125.

Following the traditional procedures for correcting standard and cone penetration resistances (Marcuson and Bieganousky, 1977; Seed, 1979; Liao and Whitman, 1986; Olsen, 1997; Robertson and Wride, 1997; Youd et al., 1997; Robertson and Wride, 1998), one can correct V_S to a reference overburden stress by (Sykora, 1987b; Robertson et al., 1992):

$$V_{S1} = V_S\left(\frac{P_a}{\sigma'_v}\right)^{0.25} \tag{2.7}$$

where

P_a = a reference stress, 100 kPa or approximately atmospheric pressure, and
σ'_v = the initial effective vertical stress in kPa.

Equation 2.7 assumes that $\sigma'_h = K_o \sigma'_v$ and K_o is a constant (≈ 0.5 at sites where liquefaction has occurred), from the relationship given in Eq. 2.6. Also, Eq. 2.7 implicitly assumes that V_S is measured with both the directions of particle motion and wave propagation polarized along principal stress directions and one of these directions is vertical.

Since the direction of wave propagation and the direction of particle motion is different with respect to the stress in the soil for each *in situ* seismic test method, some variations between measured V_S is expected. These variations are minimized by performing the tests with at least a major component of wave propagation or particle motion in the vertical direction. To have a major component of wave propagation or particle motion in the vertical direction, crosshole tests are conducted with particle motion in the vertical direction, and downhole and seismic cone tests are conducted at depths greater than the distance between the source and the borehole or cone sounding such that wave propagation is in the vertical direction.

2.3 CYCLIC SHEAR STRAIN

Liquefaction results from the rearranging of soil particles and the tendency for decrease in volume. Experimental and theoretical studies show that decrease in volume is more closely related to cyclic strain than cyclic stress (Silver and Seed, 1971); a threshold cyclic strain exists below which neither rearrangement of soil particles nor decrease in volume take place (Drnevich and Richart, 1970; Youd, 1972; Pyke et al., 1975), and no pore water pressure buildup occurs (Dobry et al., 1981; Seed et al., 1983); and that there is a predictable correlation between cyclic shear strain and pore pressure buildup of saturated soils (Martin et al., 1975; Park and Silver, 1975; Finn and Bhatia, 1981; Dobry et al., 1982; Hynes, 1988). The threshold cyclic strain is limited to a narrow range of variation, ranging from about 0.005 % for gravels to 0.01 % for normally consolidated clean sands and silty sands to 0.03 % for overconsolidated clean sands. In addition, cyclic strain-controlled test results are less affected than stress-controlled tests by factors such as density, confining stress, anisotropic confining stress, fabric and prestaining (Martin et al., 1975; Dobry and Ladd, 1980; Dobry et al., 1982; Hynes, 1988). It should also be noted that the steady state approach to liquefaction evaluation by Poulos et al. (1985) is based on a triggering strain level. These findings confirm the fact that cyclic strain is more fundamentally related to pore pressure buildup than cyclic stress, and are strong arguments in favor of a cyclic strain approach to liquefaction evaluation.

Cyclic shear strain and cyclic shear stress can be related by the following equation:

$$\gamma_{av} = \frac{\tau_{av}}{(G)_{\gamma_{av}}} \tag{2.8}$$

where

γ_{av} = the average peak cyclic shear strain during a cyclic stress-controlled test of uniform cyclic shear stress τ_{av} which results in triggering of liquefaction, and

$(G)_{\gamma_{av}}$ = the secant shear modulus at γ_{av} during the same cyclic test.

In the cyclic strain approach proposed by Dobry et al. (1982), the average cyclic shear strain caused by an earthquake is estimated from:

$$\gamma_{av} = 0.65 \frac{a_{max}}{g} \frac{\sigma_v r_d G_{max}}{\rho V_S^2 (G)_{\gamma_{av}}} \tag{2.9}$$

Equation 2.9 is obtained by combining Eqs. 1.1, 2.1 and 2.8. The variation of shear modulus with strain is commonly expressed in terms of $(G)_{\gamma_{av}}/G_{max}$, called the *modulus reduction factor.* The modulus reduction factor can be estimated from an experimentally determined correlation. Neither pore pressure buildup nor liquefaction will occur when γ_{av} is less than the threshold strain. When γ_{av} is greater than the threshold strain, then pore pressure buildup can occur. The amount of pore pressure buildup can also be estimated from an experimentally determined correlation.

R. Dobry (personal communication to R. D. Andrus, 1996) also derived a relationship between V_{S1} and CSR for constant average cyclic shear strain using Eqs. 1.1 and 2.8. Combining Eqs. 1.1 and 2.8, and dividing both sides by σ'_v leads to:

$$\frac{\tau_{av}}{\sigma'_v} = \gamma_{av} \left(\frac{\rho}{\sigma'_v} \right) \frac{(G)_{\gamma_{av}}}{G_{max}} V_S^2 \tag{2.10}$$

For an overburden stress of 100 kPa, $V_S = V_{S1}$ and curves of constant average cyclic strain can be expressed by:

$$CSR = \frac{\tau_{av}}{\sigma'_v} = f(\gamma_{av})\ V_{S1}^2 \tag{2.11}$$

where

$$f(\gamma_{av}) = \gamma_{av} \left(\frac{\rho}{P_a} \right) \frac{(G)_{\gamma_{av}}}{G_{max}} \tag{2.12}$$

Equation 2.11 provides an analytical basis for extending liquefaction resistance curves to zero at $V_{S1} = 0$, and provides a means for establishing curves at low values of V_{S1} (say $V_{S1} \leq 125$ m/s).

2.4 MAGNITUDE SCALING FACTOR

In developing the simplified procedure, Seed and Idriss (1982) collected SPT blow count measurements from several sites where surface effects of liquefaction were or were not observed during earthquakes with magnitudes of about 7.5. They plotted cyclic stress ratios and corrected blow counts for the clean sand (silt and clay content $\leq$ 5 %) sites, and drew a curve to bound the liquefaction data points. For earthquakes with magnitude other than 7.5, Seed and Idriss proposed magnitude scaling factors to adjust the curve bounding the liquefaction data points for magnitude 7.5 earthquakes.

Table 2.1 presents the magnitude scaling factors developed by Seed and Idriss (1982), as well as the magnitude scaling factors developed by other investigators in recent years. These magnitude scaling factors were derived from laboratory test results and representative cycles of loading (Seed and Idriss, 1982; Idriss, personal communication to T. L. Youd, 1995; Idriss, 1998; Idriss, 1999), correlations of field performance data and blow count measurements (Ambrasey, 1988; Youd and Noble, 1997), estimates of seismic energy for laboratory and field data (Arango, 1996), and correlations of field performance data and *in situ* V_S measurements (Andrus and Stokoe, 1997). Figure 2.3 shows a plot of the various magnitude scaling factors along with the range recommended by the 1996 NCEER workshop (Youd et al., 1997).

Table 2.1 - Magnitude Scaling Factors Obtained by Various Investigators. (modified from Youd and Noble, 1997)

Moment Magnitude, M_w	Magnitude Scaling Factor (*MSF*)										
	Seed & Idriss (1982)	Idriss (personal communication to T. L. Youd, 1995)	Idriss (1998)	Idriss (1999)	Ambraseys (1988)	Youd & Noble (1997) P_L, %			Arango (1996)		Andrus & Stokoe (1997)
						< 20	< 30	< 50			
(1)	(2)	(3)	(4)	(5)	(6)	(7)	(8)	(9)	(10)	(11)	(12)
5.5	1.43	2.20	1.625	1.68	2.86	2.86	3.42	4.44	3.00	2.20	2.8*
6.0	1.32	1.76	1.48	1.48	2.20	1.93	2.35	2.92	2.00	1.65	2.1
6.5	1.19	1.44	1.28	1.30	1.69	1.34	1.66	1.99	1.60	1.40	1.6
7.0	1.08	1.19	1.12	1.14	1.30	1.00	1.20	1.39	1.25	1.10	1.25
7.5	**1.00**	**1.00**	**0.99**	**1.00**	**1.00**			**1.00**	**1.00**	**1.00**	**1.0**
8.0	0.94	0.84	0.88	0.87	0.67			0.73	0.75	0.85	0.8*
8.5	0.89	0.72	0.79	0.76	0.44			0.56			0.65*

*Extrapolated from scaling factors for M_w = 6, 6.5, 7, and 7.5 using $MSF = (M_w/7.5)^{-3.3}$.

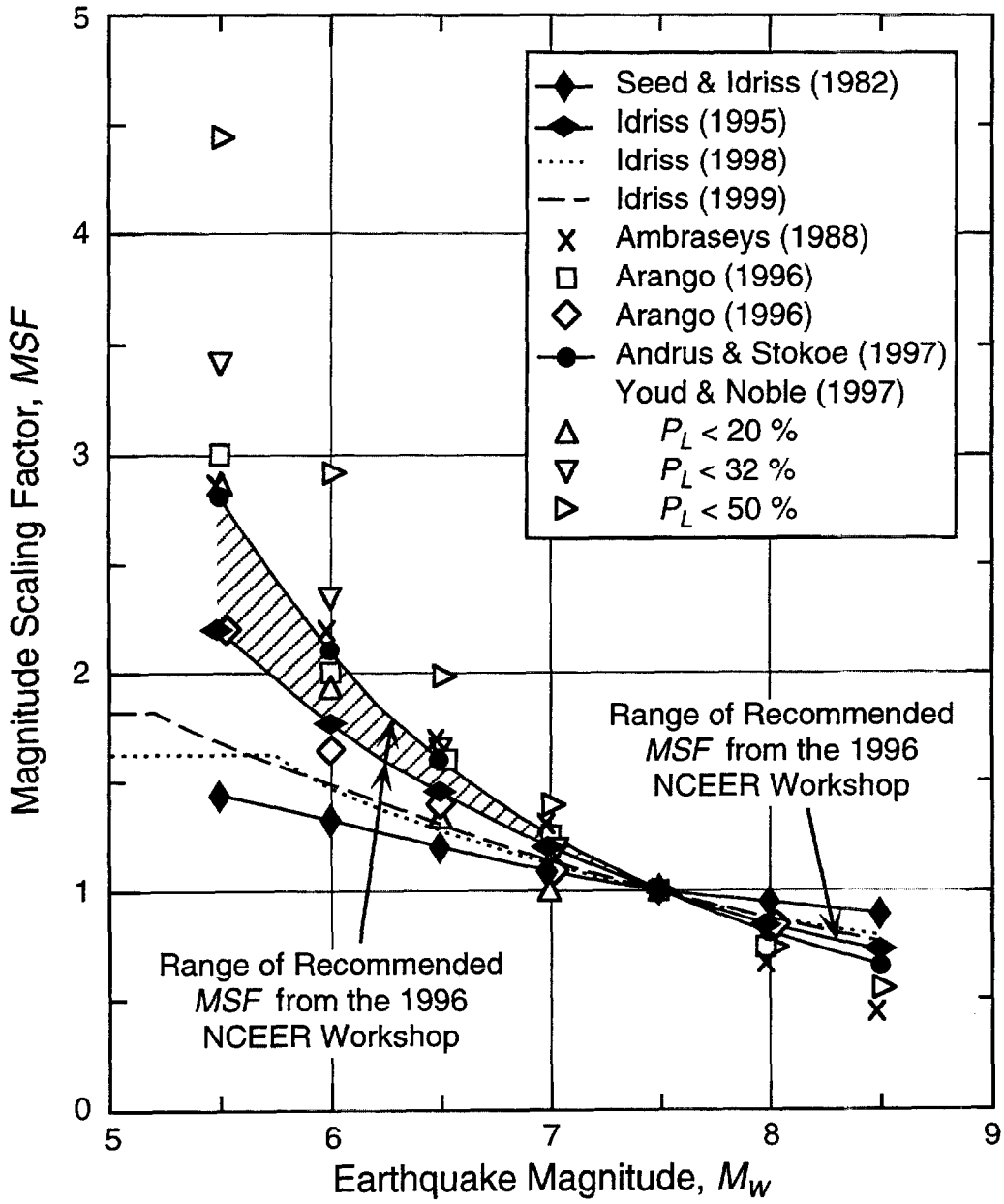

Fig. 2.3 - Magnitude Scaling Factors Derived by Various Investigators with Range Recommended by the 1996 NCEER Workshop (after Youd et al., 1997; Youd and Noble, 1997).

Although the 1996 NCEER workshop (Youd et al., 1997) recommended a range of magnitude scaling factors for engineering practice, a consensus has not yet been reached by the workshop participants. At the August 1998 MCEER workshop, some concerns were expressed about the upper limit of the recommended range. Also, a revised set of magnitude scaling factors and stress reduction coefficients (see Section 2.1.3.2) were proposed by I. M. Idriss. The magnitude scaling factors recommended by the 1996 NCEER workshop and the revised factors proposed by Idriss (1998; 1999) are discussed below.

2.4.1 Factors Recommended by 1996 NCEER Workshop

The magnitude scaling factors recommended by the 1996 NCEER workshop (Youd et al., 1997) can be represented by:

$$MSF = \left(\frac{M_w}{7.5}\right)^n \tag{2.13}$$

where

MSF = the magnitude scaling factor,
M_w = moment magnitude, and
n = an exponent.

The lower bound for the range of magnitude scaling factors recommended by the 1996 NCEER workshop is defined with n = -2.56 (Idriss, personal communication to T. L. Youd, 1995) for earthquakes with magnitude $\leq$ 7.5. The upper bound of the recommended range is defined with n = -3.3 (Andrus and Stokoe, 1997) for earthquakes with magnitude $\leq$ 7.5. For earthquakes with magnitude > 7.5, the recommended factors are defined with n = -2.56. Magnitude scaling factors defined by Eq. 2.13 should be used with r_d values given in Fig. 2.1.

2.4.2 Revised Factors Proposed by Idriss (1998; 1999)

The magnitude scaling factors proposed by Idriss (1998; 1999) are derived using laboratory data from Yoshimi et al. (1984) and a revised relationship between representative cycles of loading and earthquake magnitude. The 1998 factors are defined by the following equation:

$$MSF = 37.9\ (M_w)^{-1.81} \quad \text{for } M_w > 5.75 \tag{2.14a}$$

$$MSF = 1.625 \quad \text{for } M_w \leq 5.75 \tag{2.14b}$$

The 1999 factors are defined by the following equation:

$$MSF = 6.9 \exp\left(\frac{-M_w}{4}\right) - 0.06 \qquad \text{for } M_w > 5.2 \qquad (2.15a)$$

$$MSF = 1.82 \qquad \text{for } M_w \leq 5.2 \qquad (2.15b)$$

Figure 2.3 shows the magnitude scaling factors defined by Eqs. 2.14 and 2.15. The difference between the 1998 and 1999 magnitude scaling factors proposed by Idriss is small. Magnitude scaling factors defined by Eqs. 2.14 and 2.15 should be used with r_d values given in Fig. 2.2.

2.4.3 Comparison of Magnitude Scaling Factors

The proposed relationships for *MSF* can be compared directly by combining them with the appropriate stress reduction coefficient into one factor. This factor is the product of r_d and the reciprocal of *MSF*. Figure 2.4 presents values of r_d/MSF for the range recommended by the 1996 NCEER workshop (Youd et al., 1997) and those proposed by Idriss (1999). As shown in the figure, there is not much difference between the two sets of r_d/MSF values for magnitude of 7.5 and depth less than 11 m. At magnitudes near 5.5 and shallow depths, the difference between r_d/MSF values proposed by Idriss (1999) and values recommended by the 1996 NCEER workshop is as much as 50 %.

The magnitude scaling factors recommended by the 1996 NCEER workshop (Youd et al., 1997) and the revised magnitude scaling factors proposed by Idriss (1999) will be considered in Chapter 4 to establish the recommended liquefaction resistance relationship for magnitude 7.5 earthquakes.

2.5 CYCLIC RESISTANCE RATIO

The value of *CSR* separating liquefaction and non-liquefaction occurrences for a given V_{S1} is called the *cyclic resistance ratio, CRR*. Seven proposed relationships between V_{S1} and *CRR* are compared in Fig. 2.5 and briefly discussed below.

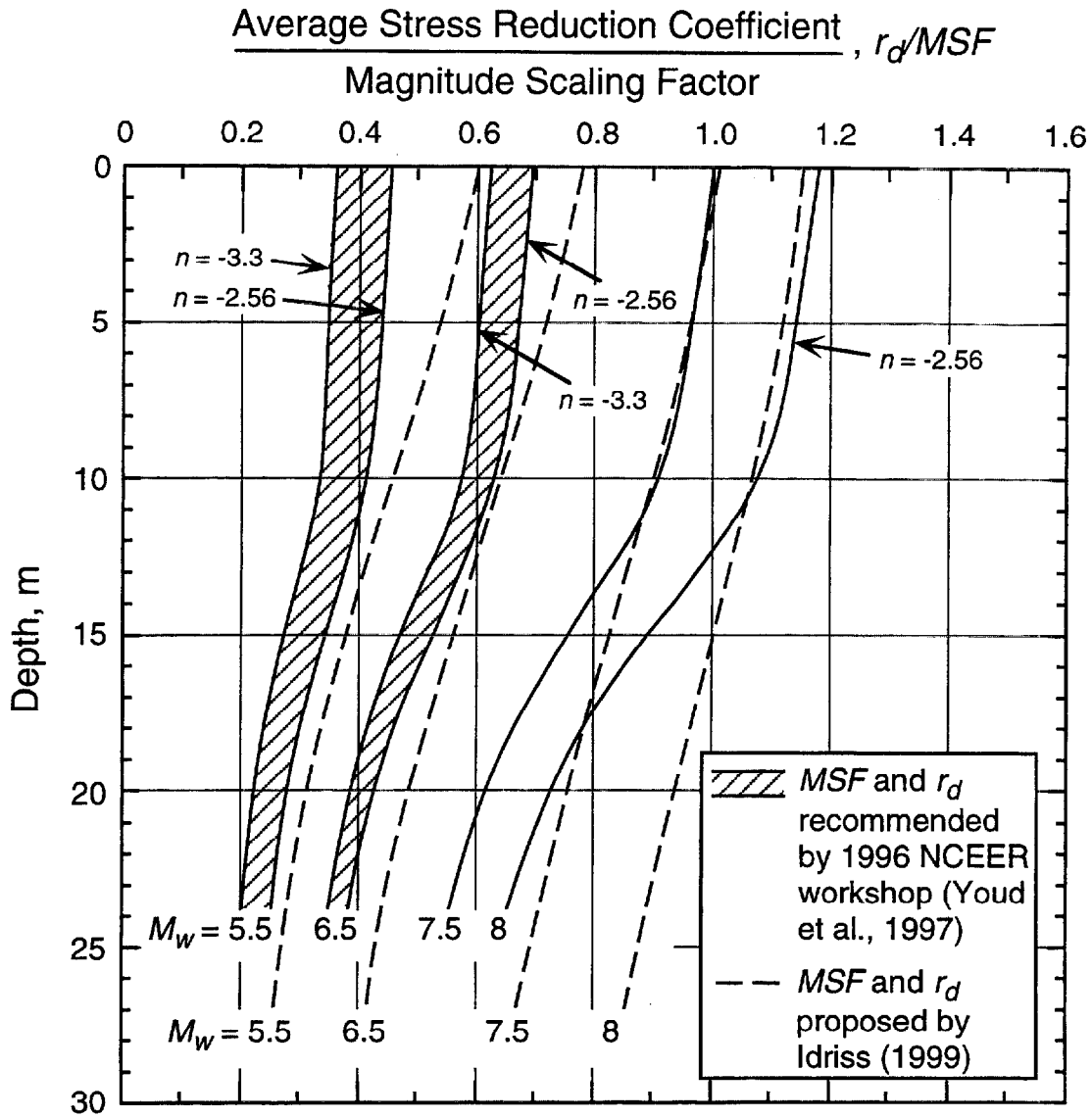

Fig. 2.4 - Variation of r_d/MSF with Depth for Various Magnitudes and Proposed Relationships.

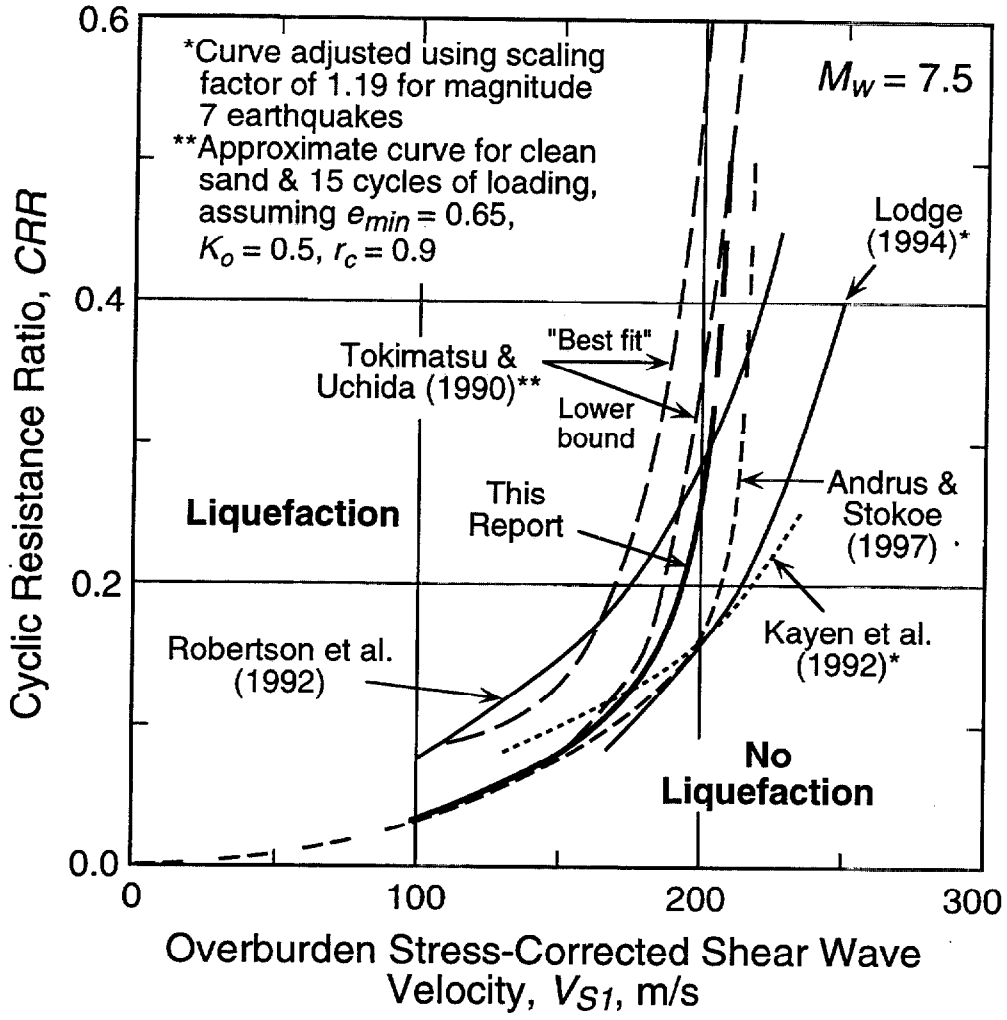

Fig. 2.5 - Comparison of Seven Relationships Between Liquefaction Resistance and Overburden Stress-Corrected Shear Wave Velocity for Clean Granular Soils.

2.5.1 Relationship by Tokimatsu and Uchida (1990)

The "best-fit" curve by Tokimatsu and Uchida (1990) shown in Fig. 2.5 was determined from laboratory cyclic triaxial test results for various sands with less than 10 % fines (silt and clay) and 15 cycles of loading. Figure 2.6 presents the cyclic triaxial test results. The solid symbols in Fig. 2.6 correspond to specimens obtained by the *in situ* freezing technique. The open symbols correspond to specimens reconstituted in the laboratory. Tokimatsu and Uchida defined the cyclic resistance ratio for cyclic triaxial tests, CRR_{tx}, as the ratio of cyclic deviator stress to initial effective confining stress, $\sigma_d/2\sigma'_o$, when the double-amplitude (or peak-to-peak) axial strain, DA, reaches 5 %. They measured the elastic shear modulus of the specimen at a shear strain of 10^{-3} % just prior to the liquefaction test. This small-strain shear modulus was normalized to correct for the influence of confining pressure and void ratio by:

$$G_N = \frac{G_{max}}{f(e_{min})(\sigma'_m)^{2/3}} \tag{2.16}$$

and

$$f(e_{min}) = \frac{(2.17-e_{min})^2}{1+e_{min}} \tag{2.17}$$

where

G_N = the normalized shear modulus,
e_{min} = the minimum void ratio determined by standard test method, and
σ'_m = the mean effective confining stress.

Tokimatsu and Uchida selected an exponent of 2/3 rather than 1/2, as determined by Hardin and Drnevich (1972), because it seemed that a slightly better correlation could be obtained. Values of e_{min} ranged from 0.61 to 0.91 for the sands tested. The actual values of void ratio in each test were greater than e_{min}, with values ranging from about 0.65 to about 1.4.

By combining Eqs. 1.1 and 2.16, one obtains the following relationship for converting G_N to mean stress-corrected V_S:

$$V_{S1m} = V_S\left(\frac{1}{\sigma'_m}\right)^{0.33} = \left(\frac{G_N f(e_{min})}{\rho}\right)^{0.5} \tag{2.18}$$

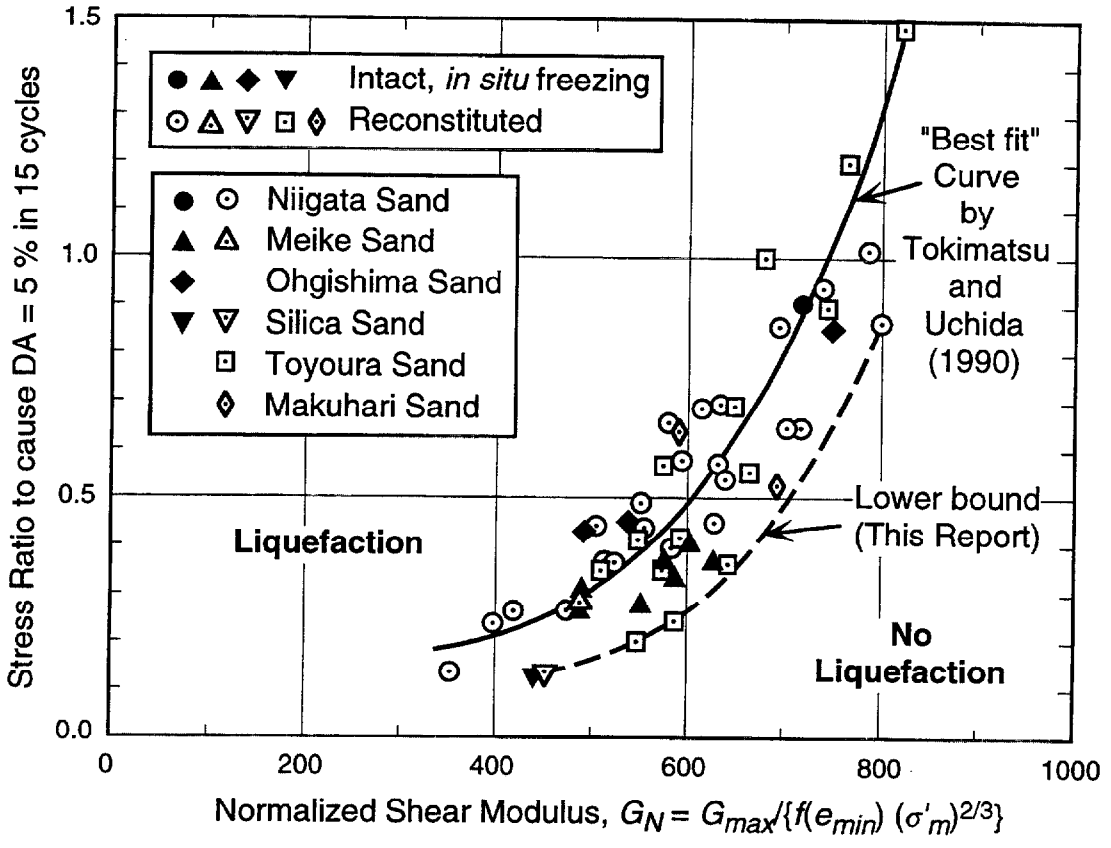

Fig. 2.6 - Relationship Between Liquefaction Resistance and Normalized Shear Modulus for Various Sands with Less than 10 % Fines Determined by Cyclic Triaxial Testing. (modified from Tokimatsu and Uchida, 1990)

where

V_{S1m} = mean stress-corrected V_S, and
σ'_m = the mean effective confining stress in kgf/cm^2 (1 kgf/cm^2 = 98 kPa).

Tokimatsu and Uchida (1990) suggested using 0.65 as an average value of e_{min} for clean sands.

The overburden stress-corrected V_S and V_{S1m} can be related by:

$$V_{S1m} = V_S\left(\frac{1}{\sigma'_v}\right)^{0.33}\left(\frac{3}{1+2K_o}\right)^{0.33} \approx V_{S1}\left(\frac{1}{\sigma'_v}\right)^{0.08}\left(\frac{3}{1+2K_o}\right)^{0.33} \qquad (2.19)$$

where

K_o = the coefficient of lateral earth pressure at rest ($=\sigma'_h/\sigma'_v$).

Values of V_{S1} for the "best fit" curve by Tokimatsu and Uchida (1990) shown in Fig. 2.5 are determined (This report; after Tokimatsu et al., 1991a) from Fig. 2.6 using Eqs. 2.18 and 2.19, and assuming $K_o = 0.5$, $e_{min} = 0.65$, $\sigma'_m = 100$ kPa, and soil density of 1.9 Mg/m^3.

For converting CRR_{tx} to an equivalent field *CRR*, Tokimatsu and Uchida (1990) suggested the following expression originally proposed by Seed (1979):

$$CRR = \frac{(1+2K_o)}{3} r_c\,(CRR_{tx}) \qquad (2.20)$$

where

r_c = a constant to account for the effects of multi-directional shaking with a value between 0.9 and 1.0.

Values of *CRR* for the "best fit" curve by Tokimatsu and Uchida shown in Fig. 2.5 are determined from Fig. 2.6 using Eq. 2.20 and assuming $K_o = 0.5$ and $r_c = 0.9$.

Since the other liquefaction resistance relationships shown in Fig. 2.5 were drawn to bound liquefaction case histories, the more conservative "lower bound" curve for the laboratory test results by Tokimatsu and Uchida (1990) is also shown. This curve was drawn (This report) from Fig. 2.6 following the procedure outlined above.

2.5.2 Relationship by Robertson et al. (1992)

The bounding curve by Robertson et al. (1992) was developed using field performance data from primarily sites in the Imperial Valley, California, along with data from four other sites, as shown in Fig. 2.7. The soil at these sites contained as much as 35 % fines. Robertson et al. corrected V_S using Eq. 2.7. The shape of their relationship was based on the analytical results of Bierschwale and Stokoe (1984). They reasoned that the curve should pass close to the Imperial Valley (Wildlife site) data point, since liquefaction did and did not occur at this site during the 1987 Superstition Hills (M_w = 6.5) and Elmore Ranch (M_w = 6.2) earthquakes, respectively. Robertson et al. used the magnitude scaling factors suggested by Seed (1979), similar to factors listed in Column 2 of Table 2.1, to position their curve for magnitude 7.5 earthquakes.

2.5.3 Relationship by Kayen et al. (1992)

Kayen et al. (1992) studied four sites that did and did not liquefy during the 1989 Loma Prieta, California, earthquake (M_w = 7.0). The four sites are: Port of Richmond, Bay Bridge Toll Plaza, Port of Oakland, and Alameda Bay Farm Island South Loop Road. The fines content for soils at these sites ranged from less than 5 % to as much as 57 %. Values of V_S were measured by the SCPT method and corrected for overburden stress using Eq. 2.7. Figure 2.8 presents their data and bounding curve. The curve was adjusted for magnitude 7.5 earthquakes assuming a *MSF* of 1.19 (see Column 3 of Table 2.1), as shown in Fig. 2.5.

2.5.4 Relationship by Lodge (1994)

Lodge (1994) considered the same sites that Kayen et al. (1992) studied, as well as other sites shaken by the 1989 Loma Prieta earthquake. The curve by Lodge was developed as follows. First, cyclic stress ratios for the entire soil profile at each site were calculated. Second, available SPT blow counts were corrected for overburden pressure and energy. Soil layers with high and low liquefaction potential were identified with the procedure of Seed et al. (1985). Soil layers with corrected blow count within 3 of the SPT-based curve were eliminated due to uncertainties in the correlation. Third, V_S measurements from SCPT and crosshole tests were corrected for overburden stress using Eq. 2.7. Fourth, on a "meter by meter" basis, values of V_{S1} and cyclic stress ratio were plotted for both layer types, those which were predicted liquefiable and those which were predicted non-liquefiable. Fifth, published data for sites shaken by the 1983 Borah Peak, Idaho, and 1964 Niigata, Japan, earthquakes were added to the plot. Finally, a curve was drawn to include all liquefiable layers, as shown in Fig. 2.9. Figure 2.5 shows the curve by Lodge adjusted for magnitude 7.5 earthquakes assuming a *MSF* of 1.19 (see Column 3 of Table 2.1).

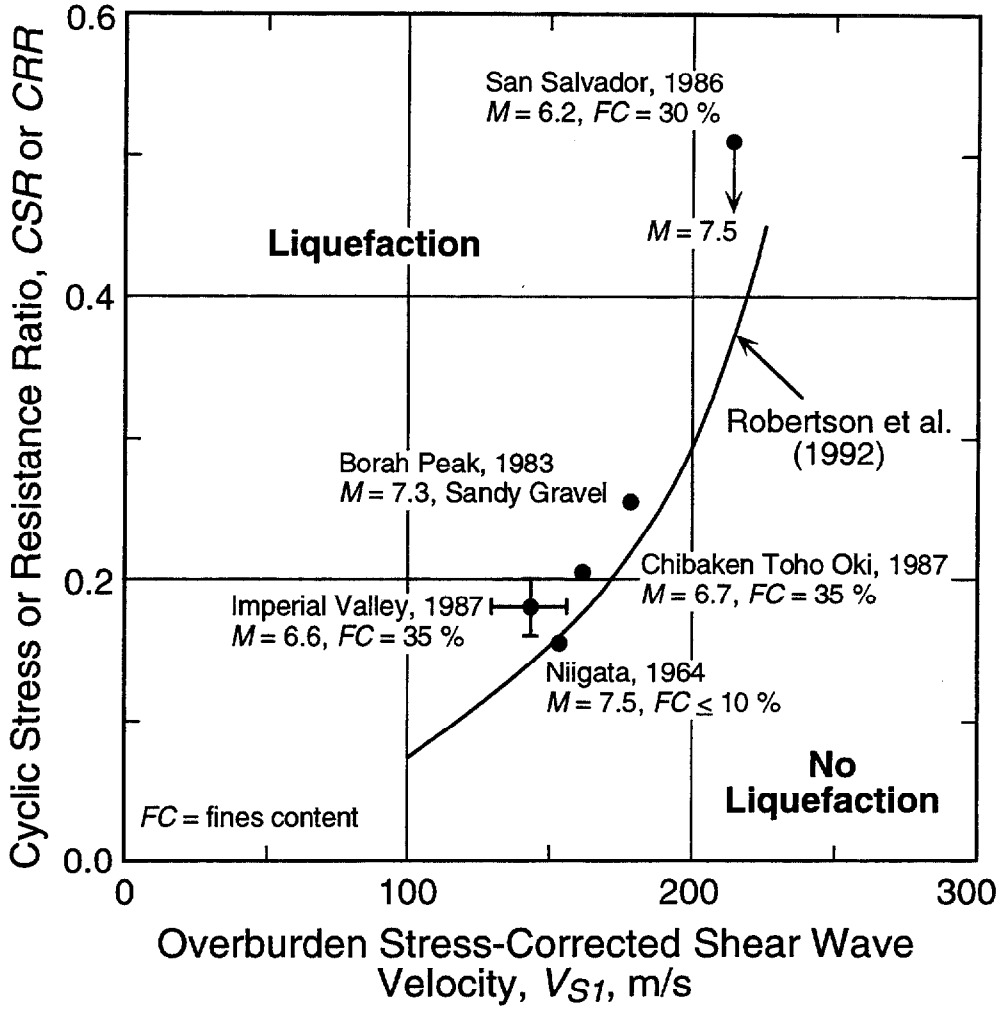

Fig. 2.7 - Liquefaction Resistance Relationship for Magnitude 7.5 Earthquakes and Case History Data from Robertson et al. (1992).

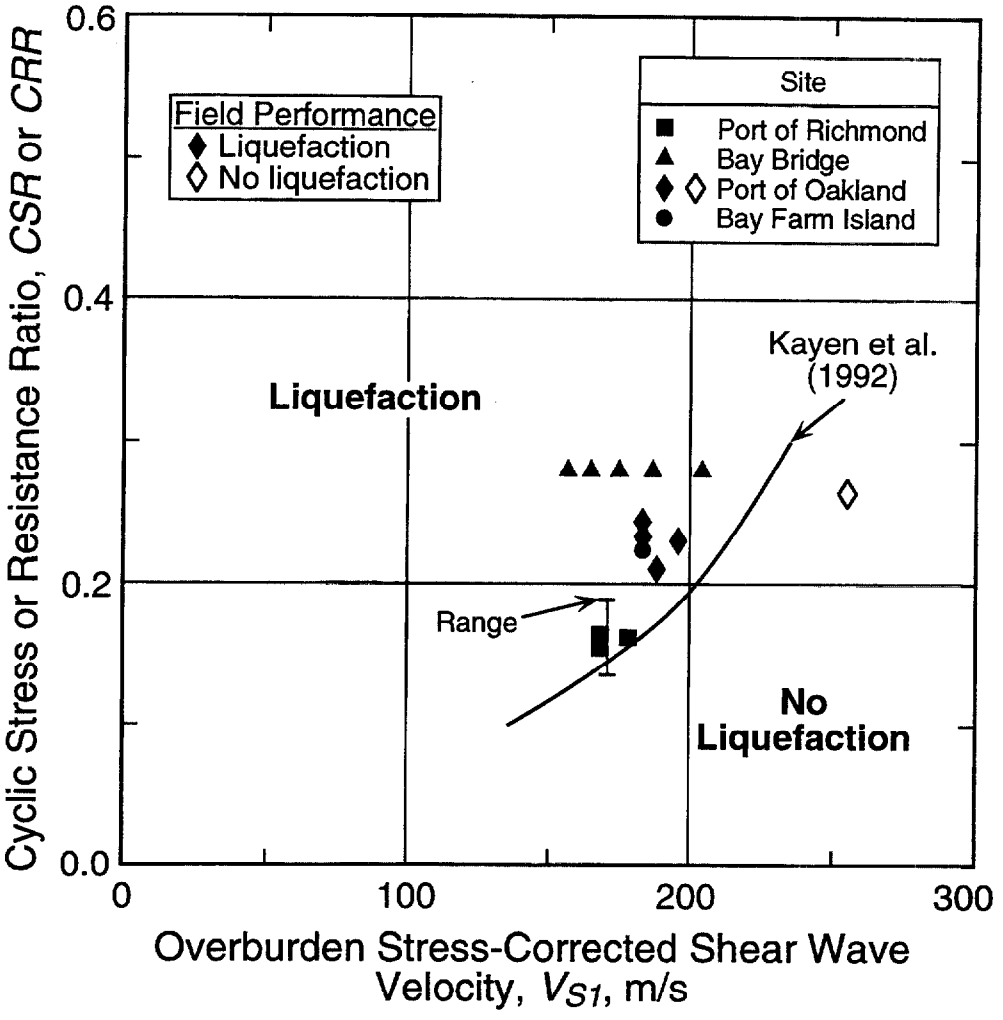

Fig. 2.8 - Liquefaction Resistance Relationship for Magnitude 7 Earthquake and Case History Data from Kayen et al. (1992).

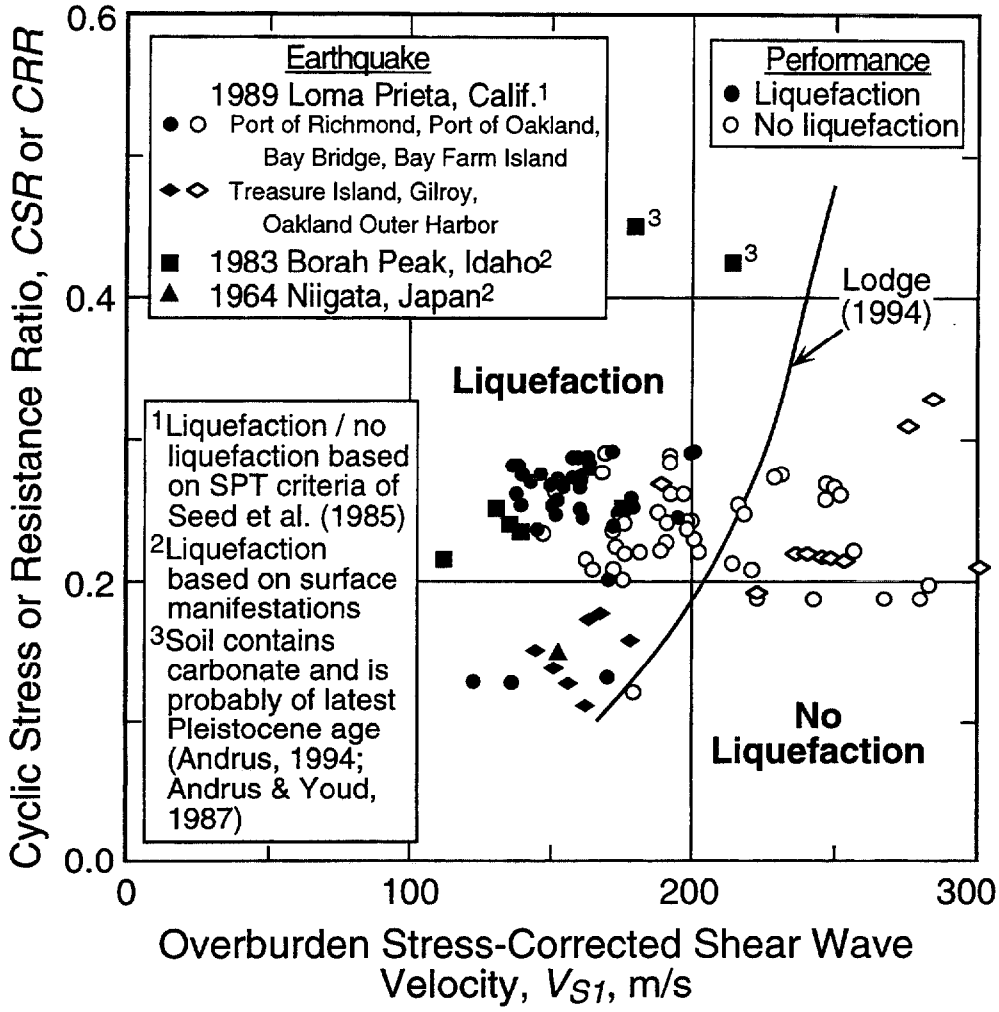

Fig. 2.9 - Liquefaction Resistance Relationship for Magnitude 7 Earthquakes and Case History Data from Lodge (1994).

2.5.5 Relationship by Andrus and Stokoe (1997)

The curve by Andrus and Stokoe (1997) shown in Fig. 2.5 was developed for the proceedings of the 1996 NCEER workshop. Several suggestions were offered at, and after, the workshop concerning how site variables should be define, as well as the shape of the boundary curve separating liquefaction and no liquefaction. Following the suggestions and using field performance data from 20 earthquakes and *in situ* V_S measurements from over 50 sites in soils ranging from clean fine sand to sandy gravel with cobbles to profiles including silty clay layers, Andrus and Stokoe constructed curves for uncemented, Holocene-age soils with various fines content, FC. The values of V_S were corrected using Eq. 2.7. The curve for $FC \leq 5$ % by Andrus and Stokoe along with the case history data are presented in Fig. 2.10

The shape of the curve by Andrus and Stokoe (1997) is based on a modified relationship between V_{S1} and CSR for constant average cyclic shear strain suggested by R. Dobry (see Section 2.3). Andrus and Stokoe reasoned that the curve separating liquefiable and non-liquefiable soils would become asymptotic to some limiting upper value of V_{S1}. This assumption is equivalent to the assumption commonly made in the SPT- and CPT-based procedures where liquefaction is considered not possible above a corrected blow count of about 30 (Seed et al., 1985; Youd et al., 1997) and a corrected tip resistance of about 160 (Youd et al., 1997; Robertson and Wride, 1998). Upper limits for blow count and V_{S1} are explained by the tendency of dense soils to exhibit dilative behavior at large strains, causing negative pore water pressures. While it is possible in a dense soil to generate pore water pressures close to the confining stress if large cyclic strains or many cycles are applied to the soil, the amount of water expelled during reconsolidation is dramatically less for dense soils than for loose soils. As explained by Dobry (1989), in dense soils, settlement is insignificant and no sand boils or engineering failure take place because of the small amount of water expelled. This is important because the definition of liquefaction used to classify the case histories here, as well as in the penetration-based simplified procedures, is based on surface manifestations.

Thus, Andrus and Stokoe (1997) modified Eq. 2.11 to:

$$CRR = \left\{ a\left(\frac{V_{S1}}{100}\right)^2 + b\left(\frac{1}{V_{S1}^* - V_{S1}} - \frac{1}{V_{S1}^*}\right)\right\} MSF \qquad (2.21)$$

where

V_{S1}^* = the limiting upper value of V_{S1} for liquefaction occurrence, and
a, b = curve fitting parameters.

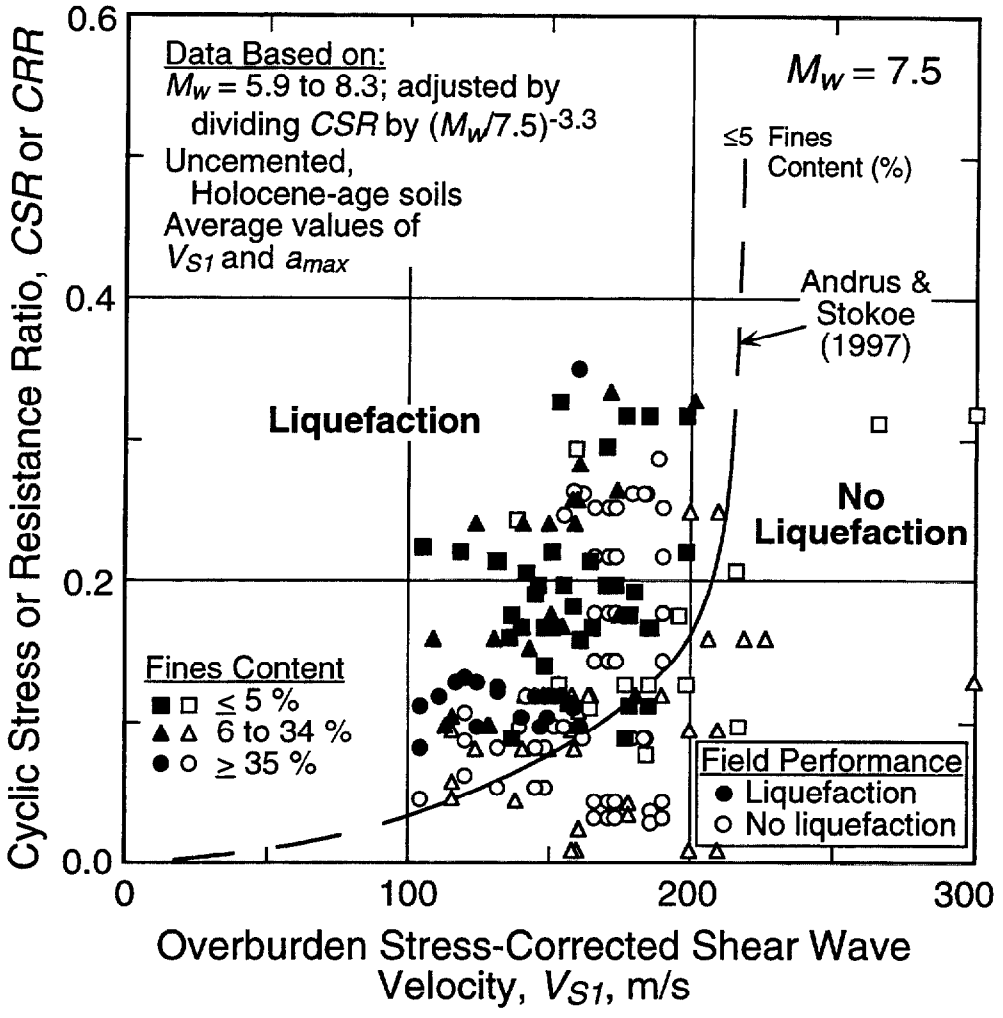

Fig. 2.10 - Liquefaction Resistance Relationship for Magnitude 7.5 Earthquakes and Uncemented Clean Soils of Holocene Age with Case History Data from Andrus and Stokoe (1997).

The first term in Eq. 2.21 is a form of Eq. 2.11, assuming $f(\gamma_{av})$ is independent of initial effective confining pressure and of pore water pressure buildup. The second term is a hyperbola with a small value at low values of V_{S1}, and a very large value as V_{S1} approaches V_{S1}^*.

The curve by Andrus and Stokoe (1997) shown in Figs. 2.5 and 2.10 is defined by Eqs. 2.13 and 2.21 with $a = 0.03$, $b = 0.9$, $n = -3.3$, and $V_{S1}^* = 220$ m/s.

2.5.6 Relationship Proposed in This Report

Since the publication of the 1996 NCEER workshop proceedings (Youd and Idriss, eds., 1997), the case history data compiled by Andrus and Stokoe (1997) have been revised, based on new information, and expanded to include field performance data from 26 earthquakes and more than 70 measurements sites. Also, the 1998 MCEER workshop was held to discuss developments since the 1996 workshop. From the suggestions given at the second workshop and using the expanded database, the curve proposed by Andrus and Stokoe (1997) is revised in this report. The case history data and the revised curve for uncemented soils with $FC \leq 5$ % are shown in Fig. 2.11. Chapter 4 discusses the development of the revised curve.

2.6 SUMMARY

A simplified procedure for evaluating liquefaction resistance of soils using V_S measurements was outlined in this chapter. Also discussed are seven proposed relationships between *CRR* and V_{S1}. Many of the differences among the seven curves (see Fig. 2.5) can be explained by the following three factors: (1) The "best-fit" curve by Tokimatsu and Uchida (1990) is more of a median curve, while the other curves bound the liquefaction case history data. (2) Portions of the proposed curves are based on limited data, and the investigator(s) have assumed different levels of conservatism. (3) Methods for selecting some site variables and correction factors are different among investigator(s).

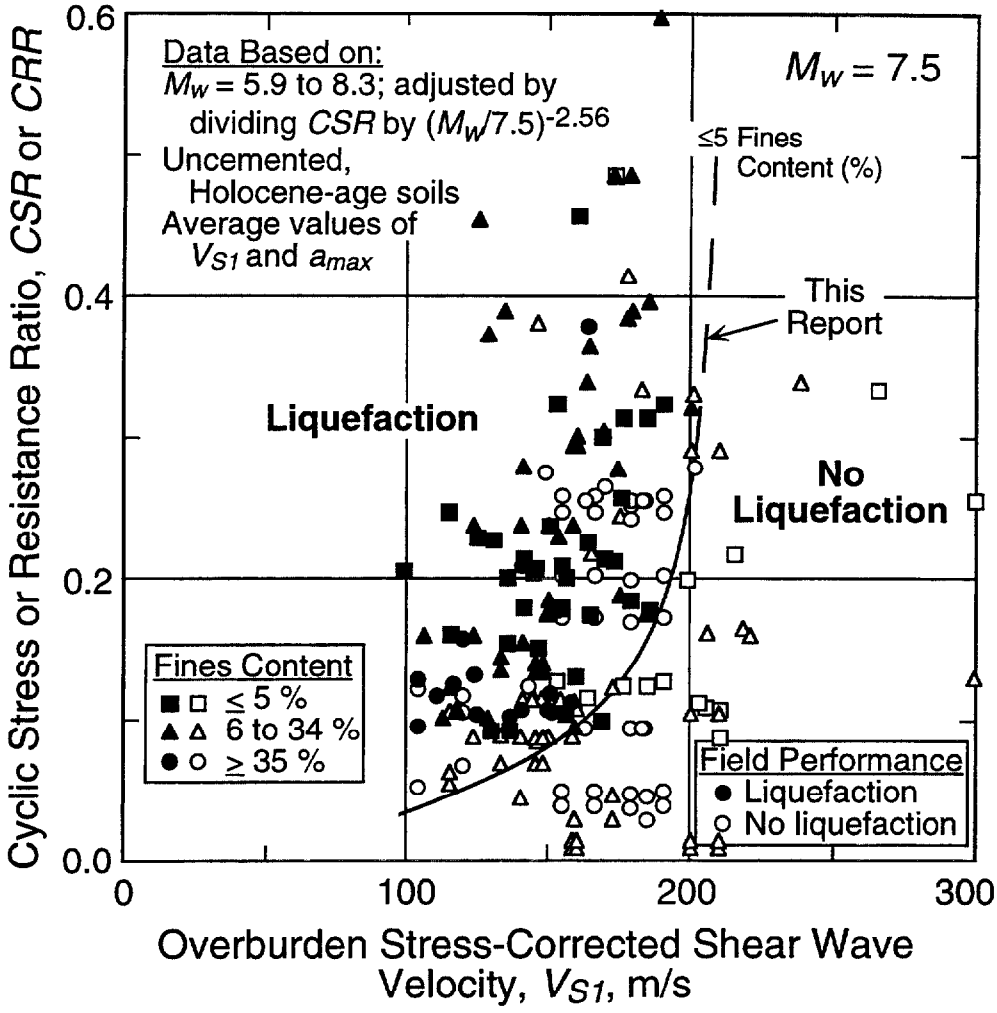

Fig. 2.11 - Revised Liquefaction Resistance Relationship for Magnitude 7.5 Earthquakes and Uncemented Clean Soils of Holocene Age with Case History Data from This Report.

CHAPTER 3

CASE HISTORY DATA AND THEIR CHARACTERISTICS

Shear wave velocity measurements have been made for field liquefaction studies at many sites during the past fifteen years. Table 3.1 lists over 70 sites and 26 earthquakes that have been investigated. Of the 26 earthquakes listed, 9 occurred in the United States; and the other 15 in Japan, Taiwan, and China. The field performance information for these earthquakes along with the V_S measurements provides an important opportunity to determine the relationship between liquefaction resistance and V_S directly from case histories. A summary of available case history data is presented in Appendix C. This chapter describes the site variables and characteristics of the database.

3.1 SITE VARIABLES AND DATABASE CHARACTERISTICS

3.1.1 Earthquake Magnitude

Earthquake magnitudes for the 26 earthquakes listed in Table 3.1 range from 5.3 to 8.3, based on the moment magnitude scale. Moment magnitude is the scale most commonly used for engineering applications, and is the preferred scale for liquefaction resistance calculations (Youd et al., 1997). When other magnitude scales are reported by the investigator(s), they are converted to M_w using the relationship of Heaton et al. (1982) shown in Fig. 3.1.

3.1.2 Shear Wave Velocity Measurement

Shear wave velocity measurements were made with 139 test arrays at the more than 70 investigation sites listed in Table 3.1. A test array is defined in this report as the two boreholes used for crosshole measurements, the borehole and source used for downhole measurements, the cone sounding and source used for seismic cone measurements, the borehole used for suspension logging measurements, or the line of receivers used for Spectral-Analysis-of-Surface-Waves (SASW) measurements. Of the 139 test arrays, 39 are crosshole, 21 downhole, 27 seismic cone, 15 suspension logger, 36 SASW, and one is unknown.

Table 3.1 - Earthquakes and Sites Used to Establish Liquefaction Resistance Curves

Earthquake (1)	Moment Magnitude (2)	Site (3)	Reference (4)
1906 San Francisco, Calif.	7.7	Coyote Creek; Salinas River (North, South)	Youd & Hoose (1978); Barrow (1983); Bennett & Tinsley (1995)
1957 Daly City, California	5.3	Marina District (2, 3, 4, 5, School)	Kayen et al. (1990); Tokimatsu et al. (1991b); T. L. Youd (personal communication to R. D. Andrus, 1999)
1964 Niigata, Japan	7.5	Niigata City (A1, C1, C2, Railway Station)	Yoshimi et al. (1984; 1989); Tokimatsu et al. (1991a)
1975 Haicheng, China	7.3	Chemical Fiber; Construction Building; Fishery & Shipbuilding; Glass Fiber; Middle School; Paper Mill	Arulanandan et al. (1986)
1979 Imperial Valley, Calif. 1981 Westmorland, Calif. 1987 Elmore Ranch, Calif. 1987 Superstition Hills, Calif.	6.5 5.9 5.9 6.5	Heber Road (Channel fill, Point bar); Kornbloom; McKim; Radio Tower; Vail Canal; Wildlife	Bennett et al. (1981; 1984); Sykora & Stokoe (1982); Youd & Bennett (1983); Bierschwale & Stokoe (1984); Stokoe & Nazarian (1984); Dobry et al. (1992); Youd & Holzer (1994)
1980 Mid-Chiba, Japan 1985 Chiba-Ibaragi-Kenkyo, Japan	5.9 6.0	Owi Island No. 1	Ishihara et al. (1981; 1987)
1983 Borah Peak, Idaho	6.9	Andersen Bar; Goddard Ranch; Mackay Dam Downstream Toe; North Gravel Bar; Pence Ranch	Youd et al. (1985); Stokoe et al. (1988a); Andrus et al. (1992); Andrus (1994)
1986 Event LSST2, Taiwan Event LSST3, Taiwan Event LSST4, Taiwan Event LSST6, Taiwan Event LSST7, Taiwan Event LSST8, Taiwan Event LSST12, Taiwan Event LSST13, Taiwan Event LSST16, Taiwan	5.3 5.5 6.6 5.4 6.6 6.2 6.2 6.2 7.6	Lotung LSST Facility	Shen et al. (1991); EPRI (1992)
1987 Chiba-Toho-Oki, Japan	6.5	Sunamachi	Ishihara et al. (1989)

Table 3.1 (cont.) - Earthquakes and Sites Used to Establish Liquefaction Resistance Curves.

Earthquake (1)	Moment Magnitude (2)	Site (3)	Reference (4)
1989 Loma Prieta, Calif.	7.0	Bay Bridge Toll Plaza, Bay Farm Island (Dike, South Loop Road); Port of Oakland; Port of Richmond	Stokoe et al. (1992); Mitchell et al. (1994)
		Coyote Creek; Salinas River (North, South);	Barrow (1983); M. J. Bennett (personal communication to R. D. Andrus, 1995); Bennett and Tinsley (1995)
		Marina District (2, 3, 4, 5, school)	Kayen et al. (1990); Tokimatsu et al. (1991b)
		Moss Landing (Harbor Office, Sandholdt Road, State Beach)	Boulanger et al. (1995); Boulanger et al. (1997)
		Santa Cruz (SC02, SC03, SC04, SC05, SC13, SC14)	Hryciw (1991); Hryciw et al. (1998)
		Treasure Island Fire Station	Hryciw et al. (1991); Redpath (1991); Gibbs et al. (1992); Furhriman (1993); Andrus (1994); de Alba et al. (1994)
		Treasure Island Perimeter (Approach to Pier, UM03, UM05, UM06, UM09)	Geomatrix Consultants (1990); Hryciw (1991); R. D. Hryciw (personal communication to R. D. Andrus, 1998); Hryciw et al. (1998); Andrus et al. (1998a, 1998b)
1993 Kushiro-Oki, Japan	8.3	Kushiro Port (2, D)	Iai et al. (1995); S. Iai (personal communication to R. D. Andrus, 1997)
1993 Hokkaido-Nansei-Oki, Japan	8.3	Pension House	Kokusho et al. (1995a, 1995b, 1995c)
		Hakodate Port	S. Iai (personal communication to R. D. Andrus, 1997)
1994 Northridge, Calif.	6.7	Rory Lane	Abdel-Haq & Hryciw (1998)

Table 3.1 (cont.) - Earthquakes and Sites Used to Establish Liquefaction Resistance Curves.

Earthquake (1)	Moment Magnitude (2)	Site (3)	Reference (4)
1995 Hyogo-Ken Nanbu, Japan	6.9	Hanshin Expressway 5 (3, 10, 14, 25, 29); Kobe-Nishinomiya Expressway (3, 17, 23, 28)	Hamada et al. (1995); Hanshin Expressway Public Corporation (1998)
		KNK; Port Island (Downhole Array); SGK	Sato et al. (1996); Shibata et al. (1996)
		Port Island (Common Factory)	Ishihara et al. (1997); Ishihara et al. (1998)
		Kobe Port (7C); Port Island (1C, 2C)	Inatomi et al. (1997); Hamada et al. (1995)
		Kobe Port (LPG Tank Yard)	S. Yasuda (personal communication to R. D. Andrus, 1997)

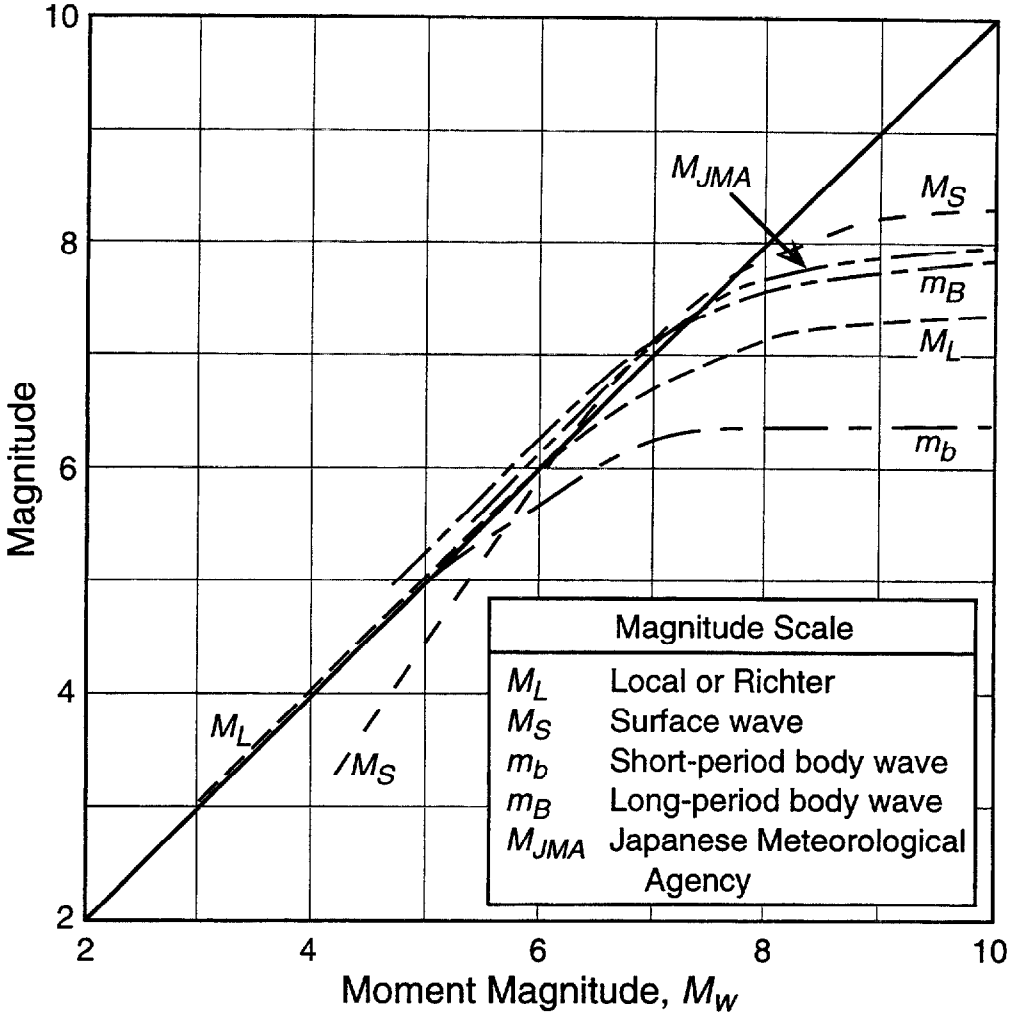

Fig. 3.1 - Relationship Between Moment Magnitude and Various Magnitude Scales (after Heaton et al., 1982).

Values of V_S reported by the investigator(s) are used directly. The one exception is for the downhole array located at the Marina District School site in San Francisco, California. A reevaluation of the field data indicates that V_S values reported for the critical layer at this site are too high. They are recalculated using the pseudo-interval method, as discussed in Section 3.2.2.

Only the crosshole measurements made with shear waves having particle motion in the vertical direction are used. Crosshole measurements near the critical layer boundary that seem high, and could represent refracted waves, are not included in the average.

Some V_S-values are from measurements made before the earthquake, others following the earthquake. No adjustments are made to compensate for changes in soil density and V_S due to ground shaking.

3.1.3 Measurement Depth

In situ V_S measurements may be reported at discrete depths or for continuous intervals, depending on the test method. When velocities are reported for continuous intervals, as is the case for downhole and SASW measurements, the depth to the center of each interval is assumed. Thus, if the reported V_S profile has ten velocity layers, it is assumed that the profile consists of ten "measurements" with depths at the center of each layer.

3.1.4 Case History

In this report, a case history is defined as a seismic event and a test array. For example, at the Treasure Island Fire Station site, crosshole measurements were made between five different pairs of boreholes, downhole measurements were made by two different investigators, seismic cone measurements were made at one location, and SASW measurements were made along one alignment. Thus, a total of nine case histories are identified for the Fire Station site and the 1989 Loma Prieta, California earthquake. At the Marina District School site, downhole measurements were made at one location. Estimates of ground surface acceleration at this site are available for the 1957 Daly City and 1989 Loma Prieta earthquakes. Thus, two case histories are identified for the Marina District School site. Combining the 26 seismic events and the 139 test arrays, a total of 225 case histories are obtained with 149 from the United States, 36 from Taiwan, 34 from Japan, and 6 from China.

The two exceptions to this definition are the Owi Island No. 1 and Moss Landing Sandholdt Road UC-4 sites where additional subsurface information is available. At Owi Island, pore pressure transducers recorded pore-water pressure buildup for two separate layers. At Moss Landing, inclinometer measurements indicated lateral movement in an upper loose layer and no lateral movement in a lower dense layer. Thus, two case histories are identified for each of these two test arrays.

3.1.5 Liquefaction Occurrence

It is important to realize that the occurrence of liquefaction, in this evaluation, is based on the appearance of surface evidence, such as sand boils, ground cracks and fissures, and ground settlement. Case histories are classified as non-liquefaction when no liquefaction effects were observed. At the Owi Island No. 1, Lotung LSST Facility, Sunamachi, Wildlife (1987 earthquakes), and Port Island sites, the assessment of liquefaction or non-liquefaction occurrence is supported by pore-water pressure measurements. Figure 3.2 shows the distribution of case histories with earthquake magnitude. Of the 225 case histories, 90 are liquefaction case histories and 135 are non-liquefaction case histories.

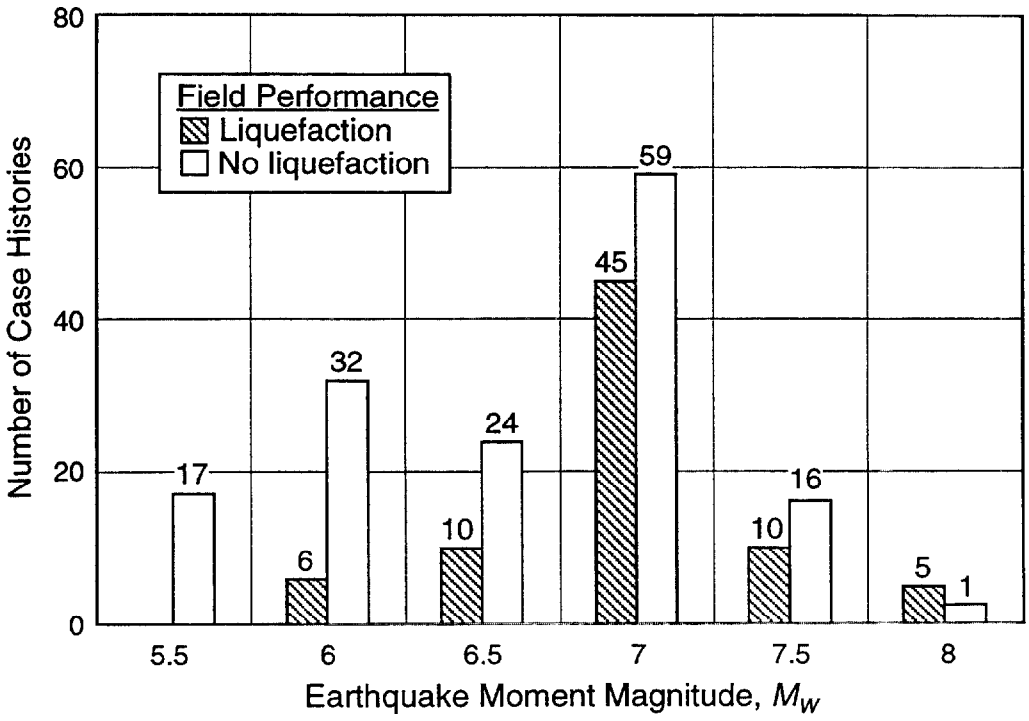

Fig. 3.2 - Distribution of Liquefaction and Non-Liquefaction Case Histories by Earthquake Magnitude.

3.1.6 Critical Layer

The critical layer is the layer of non-plastic soil below the ground water table where values of V_{S1}, as defined in Chapter 2, and penetration resistance are generally the least, and where the cyclic stress ratio relative to V_{S1} is the greatest. Figure 3.3 presents the cumulative relative frequency distribution for the case histories by critical layer thickness. Critical layer thicknesses range from 1 m to as much as 13 m. About 50 % of the case histories have a critical layer thickness less than 3.5 m; 90 % of the case histories have a critical layer thickness less than 7 m.

Figure 3.4 presents the cumulative relative frequency distribution for the case histories by average V_S measurement depth in the critical layer. The average depths of the V_S measurements are between 2 m and 11 m for nearly all case histories. Over 50 % of the case histories have average measurement depths less than 5.5 m. About 90 % of the case histories have average measurement depths less than 8 m.

Materials comprising the critical layers range from clean fine sand to sandy gravel with cobbles to profiles including silty clay layers. Figure 3.5 summarizes the average fines content (silt and clay) for the case histories grouped according to earthquake moment magnitude. Of the 225 case histories, 57 are for soils with 5 % or less fines, 98 for soils with 6 % to 34 % fines, and 70 for soils with 35 % or more fines. About 20 % of the case histories are for soils containing more than 10 % gravel.

About 70 % of the case histories are for natural soils deposits, with many formed by alluvial processes. The other 30 % are for hydraulic or dumped fills. Eight of the fills have been densified by soil improvement techniques.

At least 85 % of the case histories are of Holocene age (< 10 000 years). While the age of the other 15 % is unknown, they are believed to be also of Holocene age.

3.1.7 Ground Water Table

The ground water table for nearly all case histories lies between depths of 0.5 m and 6 m, as shown in Fig. 3.6. Nearly 60 % of the case histories have water table depths less than 2 m. About 90 % of the case histories have water table depths less than 4.5 m.

Artesian pressures are reported for the Lotung Large-Scale Seismic Test (LSST) Facility site in Taiwan. At this site, the pore-water pressure distribution is assumed to vary linearly from a pressure head of 8.1 m at a depth of 7 m to a pressure head of 1.9 m at a depth of 2 m.

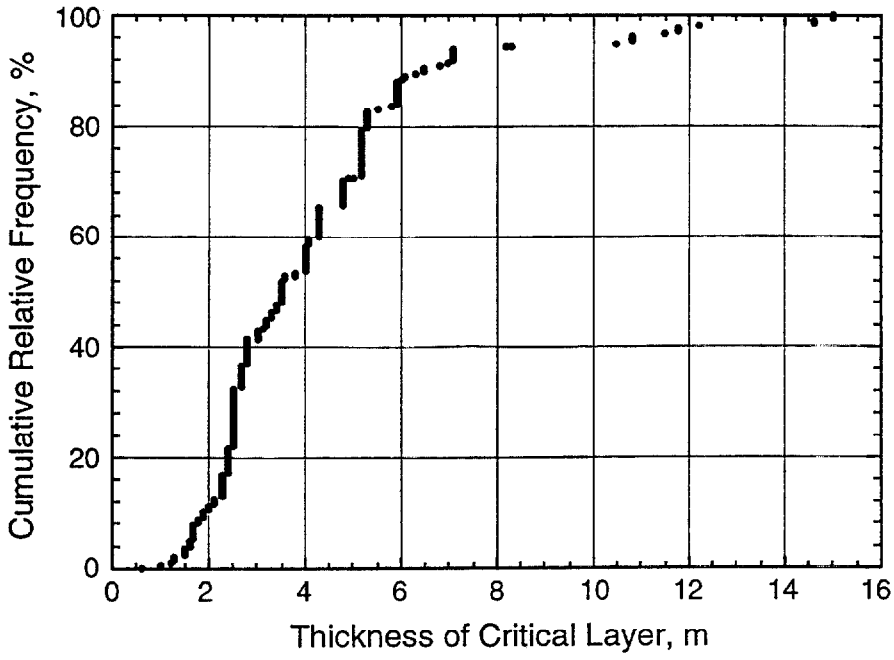

Fig. 3.3 - Cumulative Relative Frequency of Case History Data by Critical Layer Thickness.

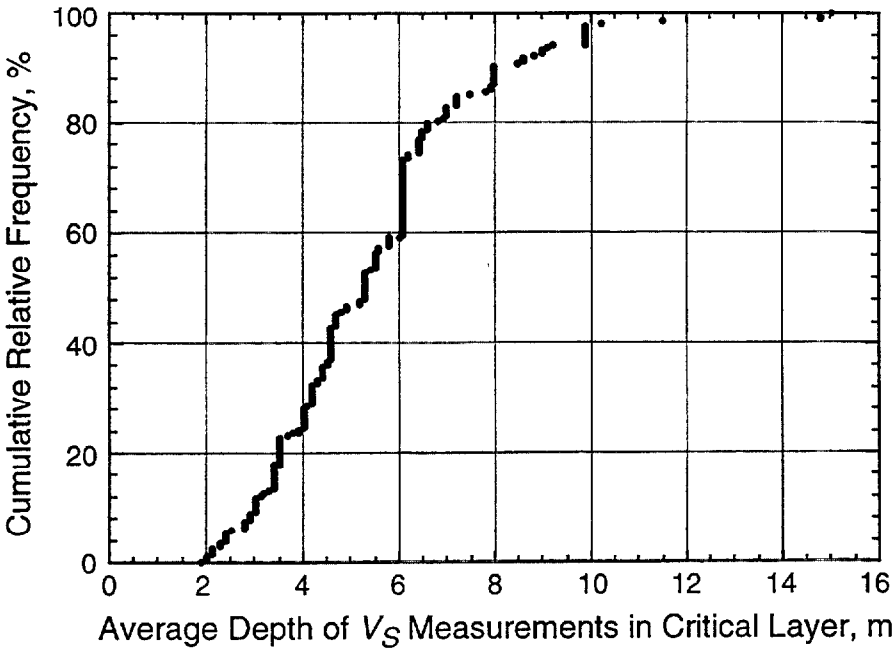

Fig. 3.4 - Cumulative Relative Frequency of Case History Data by Average Depth of V_S Measurements in Critical Layer.

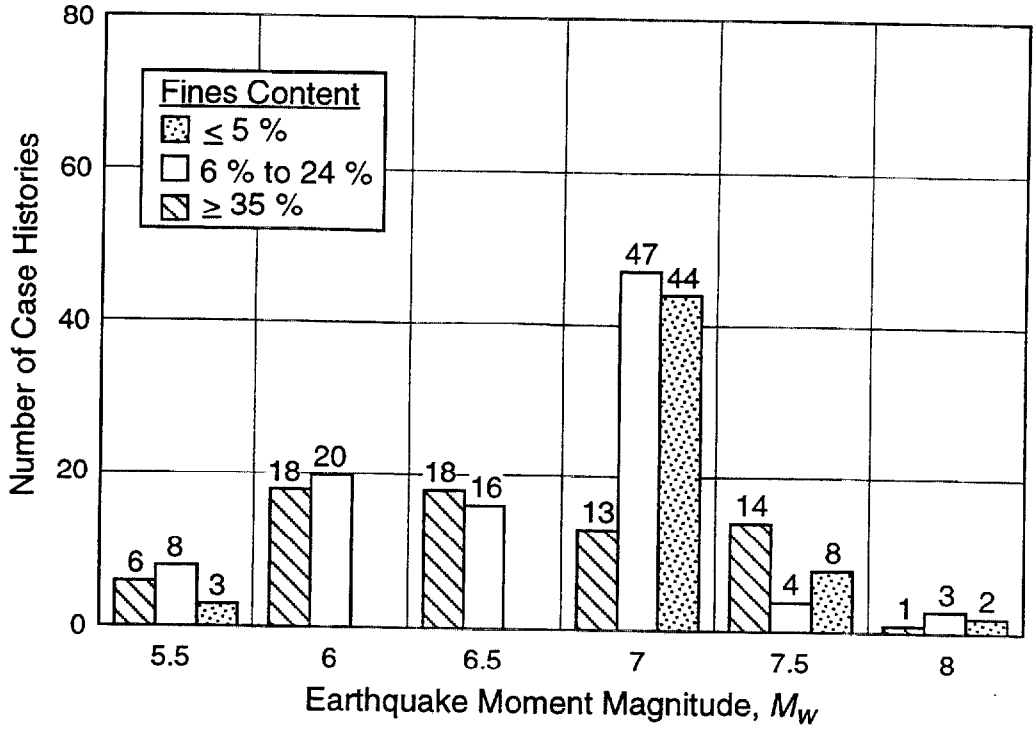

Fig. 3.5 - Distribution of Case Histories by Earthquake Magnitude and Average Fines Content.

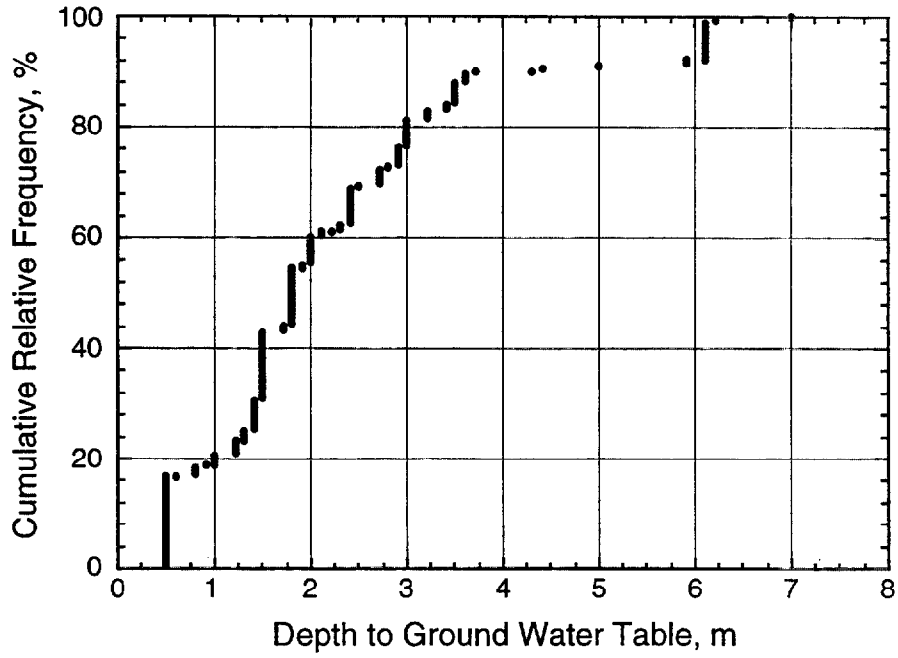

Fig. 3.6 - Cumulative Relative Frequency of Case History Data by Depth to the Ground Water Table.

3.1.8 Total and Effective Overburden Stresses

Values of total and effective overburden stresses are estimated using densities reported by the investigator(s). When no densities are reported, typical values for soils with similar grain size, penetration and velocity characteristics are assumed. In most instances, the assumed densities are 1.76 Mg/m^3 for soils above the water table and 1.92 Mg/m^3 for soils below the water table.

3.1.9 Average Peak Ground Acceleration

Average values of peak horizontal ground surface acceleration, a_{max}, are determined by averaging estimates reported by the investigator(s) and estimates made as part of this study using attenuation relationships developed from published ground surface acceleration data. Since many published attenuation relationships are based on both peak values obtained from ground motion records for the two horizontal directions (sometimes referred to as the randomly oriented horizontal component), the geometric mean (square root of the product) of the two peak values is used. Use of the geometric mean is consistent with the development of the SPT-based procedure (Youd et al., 1997). For the cases in this study, the difference between the geometric mean and arithmetic mean values is generally small, within about 5 %.

3.1.10 Average Cyclic Stress Ratio

Cyclic stress ratios, *CSR*, are first calculated for each "measurement" depth within the critical layer using Eq. 2.1, and then averaged. Values of r_d are estimated using the average by Seed and Idriss (1971) shown in Fig. 2.1. These r_d values are used to follow the traditional format of the SPT- and CPT-based procedures where the magnitude scaling factor is used to account for all effects of earthquake magnitude.

3.1.11 Average Overburden Stress-Corrected Shear Wave Velocity

Values of V_s within the critical layer are first corrected for overburden stress using Eq. 1.4, and then averaged. The number of values included in the average range from 1 to 22 (see Appendix C). About 80 % of the case histories have 2 to 7 values in the average. No adjustments are made for possible variations between seismic test methods due to different source-receiver orientations with respect to the stress state in the soil. In the calculations, each site is assumed to be level ground.

3.2 SAMPLE CALCULATIONS

Calculations for two sites shaken by the 1989 Loma Prieta, California earthquake (M_w = 7.0) are presented below to illustrate how values of *CSR* and overburden stress-corrected shear wave velocity, V_{S1}, are determined. The two sites are Treasure Island Fire Station and Marina District School.

3.2.1 Treasure Island Fire Station

Treasure Island is a man-made island located in the San Francisco Bay along the Bay Bridge between the cities of San Francisco and Oakland. It was constructed in 1936-37 by hydraulic filling behind a perimeter rock dike.

Extensive field tests have been conducted at the fire station on Treasure Island. Figure 3.7 presents two V_S profiles for the site. The V_S profile determined by crosshole testing is from Fuhriman (1993). The other V_S profile is based on unpublished SASW test results by The University of Texas at Austin in 1992. Also presented in Fig. 3.7 is the soil profile for the site. From the description by de Alba et al. (1994), the upper 4.5 m of soil consists of silty sand fill, possibly formed by dumping. Between depths of 4.5 m and 12.2 m, the soil consists of silty sand to clayey sand, formed by hydraulic filling. Beneath the hydraulic fill are natural clayey soils. The ground water table lies near the ground surface at a depth of 1.4 m. The critical layer is determined to be between depths of 4.5 m and 7 m, where the soil is non-plastic, lies below the water table, and exhibits the lowest values of V_{S1} relative to the highest values of CSR in the layer (see Fig. 5.1).

During the 1989 Loma Prieta earthquake, a seismograph station at the fire station recorded ground surface accelerations. The peak values in the two horizontal accelerometer records are 0.16 g and 0.11 g (Brady and Shakal, 1994). Unlike recordings at other seismograph stations located on soft-soils in the Bay area, there is a sudden drop in the recorded acceleration at about 15 seconds and small motion afterwards (Idriss, 1990). De Alba et al. (1994) attribute this behavior to liquefaction of an underlying sand. However, no sand boils or ground cracks occurred at the site. The nearest liquefaction effect observed is a sand boil located 100 m from the site (Geometric Consultants, 1990; Bennett, 1994; Power et al., 1998). Thus, this site is classified as a non-liquefaction site during this event by the definition given in Section 3.1.4.

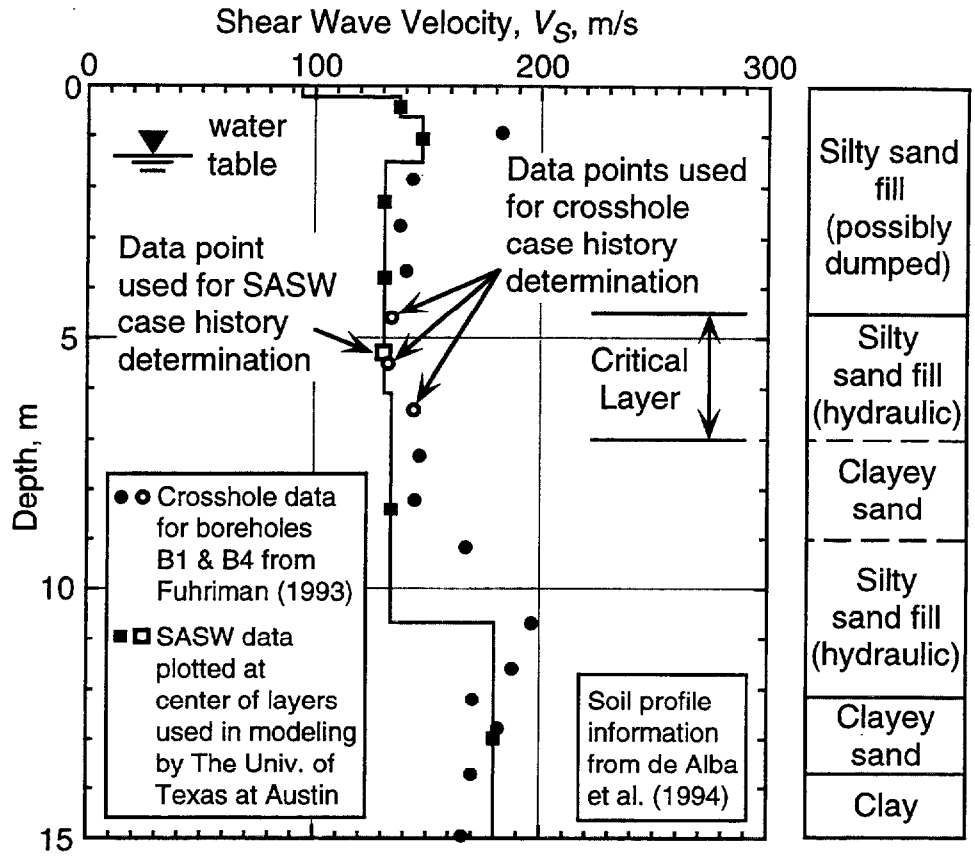

Fig. 3.7 - Shear Wave Velocity and Soil Profiles for the Treasure Island Fire Station Site.

Sample calculations for the crosshole and SASW test arrays are summarized in Tables 3.2 and 3.3, respectively. The data points used in the calculations are shown by the open symbols in Fig. 3.7. Total and effective overburden stresses are calculated assuming densities of 1.76 Mg/m^3 above the water table and 1.92 Mg/m^3 below the water table. Stress reduction coefficients are estimated using the average curve by Seed and Idriss (1971) shown in Fig. 2.1. The geometric mean of the two peak values observed in the horizontal ground surface acceleration records is 0.13 g. Using these parameters, values of CSR and V_{S1} are calculated for the crosshole measurement at depth of 4.6 m as follows:

$$CSR = 0.65\left(\frac{a_{max}}{g}\right)\left(\frac{\sigma_v}{\sigma'_v}\right)r_d \qquad (3.1)$$

$$= 0.65\left(\frac{0.13g}{g}\right)\left(\frac{84.0}{52.7}\right)0.97 = 0.131$$

and

$$V_{S1} = V_S\left(\frac{P_a}{\sigma'_v}\right)^{0.25} = 134\left(\frac{100}{52.7}\right)^{0.25} = 158 \text{ m/s} \qquad (3.2)$$

Representative values of CSR and V_{S1} used to defined the two case histories are determined by averaging values for each "measurement" depth within the critical layer, as shown in Tables 3.2 and 3.3.

3.2.2 Marina District School

Downhole seismic tests were conducted at the Winfield Scott School in the Marina District of San Francisco by Kayen et al. (1990). Figure 3.8 presents soil and velocity profiles for the site. The critical layer lies between depths of 2.7 m, the ground water table depth, and 4.3 m, the base of sand fill. The average V_S profile shown in Fig. 3.8 was determined by Kayen et al., and was based on best-fit line segments through travel time measurements plotted versus depth. The second V_S profile is determined using the pseudo-interval method (This Report), as illustrated in Fig. 3.9. Both methods should provide similar average values over the same depth interval. However, the layering assumed for the best-fit line segment method does not seem appropriate for the fill. For this reason, values of V_S based on the pseudo-interval method are used in this analysis.

Table 3.2 - Sample Calculations for the Treasure Island Fire Station Site, Crosshole Test Array B1- B4, and the 1989 Loma Prieta Earthquake.

Measurement Number (1)	Average Depth, m (2)	Measured Shear Wave Velocity, V_s, m/s (3)	Total Overburden Stress[1], kPa (4)	Effective Overburden Stress[1], kPa (5)	Stress Reduction Coefficient[2], r_d (6)	Cyclic Stress Ratio[3], CSR (7)	Overburden Stress-Corrected Shear Wave Velocity, V_{s1}, m/s (8)
1	4.57	134	84.0	52.7	0.97	0.13	158
2	5.49	133	111.3	60.9	0.96	0.14	150
3	6.40	144	118.5	69.2	0.95	0.14	158
Average	5.5	137	101.3	60.9	0.96	0.14	155

[1]Assuming water table at 1.4 m; and material densities are 1.76 Mg/m^3 above the water table and 1.92 Mg/m^3 below the water table.

[2]Based on average values determined by Seed and Idriss (1971).

[3]Assuming peak horizontal ground surface acceleration is 0.13 g.

Table 3.3 - Sample Calculations for the Treasure Island Fire Station Site, SASW Test Array, and the 1989 Loma Prieta Earthquake.

Measurement Number (1)	Average Depth, m (2)	Measured Shear Wave Velocity, V_s, m/s (3)	Total Overburden Stress[1], kPa (4)	Effective Overburden Stress[1], kPa (5)	Stress Reduction Coefficient[2], r_d (6)	Cyclic Stress Ratio[3], CSR (7)	Overburden Stress-Corrected Shear Wave Velocity, V_{s1}, m/s (8)
1	5.34	131	98.4	59.6	0.96	0.14	149
Average	5.3	131	98.4	59.6	0.96	0.14	149

[1]Assuming water table at 1.4 m; and material densities are 1.76 Mg/m^3 above the water table and 1.92 Mg/m^3 below the water table.

[2]Based on average values determined by Seed and Idriss (1971).

[3]Assuming peak horizontal ground surface acceleration is 0.13 g.

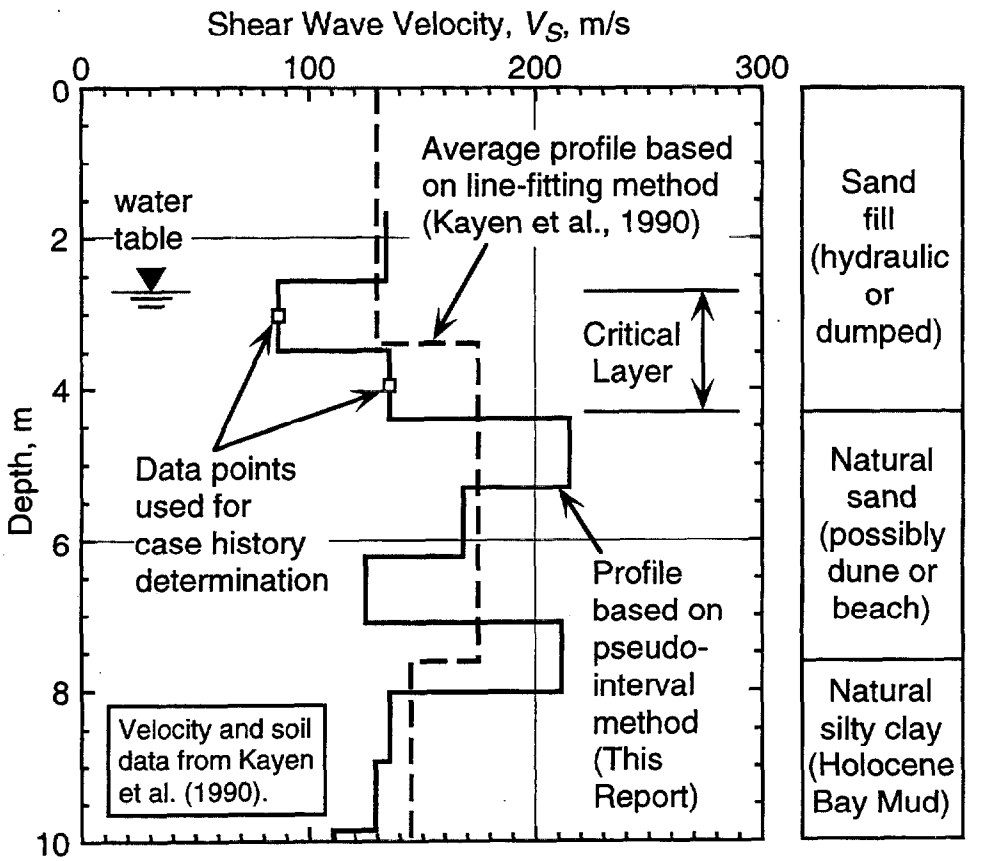

Fig. 3.8 - Shear Wave Velocity and Soil Profiles for the Marina District School Site (Kayen et al., 1990).

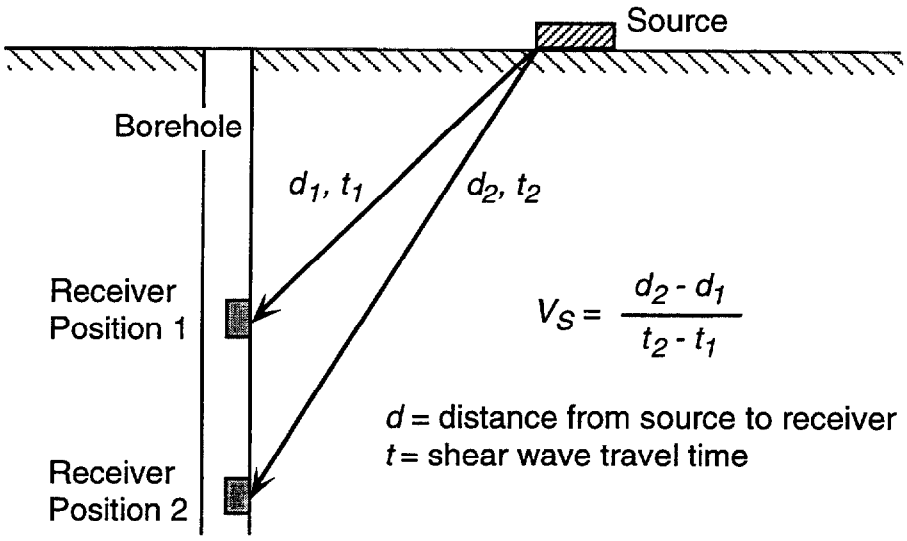

Fig. 3.9 - General Configuration of the Downhole Seismic Test Using the Pseudo-Interval Method to Calculate Shear Wave Velocity.

Many structures, pavements, and public works near the school sustained heavy damage during the 1989 earthquake (Kayen et al., 1990). This damage was due to liquefaction of the sand fill. From maps prepared by Pease and O'Rourke (1995), the site lies on the margin of the 1906 water front and artificial fill where about 40 mm of settlement occurred. Mapped sand boils and ground cracks lie just east of the site. Based on these observations, this site is classified as a liquefaction site during this earthquake.

The Marina District and Treasure Island are located about 82 km from the 1989 surface rupture. The geometric mean value of a_{max} recorded at Treasure Island during the earthquake is 0.13 g. The attenuation relationship by Idriss (1991) for 1989 strong ground motion records from soft-soil sites provides a median value of 0.16 g, assuming a distance of 82 km from surface rupture. Thus, a peak horizontal ground surface acceleration of 0.15 g, the average of these two estimates, is assumed in the analysis.

Sample calculations for the Marina District School site are summarized in Table 3.4. The locations of V_S measurements are assumed midway between receiver positions, as shown in Fig. 3.8. Total and effective overburden stresses are estimated assuming densities of 1.76 Mg/m^3 above the water table and 1.92 Mg/m^3 below the water table. The ground water table is at a depth of about 2.7 m. Average values of *CSR* and V_{S1} defining the case history are determined by averaging values for the two "measurement" depths, as shown in Table 3.4

3.3 SUMMARY

The case history data described in this chapter are limited to level and gently sloping sites with the following characteristics:

(1) average critical layer depths less than 10 m;
(2) uncemented soils of Holocene age;
(3) ground water table depths between 0.5 m and 6 m; and
(4) all V_S measurements from below the water table.

Of the 225 case histories, 57 are for soils with 5 % or less fines (silt and clay), 98 for soils with 6 % to 34 % fines, and 70 for soils with 35 % or more fines. About 20 % of the case histories are for soils containing more than 10 % gravel. Nearly 50 % of the case histories are for earthquake magnitudes near 7.

Table 3.4 - Sample Calculations for the Marina District School Site and the 1989 Loma Prieta Earthquake.

Measurement Number	Average Depth, m	Measured Shear Wave Velocity[1], V_S, m/s	Total Overburden Stress[2], kPa	Effective Overburden Stress[2], kPa	Stress Reduction Coefficient[3], r_d	Cyclic Stress Ratio[4], *CSR*	Overburden Stress-Corrected Shear Wave Velocity, V_{S1}, m/s
(1)	(2)	(3)	(4)	(5)	(6)	(7)	(8)
1	3.02	87	52.6	49.9	0.98	0.10	104
2	3.94	136	70.0	58.2	0.97	0.11	156
Average	3.5	112	61.3	54.1	0.98	0.11	130

[1]Based on pseudo-interval method.

[2]Assuming water table at 2.7 m; and material densities are 1.76 Mg/m^3 above the water table and 1.92 Mg/m^3 below the water table.

[3]Based on average values determined by Seed and Idriss (1971).

[4]Assuming peak horizontal ground surface acceleration is 0.15 g.

CHAPTER 4

LIQUEFACTION RESISTANCE FROM CASE HISTORY DATA

To establish the recommended curves for liquefaction resistance evaluation, cyclic stress ratios and shear wave velocities for the 225 case histories described in Chapter 3 are plotted in Figs. 4.1 through 4.6 for earthquakes with moment magnitudes ranging from 5.5 through 8, respectively. The plotted data have been separated into three categories: (1) sands and gravels with average fines (silt and clay) content less than or equal to 5 %; (2) sand and gravels with average fines content of 6 % to 34 %; and (3) sands and silts with average fines content greater than or equal to 35 %. Also shown in Figs. 4.1 through 4.6 are the recommended liquefaction resistance curves based on Eq. 2.21. This chapter presents the development of these curves.

4.1 LIMITING UPPER V_{S1} VALUE FOR LIQUEFACTION OCCURRENCE

Figures 4.1 through 4.6 show that the available case history data above a cyclic stress ratio of about 0.35 are limited. Thus, current estimates of V_{S1}^{*} rely in part on penetration-shear wave velocity correlations.

In the SPT-based procedure, a corrected blow count of 30 is assumed as the limiting upper value for liquefaction occurrence in clean sands above *CRR* of 0.6 and magnitude 7.5 earthquakes (Seed et al., 1985; Youd et al., 1997). Table 4.1 presents estimates of equivalent V_{S1} for corrected blow count of 30. The relationship by Ohta and Goto (1978) modified to blow count with theoretical free-fall energy of 60 % (Seed et al., 1985) suggests equivalent V_{S1} values of 207 m/s for Holocene sands and 227 m/s for Holocene gravels, assuming that a depth of 10 m is equivalent to an overburden stress of 100 kPa. The stress-corrected crosshole measurements collected by Sykora (1987b) for Holocene sands and non-plastic silty sands below the ground water table with corrected blow count between 25 and 35 exhibit an average value of 206 m/s and a standard deviation of 41 m/s. The correlation by Rollins et al. (1998a) provides a best-fit value of 232 m/s for Holocene gravels with corrected blow count of 30.

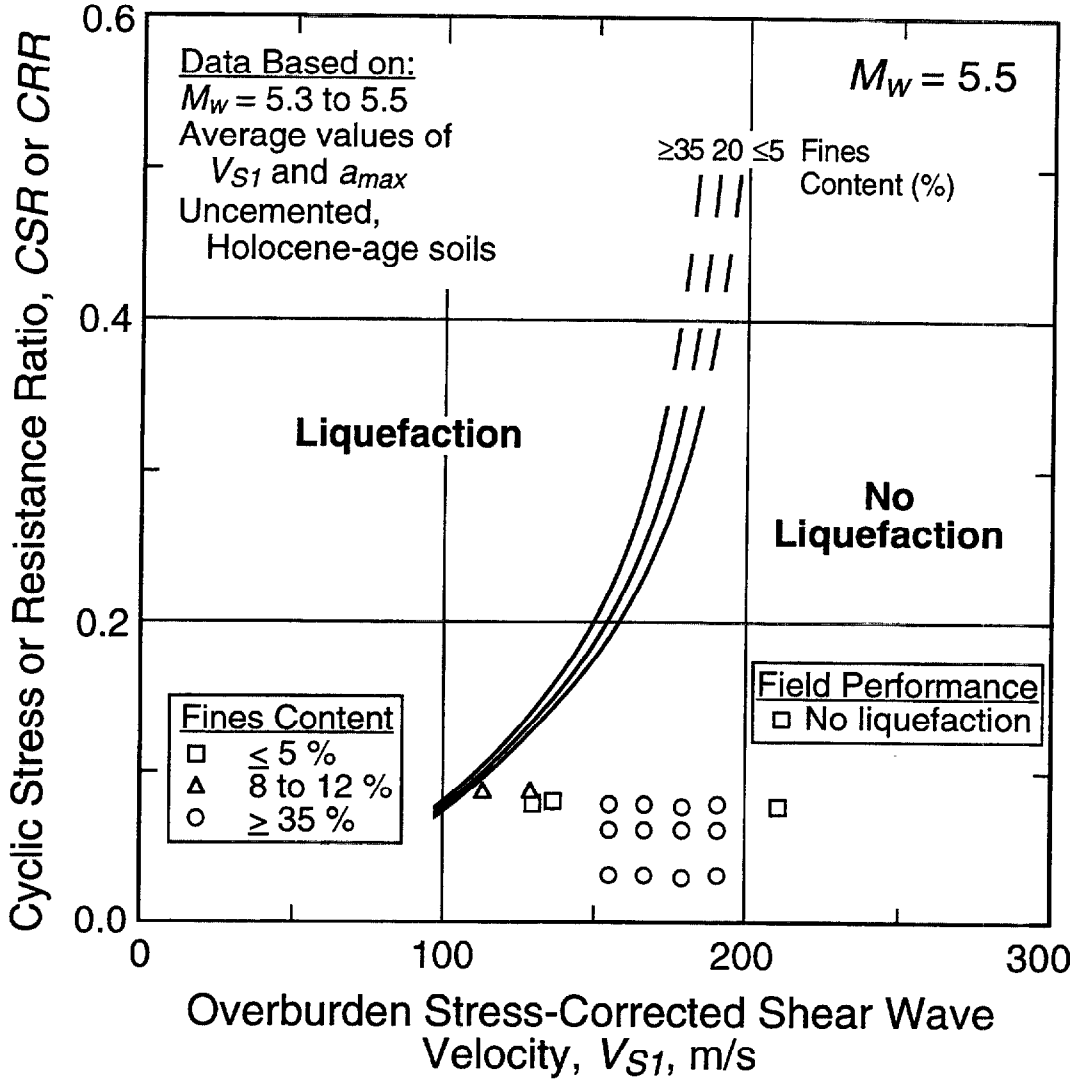

Fig. 4.1 - Case History Data for Earthquakes with Magnitude Near 5.5 Based on Overburden Stress-Corrected Shear Wave Velocity and Cyclic Stress Ratio with Recommended Liquefaction Resistance Curves.

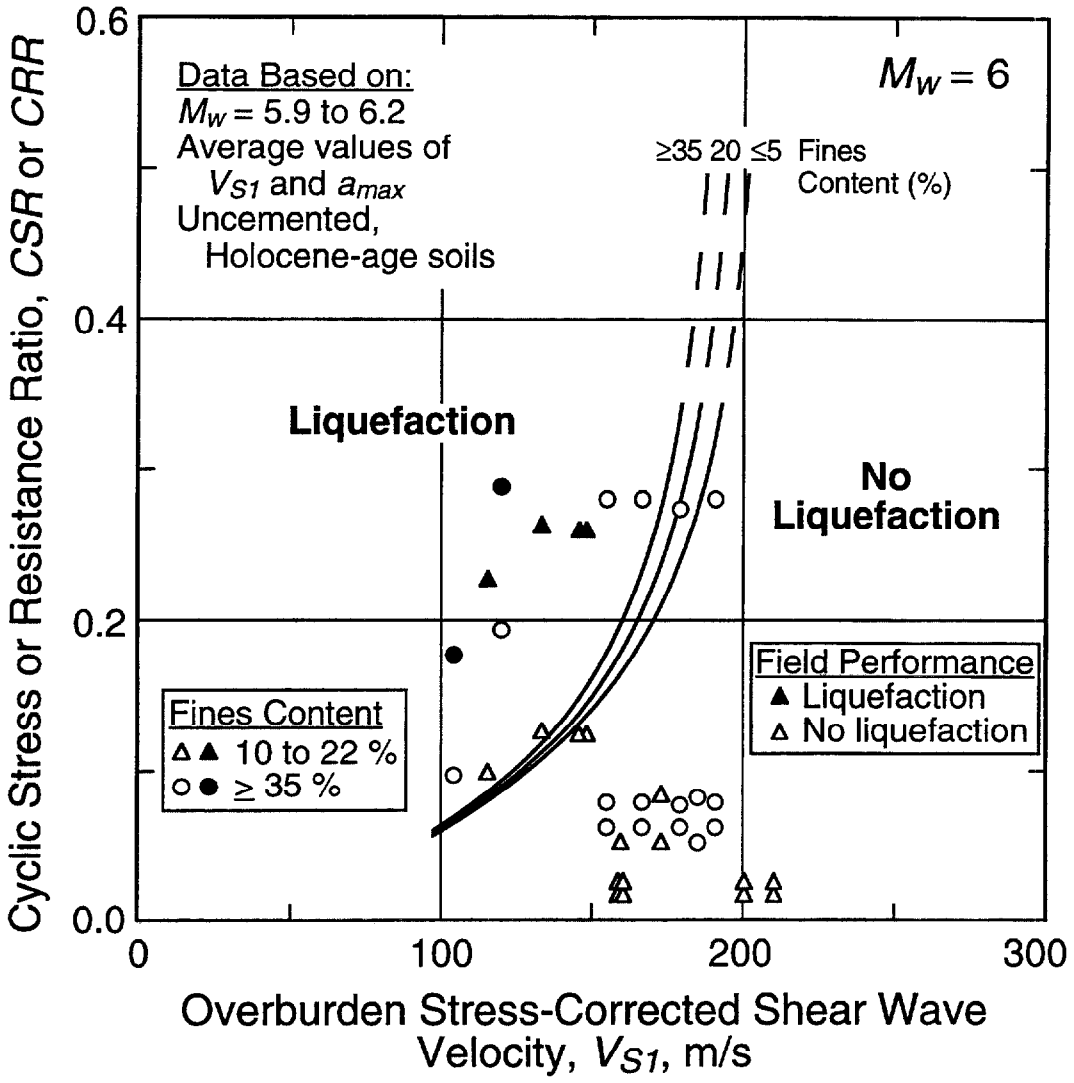

Fig. 4.2 - Case History Data for Earthquakes with Magnitude Near 6 Based on Overburden Stress-Corrected Shear Wave Velocity and Cyclic Stress Ratio with Recommended Liquefaction Resistance Curves.

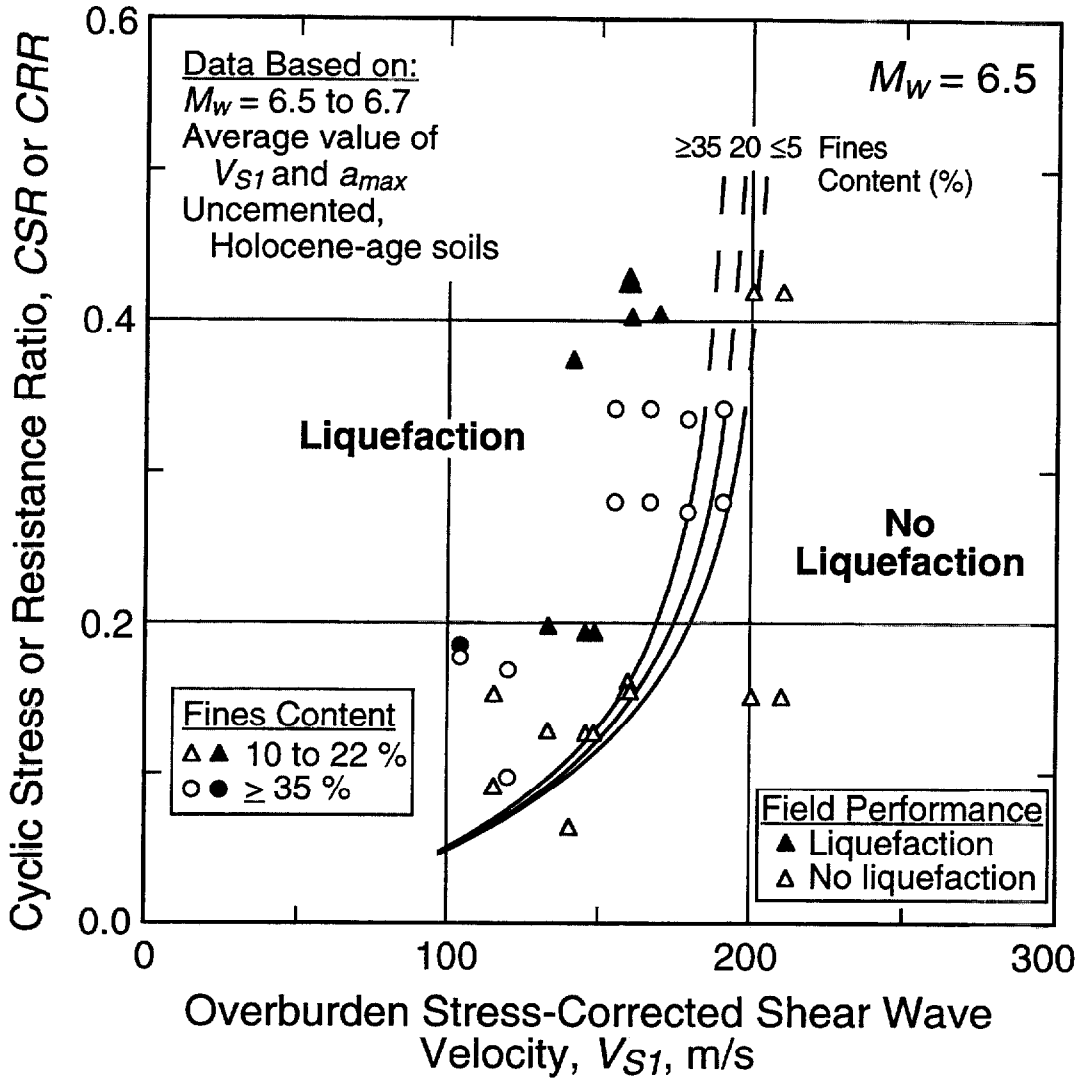

Fig. 4.3 - Case History Data for Earthquakes with Magnitude Near 6.5 Based on Overburden Stress-Corrected Shear Wave Velocity and Cyclic Stress Ratio with Recommended Liquefaction Resistance Curves.

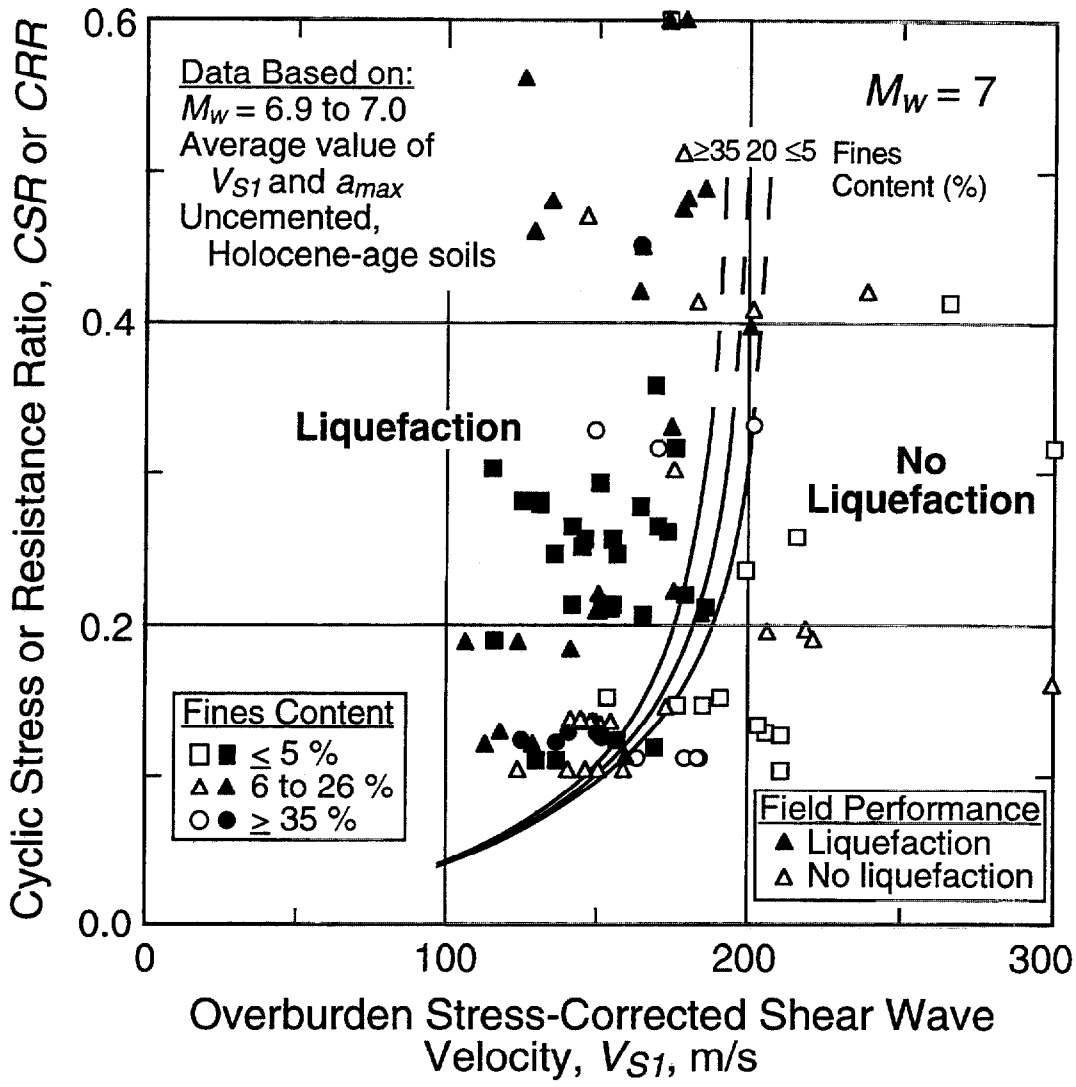

Fig. 4.4 - Case History Data For Earthquakes with Magnitude Near 7 Based on Overburden Stress-Corrected Shear Wave Velocity and Cyclic Stress Ratio with Recommended Liquefaction Resistance Curves.

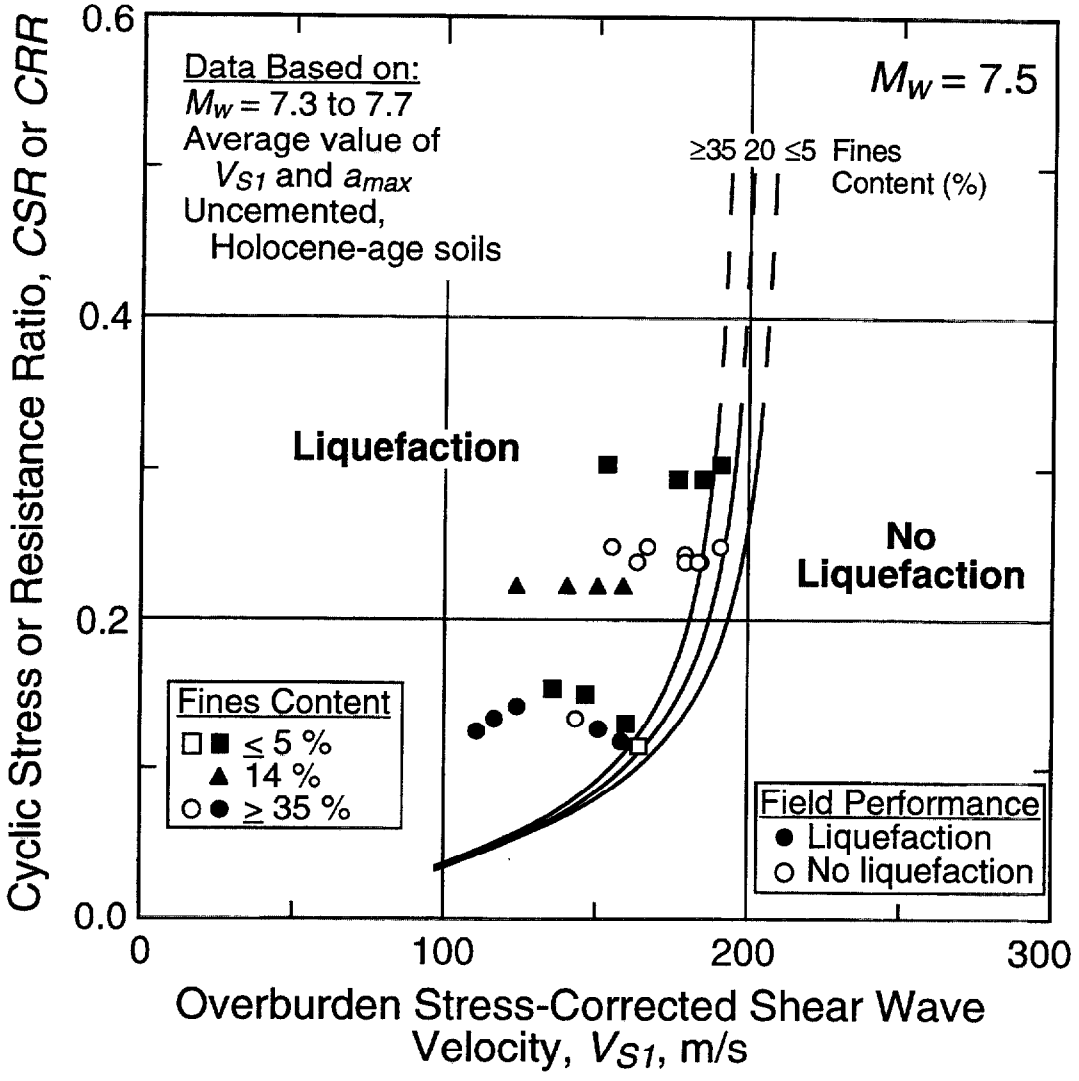

Fig. 4.5 - Case History Data for Earthquakes with Magnitude Near 7.5 Based on Overburden Stress-Corrected Shear Wave Velocity and Cyclic Stress Ratio with Recommended Liquefaction Resistance Curves.

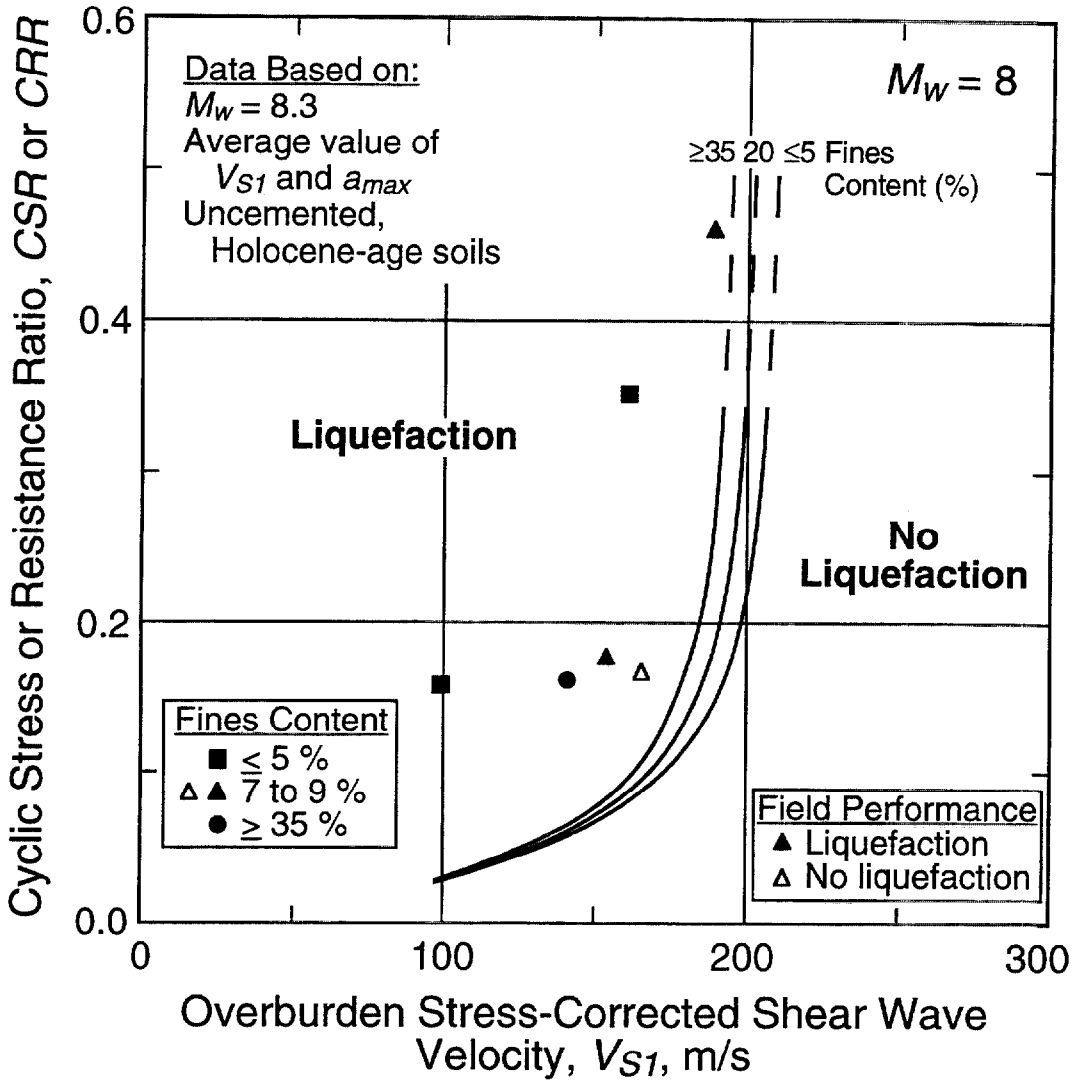

Fig. 4.6 - Case History Data for Earthquakes with Magnitude Near 8 Based on Overburden Stress-Corrected Shear Wave Velocity and Cyclic Stress Ratio with Recommended Liquefaction Resistance Curves.

Table 4.1 - Estimates of Equivalent V_{S1} for Holocene Sands and Gravels Below the Ground Water Table with Corrected SPT **Blow Count of 30.**

Reference (1)	Relationship (2)	Equivalent V_{S1} Estimate (m/s) (3)	Assumptions (4)
Ohta & Goto (1978); also given in report by Sykora (1987a, page 29)	$V_S = 69\ (N_j)^{0.173}\ z^{0.195}\ F_1 F_2$ N_j = SPT blow count measured in Japanese practice z = depth, m F_1 = 1.00 for Holocene-age soils F_2 = 1.085 for sands; 1.189 for gravel ...best-fit relationship for 289 sets of SPT and V_S measurements from Japan	207 ...for Holocene sands 227 ...for Holocene gravels	1. $N_j = 60/67\ N_{60}$ 2. $N_{60} = 30$ 3. z = 10 m is equivalent to an overburden stress of 100 kPa 4. All measurements are from below the ground water table
Sykora (1987b, page 90); This Report	Correlation between $(N_1)_{60}$ and crosshole V_S, normalized to effective overburden stress, measurements for Holocene sands and non-plastic silty sands below the ground water table at sites in U.S.A.; 16 sets of measurements (with known SPT equipment)	206 ...for Holocene sands and non-plastic silty sands below the water table ...standard deviation is 41 m/s	1. Average for V_{S1} values with $(N_1)_{60}$ between 25 and 35 2. σ'_v = 100 kPa
Rollins et al. (1998a)	$V_S = 53\ (N_{60})^{0.19}\ (\sigma'_v)^{018}$ ...best-fit relationship using equivalent N_{60}-values from Becker Penetration Tests and V_S measurements; 186 points from 7 Holocene gravel sites	232 ...for Holocene gravels ...most of data lie within ±25 % of relationship	1. $N_{60} = 30$ 2. σ'_v = 100 kPa 3. All measurements are from below the ground water table
This Report (see Fig. 4.7)	$V_{S1} = B_1\ [(N_1)_{60}]^{B2}$ $B_1 = 93.2 \pm 6.5$ $B_2 = 0.231 \pm 0.022$ ...best-fit relationship for uncemented, Holocene-age sands with less than 10 % non-plastic fines; 25 sets of average SPT and V_S measurements all from below the water table	204 ...for Holocene clean sands below the water table ...residual standard deviation is 12 m/s	1. Average for V_{S1} with $(N_1)_{60} = 30$ 2. σ'_v = 100 kPa 3. Corrected blow count based on procedures given in Seed et al. (1985) and Robertson and Wride (1997; 1998)

Rollins et al. noted that the majority of the data analyzed fall within ±25 % of their correlation. Figure 4.7 presents average values of V_{S1} and corrected blow count for soil layers with less than 10 % fines at several sites listed in Table 3.1. Also shown in Fig. 4.7 is the best-fit relationship for the plotted data. The plotted data exhibit a mean V_{S1} value of 204 m/s at a corrected blow count of 30 and a residual standard deviation, S_{res}, of 12 m/s.

In the CPT-based procedure, a normalized cone tip resistance of 160 is assumed as the limiting upper value for liquefaction occurrence in clean sand above *CRR* of 0.6 and magnitude 7.5 earthquakes (Youd et al., 1997; Robertson and Wride, 1998). Figure 4.8 presents average values of V_{S1} and normalized tip resistance for soil layers with less than 10 % fines at several sites listed in Table 3.1. Also shown in Fig. 4.8 is the best-fit relationship for the plotted data. Table 4.2 summarizes the general characteristics of the plotted data and best-fit relationship. The plotted data exhibit a mean V_{S1} value of 193 m/s at a normalized tip resistance of 160 and a residual standard deviation of 19 m/s.

From these estimates, a V_{S1} value of 210 m/s is assumed equivalent to a corrected blow count of 30 and normalized tip resistance of 160 in clean sands. A limiting upper V_{S1} value of 210 m/s for liquefaction occurrence is less than the general consensus value of 230 m/s agreed upon at the 1998 MCEER workshop. Figures 4.7 and 4.8 have been added to this report to provide additional evidence to support the use of 210 m/s as the limiting upper value of V_{S1} for clean sands and gravels.

Table 4.2 - Estimates of Equivalent V_{S1} for Holocene Sands and Gravels Below the Ground Water Table with Normalized Cone Tip Resistance of 160.

Reference (1)	Relationship (2)	Equivalent V_{S1} Estimate (m/s) (3)	Assumptions (4)
This Report (see Fig. 4.8)	$V_{S1} = B_1 (q_{c1N})^{B2}$ $B_1 = 88.2 \pm 15.5$ $B_2 = 0.154 \pm 0.037$ ...best-fit relationship for uncemented, Holocene-age sands with less than 10 % non-plastic fines; 23 sets of average SPT and V_S measurements all from below the water table	193 ...for Holocene clean sands below the water table ...residual standard deviation is 19 m/s	1. Average for V_{S1} with $q_{c1N} = 160$ 2. $\sigma'_v = 100$ kPa 3. Normalized tip resistance based on procedures given in Robertson and Wride (1997; 1998)

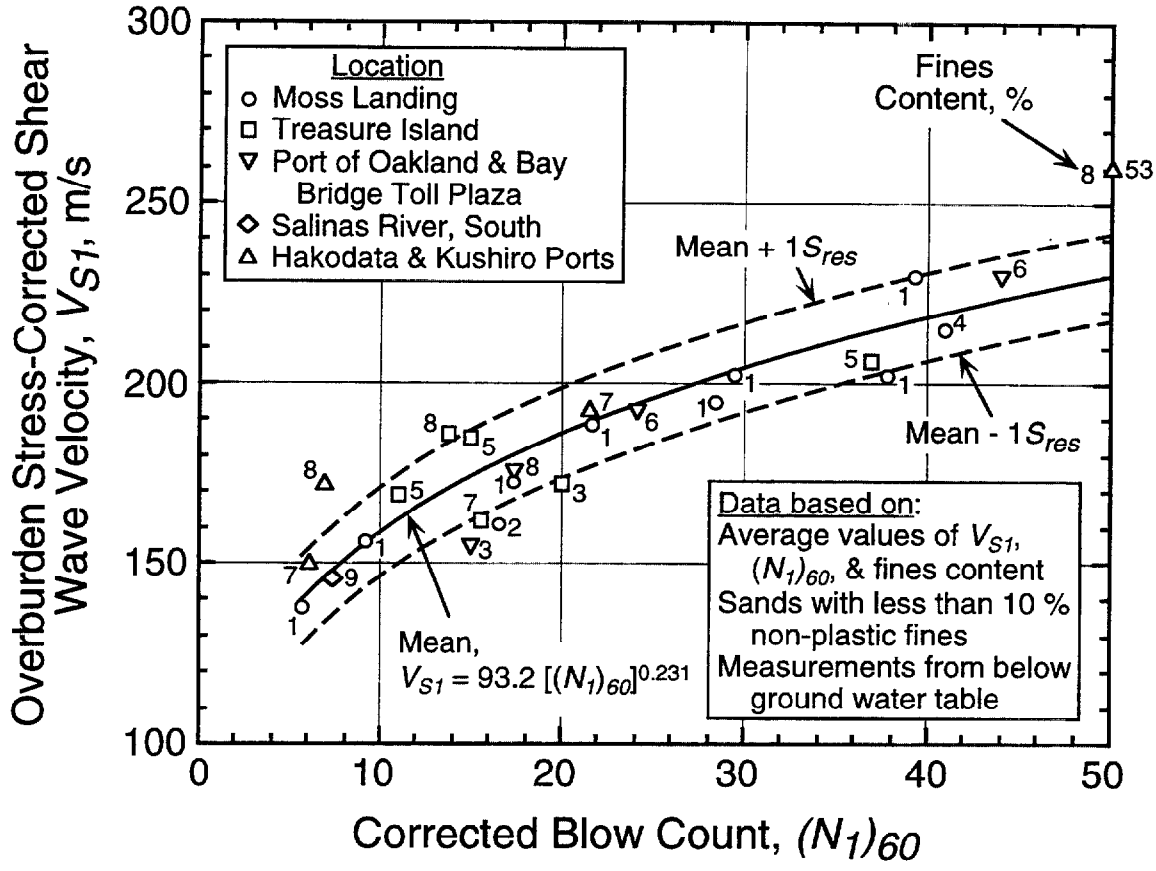

Fig. 4.7 - Variations in V_{S1} with $(N_1)_{60}$ for Uncemented, Holocene-age Sands with Less than 10 % Non-Plastic Fines.

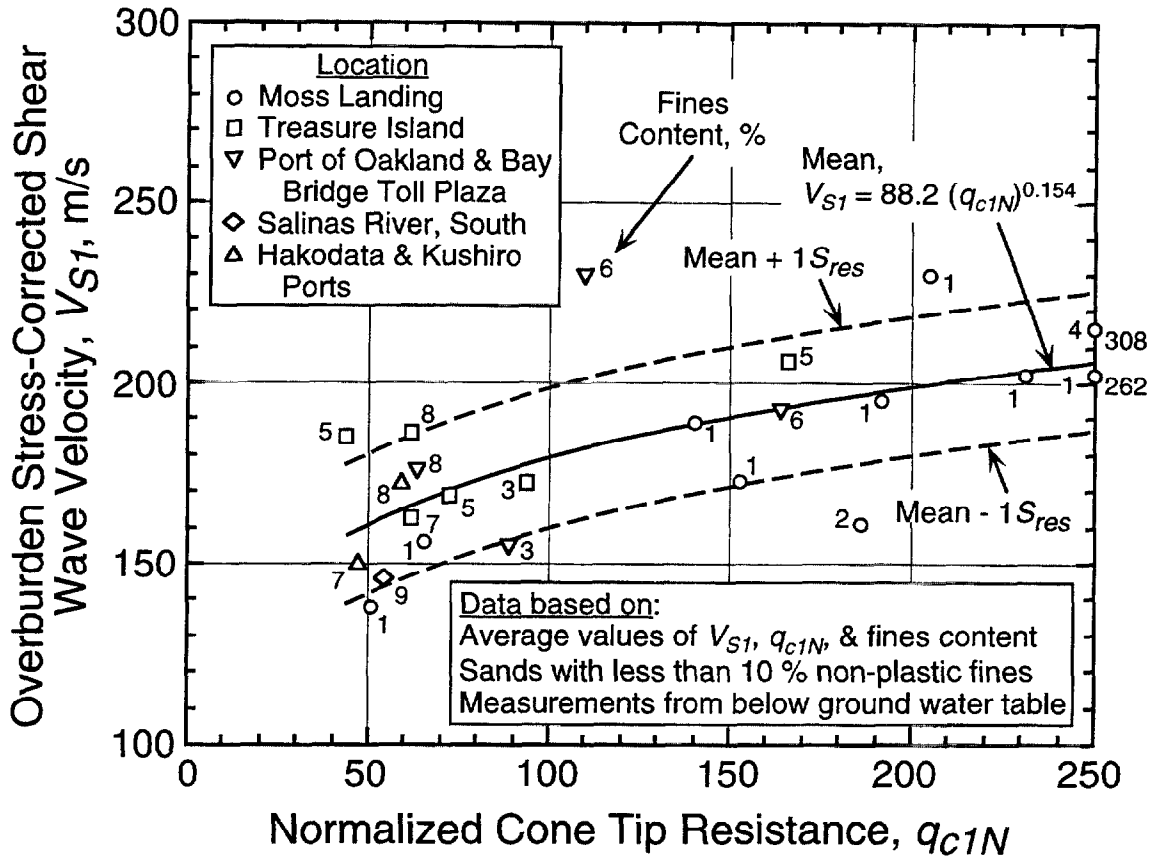

Fig. 4.8 - Variations in V_{S1} with q_{c1N} for Uncemented, Holocene-age Sands with Less than 10 % Non-Plastic Fines.

For soils with fines content greater than 35 %, the SPT-based chart by Seed et al. (1985) indicates a limiting upper corrected blow count of about 21 for liquefaction occurrence above *CRR* of 0.6. Table 4.3 presents estimates of equivalent V_{S1} for blow count of 21. The relationship by Ohta and Goto (1978) suggests equivalent V_{S1} values of 195 m/s for Holocene sands and 214 m/s for Holocene gravels. The stress-corrected crosshole collected by Sykora (1987b) for Holocene sands and non-plastic silty sands below the ground water table with corrected blow count between 16 and 26 exhibit an average value of 199 m/s and a standard deviation of 36 m/s. The correlation by Rollins et al. (1998a) provides a best-fit value of 217 m/s for Holocene gravels. From these estimates, a V_{S1} value of 195 m/s is assumed equivalent to a corrected blow count of 21 in non-plastic soils with fines content ≥ 35 %.

To permit the liquefaction resistance curves for magnitude 7.5 earthquakes shown in Fig. 4.5 to have V_{S1} values between 195 m/s and 210 m/s at *CRR* near 0.6, values of V_{S1}^* are assumed to range from 200 m/s to 215 m/s, respectively. The relationship between V_{S1}^* and fines content can be expressed by:

$$V_{S1}^* = 215 \text{ m/s} \quad \text{for sands and gravels with } FC \leq 5\ \% \qquad (4.1a)$$

$$V_{S1}^* = 215 - 0.5(FC\text{-}5) \text{ m/s} \quad \text{for sands and gravels with } 5\ \% < FC < 35\ \% \qquad (4.1b)$$

$$V_{S1}^* = 200 \text{ m/s} \quad \text{for sands and silts with } FC \geq 35\ \% \qquad (4.1c)$$

where

FC = the average fines content in percent by mass.

The *CRR*-V_{S1} curves shown in Figs. 4.1 through 4.6 provide reasonable bounds for the case history data shown above a cyclic stress ratio of 0.35, further supporting the use of V_{S1}^* values given in Eq. 4.1.

Table 4.3 - Estimates of Equivalent V_{S1} for Holocene Sands and Gravels Below the Ground Water Table with Corrected SPT **Blow Count of 21.**

Reference (1)	Relationship (2)	Equivalent V_{S1} Estimate (m/s) (3)	Assumptions (4)
Ohta & Goto (1978); also given in report by Sykora (1987a, page 29)	$V_S = 69\ (N_j)^{0.173}\ z^{0.195}\ F_1F_2$ N_j = SPT blow count measured in Japanese practice z = depth, m F_1 = 1.00 for Holocene-age soils F_2 = 1.085 for sands; 1.189 for gravel ...best-fit relationship for 289 sets of SPT and V_S measurements from Japan	195 ...for Holocene sands 214 ...for Holocene gravels	1. $N_j = 60/67\ N_{60}$ 2. $N_{60} = 21$ 3. z = 10 m is equivalent to an overburden stress of 100 kPa 4. All measurements are from below the ground water table
Sykora (1987b, page 90); This Report	Correlation between $(N_1)_{60}$ and crosshole V_S, normalized to effective overburden stress, measurements for Holocene sands and non-plastic silty sands below the water table at sites in U.S.A.; 31 sets of measurements (with known SPT equipment)	199 ...for Holocene sands and non-plastic silty sands below the water table ...standard deviation is 36 m/s	1. Average for V_{S1} values with $(N_1)_{60}$ between 16 and 26 2. σ'_v = 100 kPa
Rollins et al. (1998a)	$V_S = 53\ (N_{60})^{0.19}\ (\sigma'_v)^{018}$ ...best-fit relationship using equivalent N_{60}-values from Becker Penetration Tests and V_S measurements; 186 points from 7 Holocene gravel sites	217 ...for Holocene gravels ...most of data lie within ±25 % of relationship	1. $N_{60} = 21$ 2. σ'_v = 100 kPa 3. All measurements are from below the ground water table

4.2 CURVE FITTING PARAMETERS, *a* AND *b*

The curve fitting parameters a and b in Eq. 2.21 can be approximated from the case history data assuming the values of V_{S1}^* given in Eq. 4.1 and a *MSF* relationship. By assuming a *MSF* relationship, one can adjust the cyclic stress ratios for the case history data to magnitude 7.5 as follows:

$$CSR_{7.5} = \frac{CSR}{MSF} \tag{4.2}$$

where

CSR = the cyclic stress ratio, and
$CSR_{7.5}$ = the CSR corrected to magnitude 7.5.

Three *MSF* relationships representing the range of proposed magnitude scaling factors are considered below to establish the values of a and b.

4.2.1 Magnitude Scaling Factors Recommended by 1996 NCEER Workshop

4.2.1.1 Lower Bound of Recommended Range—Figure 4.9 presents the case history data for magnitude 5.9 to 8.3 earthquakes adjusted using the lower bound for the range of magnitude scaling factors recommended by the 1996 NCEER workshop (Youd et al., 1997). The lower bound is defined by Eq. 2.13 with n = -2.56, as discussed in Section 2.4.1. Also shown in Fig. 4.9 are three liquefaction resistance curves for earthquakes with magnitude near 7.5 and various fines content. The three curves were determined through an iterative process of varying the values of a and b until nearly all the liquefaction case histories were bound by the curves with the least amount of non-liquefaction case histories in the liquefaction region. Of the 90 liquefaction case histories, only two case histories incorrectly lie in the no liquefaction region. The final values of a and b used to draw the curves in Fig. 4.9 are 0.022 and 2.8, respectively.

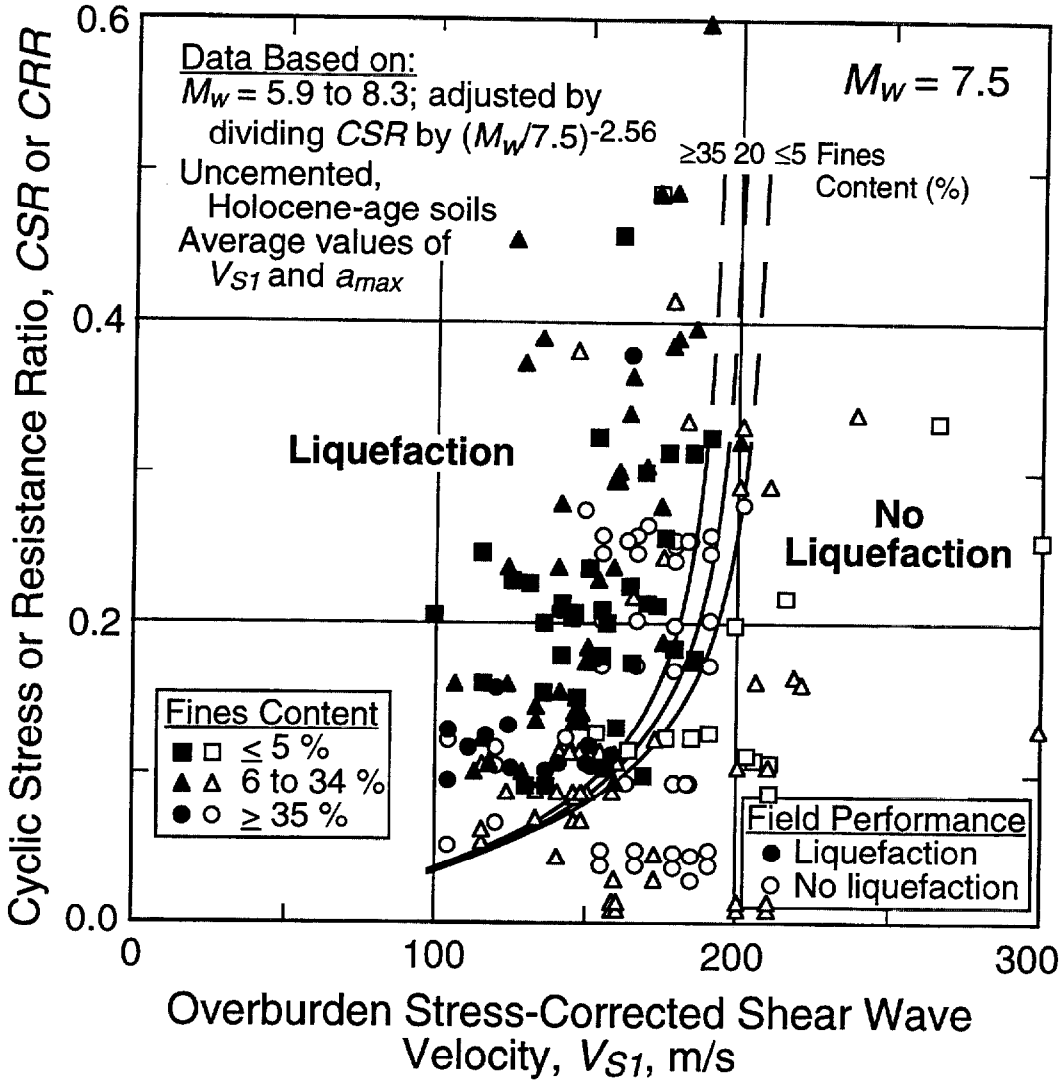

Fig. 4.9 - Curves Recommended for Calculation of *CRR* from Shear Wave Velocity Measurements Along with Case History Data Based on **Lower Bound** Values of *MSF* for the Range Recommended by the 1996 NCEER Workshop (Youd et al., 1997) and r_d Developed by Seed and Idriss (1971).

The two liquefaction case histories in Fig. 4.9 that lie in the no liquefaction region are for the Treasure Island UM05 and UM09 sites. The UM05 and UM09 sites are located along the perimeter of Treasure Island. Mapped liquefaction effects generated by the 1989 Loma Prieta earthquake near the UM05 site are ground cracks with 50 to 90 mm of horizontal displacement (R. D. Hryciw, personal communication to R. D. Andrus, 1998; Power et al., 1998). The nearest mapped sand boil is located 60 m away from the site. At the UM09 site, as much as 90 mm of vertical displacement was observed adjacent to a building located 60 m inland from the site. These displacements are small compared to the meters of displacement that are expected to occur during larger ground shaking. Thus, liquefaction was marginal at the UM05 and UM09 sites, and sloping ground may have been a factor. It should be noted that similar evaluations are obtained using the SPT and CPT data for these sites. The SPT- and CPT-based evaluations for the UM05 site are discussed in Section 4.3.1.

4.2.1.2 Upper Bound of Recommended Range—Figure 4.10 presents the case history data for magnitude 5.9 to 8.3 earthquakes adjusted using the upper bound for the range of magnitude scaling factors recommended by the 1996 NCEER workshop (Youd et al., 1997). The upper bound is defined by Eq. 2.13 with n = -3.3, as discussed in Section 2.4.1. Also shown in Fig. 4.10 are the same three curves from Fig. 4.9. Many case history data plot lower in Fig. 4.10 than in Fig. 4.9, since the earthquake magnitude is less than 7.5 for most of the data. The downward shift in the liquefaction data points near the curves at *CRR* of about 0.08 is less than 0.01. This difference is not significant, and is within the accuracy of the plotted case history data.

4.2.2 Revised Magnitude Scaling Factors Proposed by Idriss (1999)

Figure 4.11 presents the case history data for magnitude 5.9 to 8.3 earthquakes adjusted using the revised magnitude scaling factors and stress reduction coefficients proposed by Idriss (1999 as discussed in Section 2.4.2. Also shown in Fig. 4.11 are the same three liquefaction resistance curves from Fig. 4.9. Many of the case history data shown in Fig. 4.11 plot higher than case history data in Fig. 4.9, since the earthquake magnitude is less than 7.5 for most of the data. The upward shift in the liquefaction data points near the curves at *CRR* of about 0.08 is less than 0.01. This difference is also not significant, and is within the accuracy of the plotted case history data.

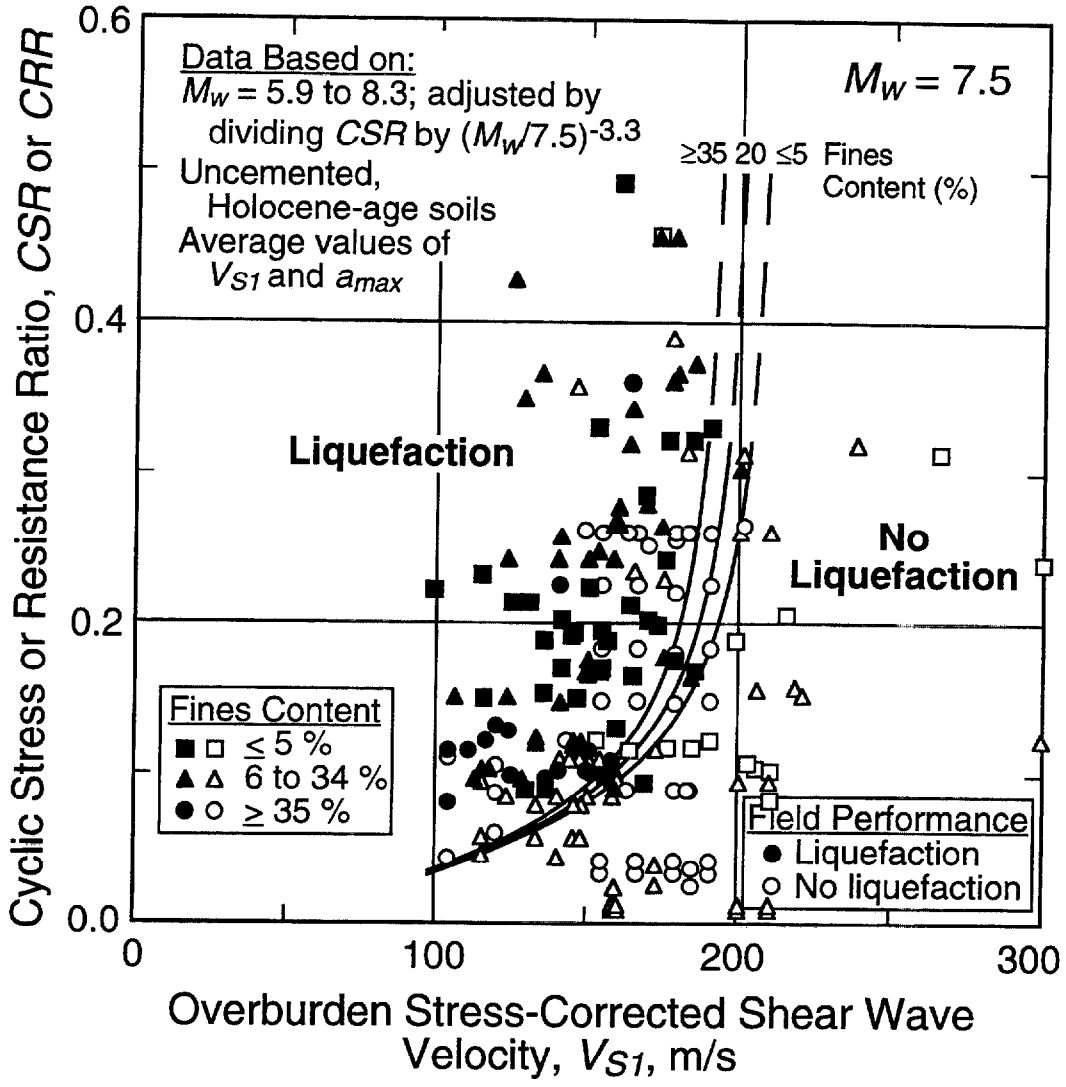

Fig. 4.10 - Curves Recommended for Calculation of *CRR* from Shear Wave Velocity Measurements Along with Case History Data Based on **Upper Bound** Values of *MSF* for the Range Recommended by the 1996 NCEER Workshop (Youd et al., 1997) and r_d Developed by Seed and Idriss (1971).

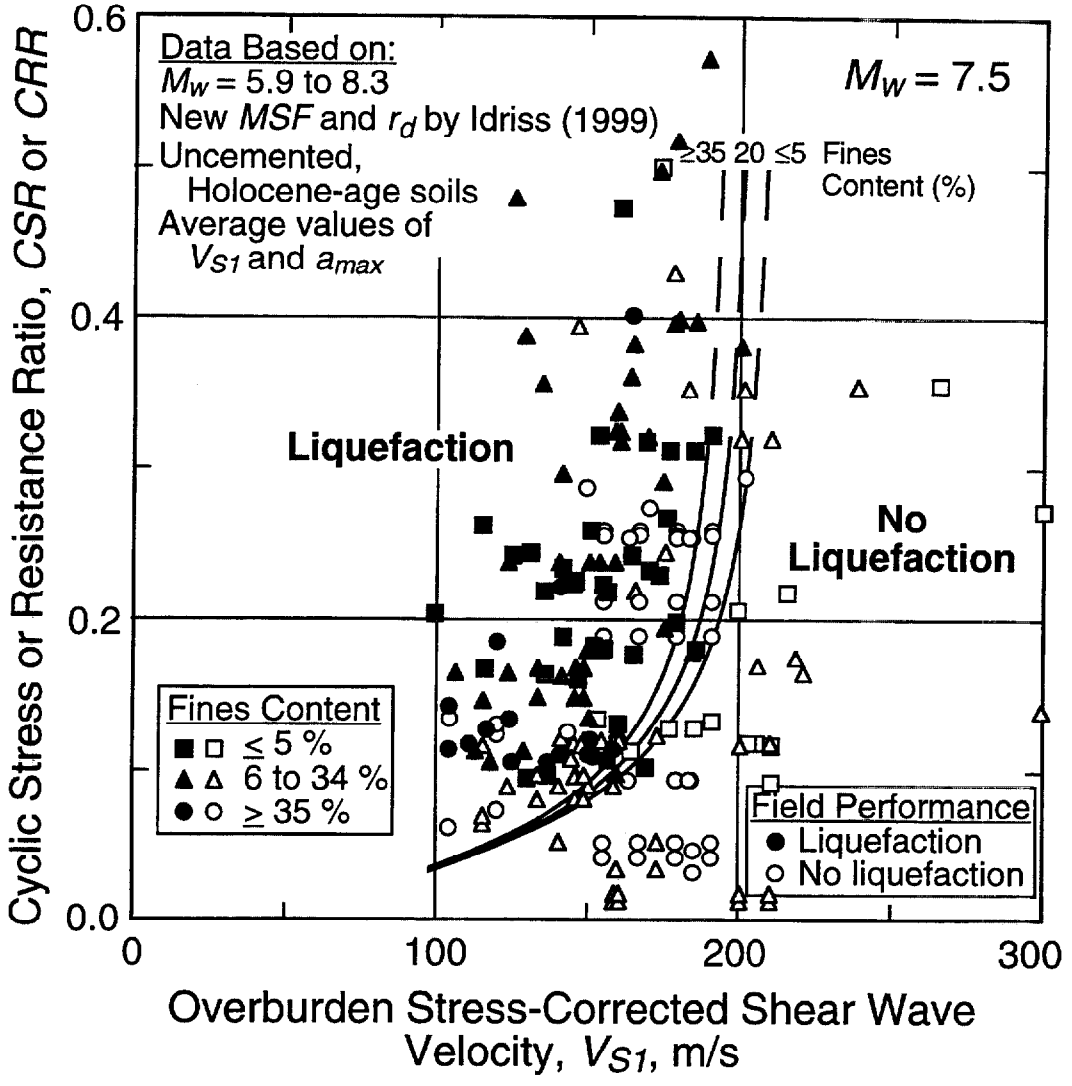

Fig. 4.11 - Curves Recommended for Calculation of *CRR* from Shear Wave Velocity Measurements Along with Case History Data Based on Revised Values of *MSF* and r_d Proposed by Idriss (1999).

The differences between the *MSF* and r_d relationships proposed by Idriss (1999) and the relationships recommended by the 1996 NCEER workshop (Youd et al., 1997) are significant at magnitudes less than about 7 (see Fig. 2.4). Figure 4.12 presents two liquefaction resistance curves for earthquakes with magnitude near 5.5 and clean soils ($FC \leq 5$ %). The upper curve was obtained by multiplying values of *CRR* defining the curve for $FC \leq 5\%$ in Fig. 4.9 by 2.2, the lower *MSF* recommended by the 1996 NCEER workshop for magnitude 5.5 earthquakes (see Eq. 2.13 with n = -2.56). The lower curve was obtained by multiplying values of *CRR* defining the curve for $FC \leq 5$ % in Fig. 4.9 by 1.68, the *MSF* proposed by Idriss (1999) for magnitude 5.5 earthquakes (see Eq. 2.15). Also shown in Fig. 4.12 are the available case history data for clean sands determined using average stress reduction coefficients proposed by Seed and Idriss (1971) and Idriss (1998). The two curves in Fig. 4.12 exhibit differences in *CRR* of about 0.02 at V_{S1} = 100 m/s and 0.1 at V_{S1} = 200 m/s.

4.3 RECOMMENDED *CRR*-V_{S1} CURVES

From the discussion presented in Sections 4.1 and 4.2, the recommended *CRR*-V_{S1} curves are defined by Eqs. 2.13, 2.21, and 4.1 with $a = 0.022$, $b = 2.8$, and $n = -2.56$. The value of -2.56 for n is recommended for determining magnitude scaling factors because it provides more conservative *CRR*-V_{S1} curves than -3.3 for magnitude less than 7.5. While the magnitude scaling factors defined by Eq. 2.13 with n = -2.56 provide less conservative *CRR*-V_{S1} curves than the factors proposed by Idriss (1999) for magnitudes less than 7.5, the findings of Ambrasey (1988), I. M. Idriss (personal communication to T. L. Youd, 1995), Arango (1996), Youd and Noble (1997), and the case history data presented in this report (see Figs. 4.2 and 4.3) support their use.

The recommended *CRR*-V_{S1} curves are shown in Figs. 4.1 through 4.6 for different magnitude earthquakes. The curves are dashed above *CRR* of about 0.35 to indicate that they are based on limited field performance data. The curves do not extend much below 100 m/s, since there are no field data to support extending them to the origin.

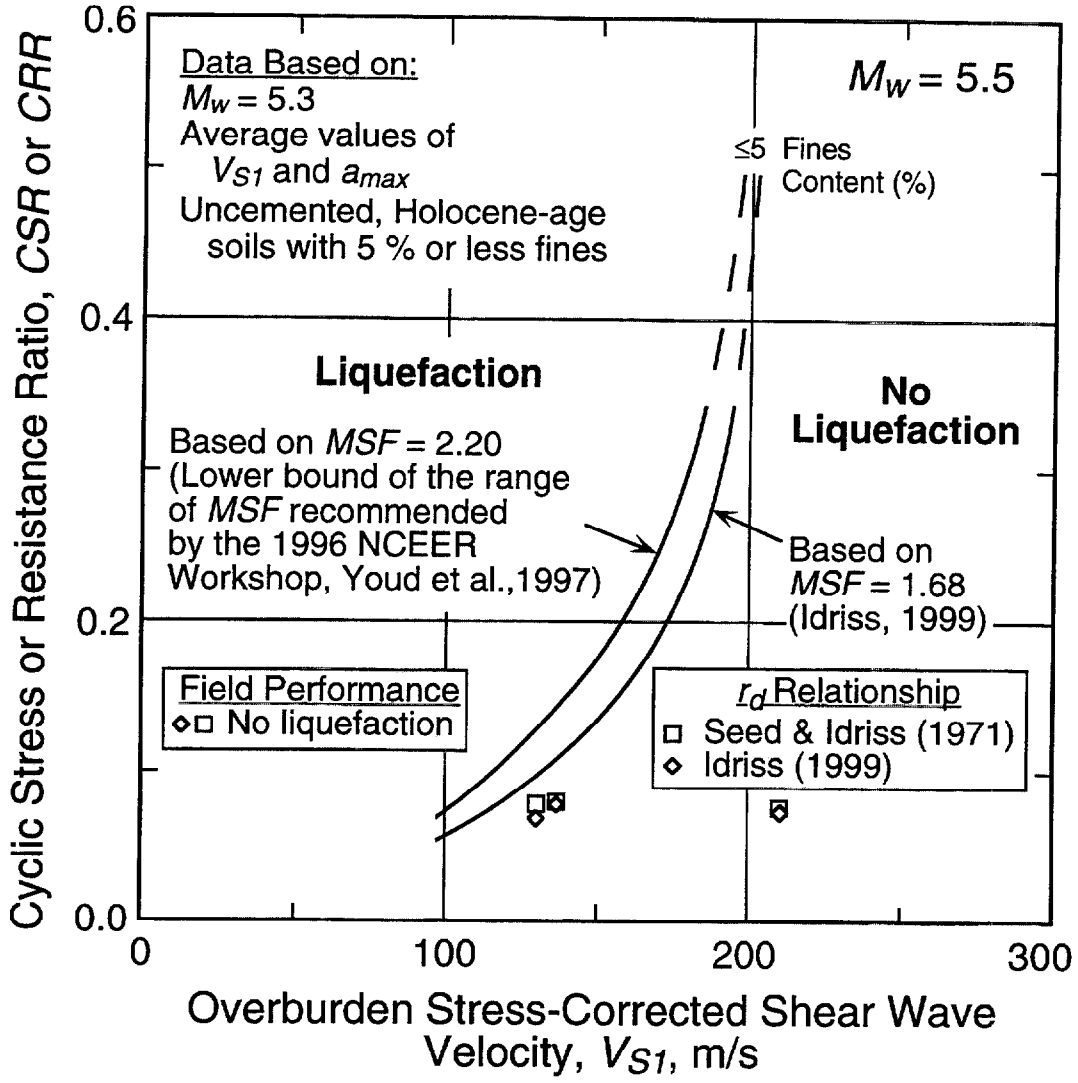

Fig. 4.12 - Comparison of Liquefaction Resistance Curves and Case History Data for Procedures Recommended by the 1996 NCEER Workshop (Youd et al., 1997) and the Revised Procedures Proposed by Idriss (1999) for Clean Sands and Earthquakes with Magnitude Near 5.5.

4.3.1 Correlations Between V_{S1} and Penetration Resistance

By plotting values with equal *CRR*, on can obtain Correlations between V_{S1} and corrected penetration resistance from the recommended *CRR*-V_{S1} relationships given in Fig. 4.5 and the 1996 NCEER workshop recommended SPT- and CPT-based relationships for magnitude 7.5 earthquakes (Youd et al., 1997).

4.3.1.1 Corrected SPT Blow Count—Figure 4.13 presents the correlation of V_{S1} with $(N_1)_{60}$ for clean soils (≤ 5 % fines) based on the recommended *CRR*-V_{S1} and *CRR*-$(N_1)_{60}$ relationships. Also shown are the field data and mean curve for sands with less than 10 % non-plastic fines from Fig. 4.7. The correlation derived from the *CRR* relationships lies between the mean and the mean $+1S_{res}$ curves. The flatter slope below $(N_1)_{60}$ of 6 exhibited by the *CRR*-based correlation can be explained by different assumed minimal values of *CRR*. The *CRR*-V_{S1} relationship for magnitude 7.5 earthquakes and $FC \leq 5$ % shown in Fig. 4.5 provides a *CRR* of 0.033 for V_{S1} = 100 m/s, the lowest V_{S1} value shown in the figure. The 1996 NCEER workshop recommended a *CRR* value of 0.05 for $(N_1)_{60} = 0$. The difference between minimal values of *CRR* is small, and is near the accuracy of both procedures.

The *CRR*-based curve shown in Fig. 4.13, along with the plotted field data, provide a simple method of comparing the V_{S1}- and $(N_1)_{60}$-based liquefaction evaluation procedures. Both procedures will provide similar predictions of liquefaction potential, when the data point lies on the *CRR*-based curve. When the data point plots below the *CRR*-based curve, the V_{S1}-based liquefaction evaluation procedure provides the more conservative prediction; and when the data point plots above the *CRR*-based curve, the SPT-based liquefaction evaluation procedure provides the more conservative prediction. Since most of the data points shown in Fig. 4.13 plot below the *CRR*-based curve, the V_{S1}-based procedure provides an overall more conservative prediction of liquefaction resistance than does the SPT-based procedure for these sites.

The data point for the Treasure Island UM05 site, which incorrectly lies in the region of no liquefaction shown in Fig. 4.9, plots just below the *CRR*-based curve, as shown in Fig. 4.13. Thus, this case history also incorrectly plots in the region of no liquefaction on the SPT-based liquefaction evaluation chart. Furthermore, the SPT-based procedure provides a slightly less conservative prediction of liquefaction resistance than the shear-wave-based procedure for this case history.

Although the *CRR*-based curve shown in Fig. 4.13 generally trends parallel to the mean curve, there is a small hump between corrected blow counts of 8 and 26. This hump suggests that either the *CRR*-V_{S1} relationship is more conservative or the *CRR*-$(N_1)_{60}$ relationship is less conservative in this range.

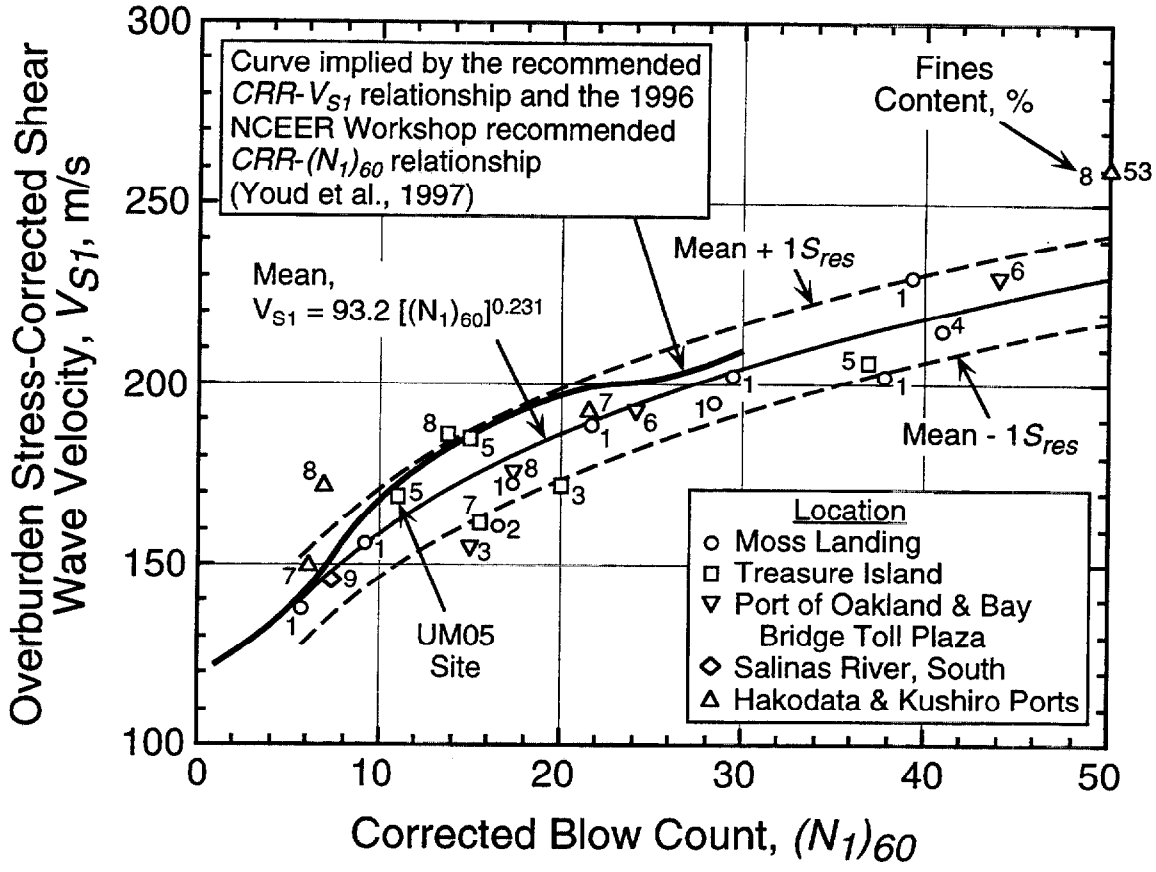

Fig. 4.13 - Relationships Between $(N_1)_{60}$ and V_{S1} for Clean Sands Implied by the Recommended CRR-V_{S1} Relationship and the 1996 NCEER Workshop Recommended CRR-$(N_1)_{60}$ Relationship (Youd et al., 1997) with Field Data for Sands with Less than 10 % Fines.

4.3.1.2 Normalized Cone Tip Resistance—Figure 4.14 presents the correlation of V_{S1} with q_{c1N} for clean sands with median grain size, D_{50}, between 0.25 mm and 2.0 mm based on the recommended CRR-V_{S1} and CRR-q_{c1N} relationships. Also shown are the field data and mean curve for clean sands with less than 10 % non-plastic fines from Fig. 4.8. The correlation derived from the CRR relationships lies between the mean and the mean $+1S_{res}$ curves for $V_{S1} \geq$ 170 m/s, indicating that the V_{S1}-based procedure provides an overall more conservative prediction of liquefaction resistance than does the CPT-based procedure for these sites. For V_{S1} < 170, the CRR-based correlation lies close to the mean curve, indicating that both procedure provide an overall similar prediction. The slope of the CRR-based correlation below q_{c1N} of 20 may be explained by the different assumed minimal values of CRR.

The data point for the Treasure Island UM05 site, which incorrectly lies in the region of no liquefaction shown in Fig. 4.9, plots on the CRR-based curve, as shown in Fig. 4.14. Thus, the CPT-based procedure provides a similar prediction of no liquefaction.

4.3.2 Cementation, Aging, and Above-the-Water-Table Correction

The recommended CRR-V_{S1} relationship is limited to the characteristics of the database, as described in Chapter 3. In areas of cemented and aged soils (> 10 000 years), and soils above the ground water table where negative pore-water pressure can increase the value of V_S measured in seismic tests, a correction factor can be added to Eq. 2.21 as follows:

$$CRR = \left\{ a\left(\frac{CV_{S1}}{100}\right)^2 + b\left(\frac{1}{V_{S1}^* - CV_{S1}} - \frac{1}{V_{S1}^*}\right)\right\} MSF \qquad (4.3)$$

where

C = a factor to correct for high values of V_{S1} caused by cementation, aging, and negative pore-water pressures.

Average estimates of C range from 0.6 to 0.8 based on the penetration-V_{S1} correlations for Pleistocene-age soils by Rollins et al. (1998a) and Ohta and Goto (1978), respectively.

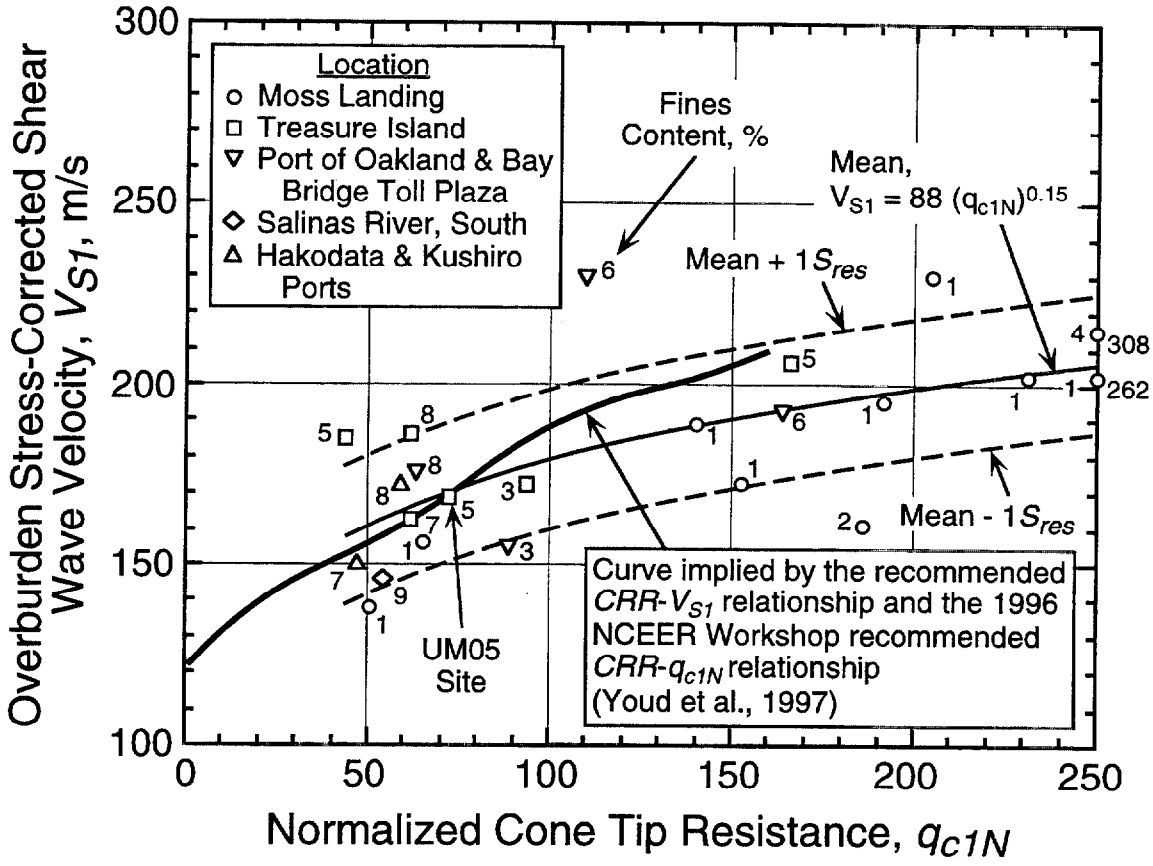

Fig. 4.14 - Relationships Between q_{c1N} and V_{S1} for Clean Sands Implied by the Recommended CRR-V_{S1} Relationship and the 1996 NCEER Workshop Recommended CRR-q_{c1N} Relationship (Youd et al., 1997) with Field Data for Sands with Less than 10 % Fines.

Figures 4.15 and 4.16 illustrate a method for estimating the value of C using SPT and CPT test results, respectively. Shown in the figures are the V_{S1}-penetration correlation curves for clean soils and silty soils implied by the recommended CRR-V_{S1} relationship and the 1996 NCEER workshop recommended CRR-penetration relationships (Youd et al., 1997). In the example, the measured values of V_{S1}, $(N_1)_{60}$, q_{c1N}, and fines content are 220 m/s, 8, 55, and 10 %, respectively. The V_{S1}-penetration correlation curves suggest a C value of 0.74 for these conditions.

The method for estimating C described above assumes that the strain level induced during penetration testing is the same strain level causing liquefaction. This may not be true since pore-water pressure buildup to liquefaction can occur at medium strains in several loading cycles (Dobry et al., 1982; Seed et al., 1983).

4.3.3 High Overburden Stress Correction

To adjust cyclic resistance ratios where overburden stresses are much greater than 100 kPa, Seed (1983) developed the correction factor K_σ. This correction is applied by:

$$CRR_1 = CRR\, K_\sigma \tag{4.4}$$

where

CRR_1 = the cyclic resistance ratio at the reference overburden stress (100 kPa).

The original correction factors were derived from isotropically consolidated cyclic triaxial compression test results. They decreased almost linearly with effective overburden pressure from a value of 1.0 at 100 kPa to values ranging from 0.4 to 0.65 at 800 kPa. Modifications to these factors have been suggested based on subsequent analyses of additional cyclic triaxial and constant-volume cyclic simple shear tests (Vaid et al., 1985; Seed and Harder, 1990; Pillai and Byrne, 1994; Vaid and Thomas, 1995; Arango, 1996), as shown in Fig. 4.17. Figure 4.18 presents the relationship of minimal values of K_σ recommended by the 1996 NCEER workshop (Youd et al., 1997; Harder and Boulanger, 1997) for both sands and gravels.

Hynes and Olsen (1998) compiled and examined a database of about 150 K_σ values for gravels, sands and silt-sand mixtures at densities ranging from very loose to very dense. The database consisted of both undisturbed and reconstituted specimens. The reconstituted specimens were pluviated through air, pluviated through water, and constructed in layers by moist tamping or vibration. Hynes and Olsen compared the laboratory estimates of CRR at one

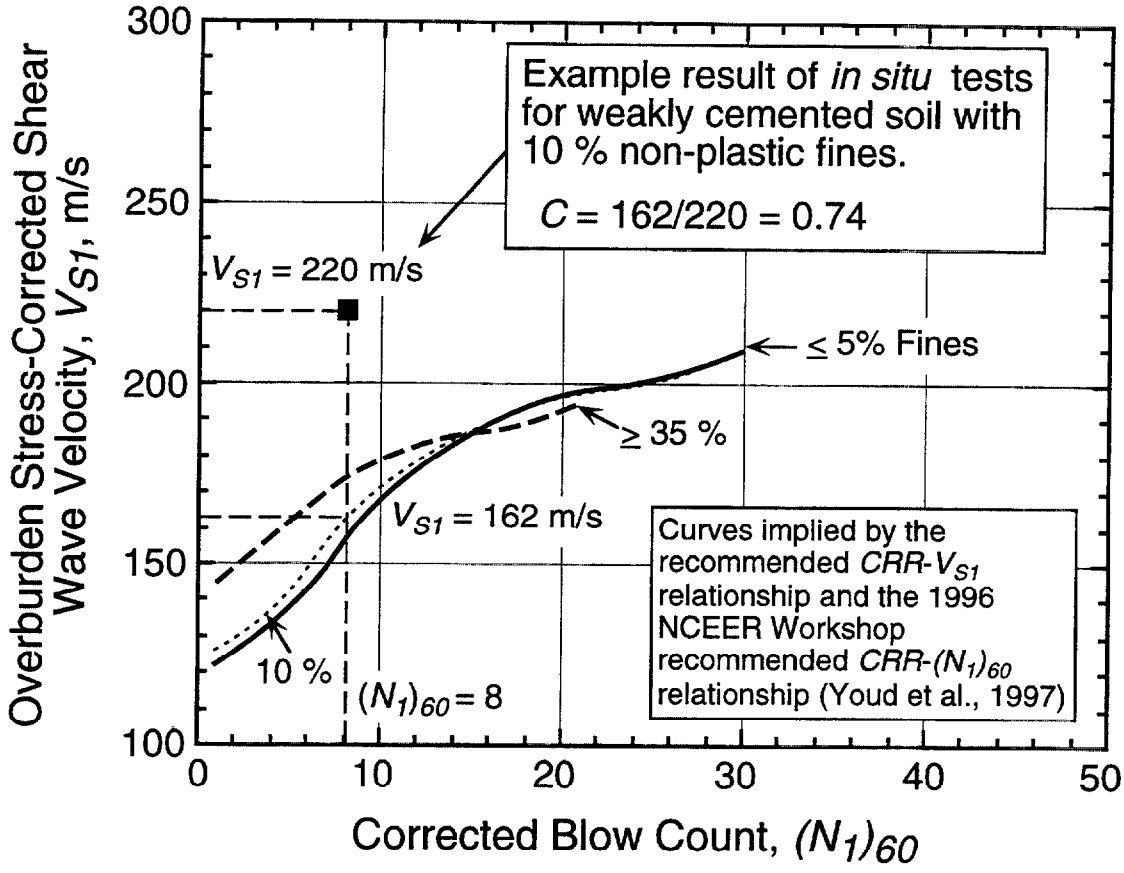

Fig. 4.15 - Relationships Between $(N_1)_{60}$ and V_{S1} Implied by the Recommended CRR-V_{S1} Relationship and the 1996 NCEER Workshop Recommended CRR-$(N_1)_{60}$ Relationship (Youd et al., 1997) with an Example for Determining the Correction Factor C at a Weakly Cemented Soil Site.

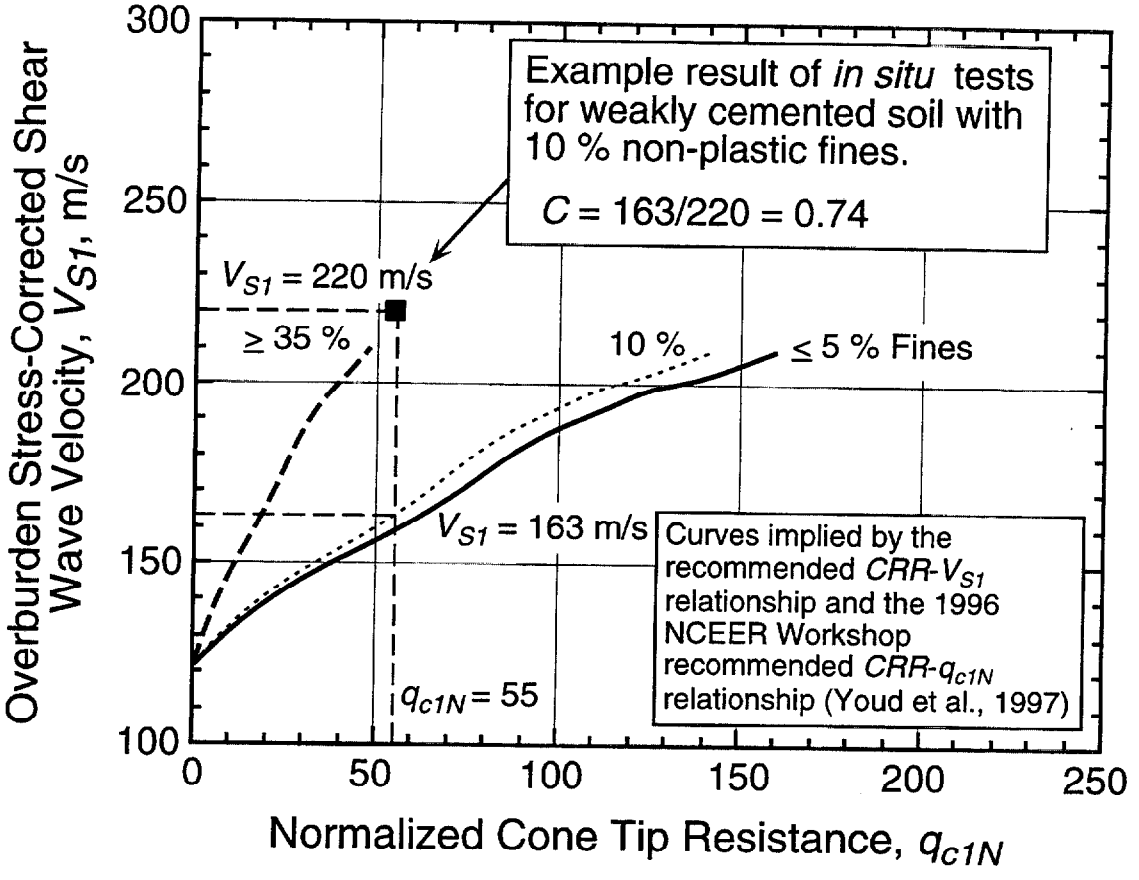

Fig. 4.16 - Relationships Between q_{c1N} and V_{S1} Implied by the Recommended $CRR\text{-}V_S$ Relationship and the 1996 NCEER Workshop Recommended $CRR\text{-}q_{c1N}$ Relationship (Youd et al., 1997) with an Example for Determining the Correction Factor C at a Weakly Cemented Soil Site.

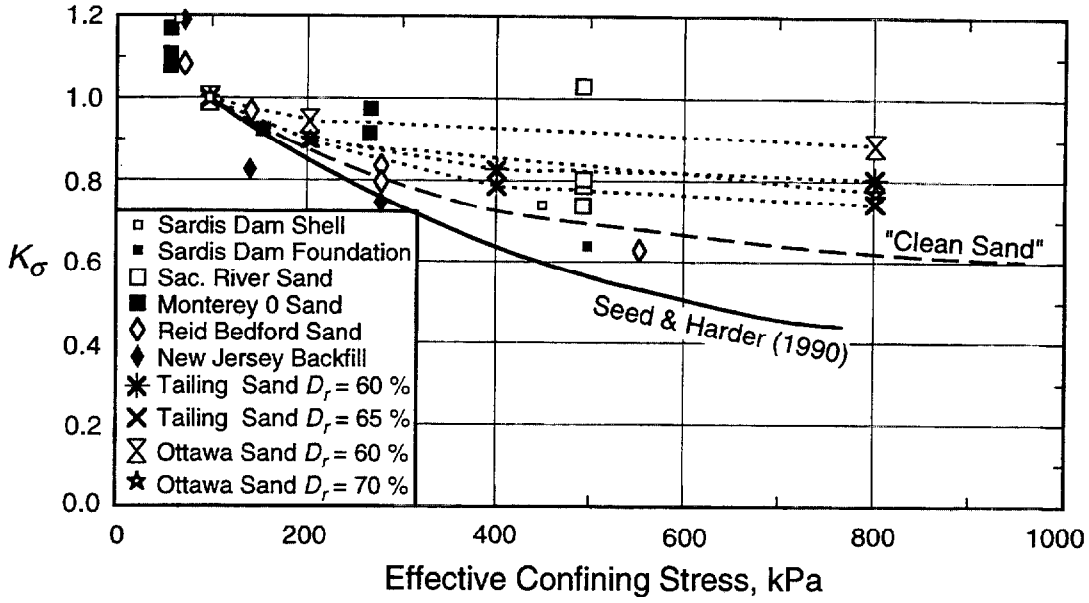

Fig. 4.17 - Values of K_σ Determined by Various Investigators (after Harder and Boulanger, 1997).

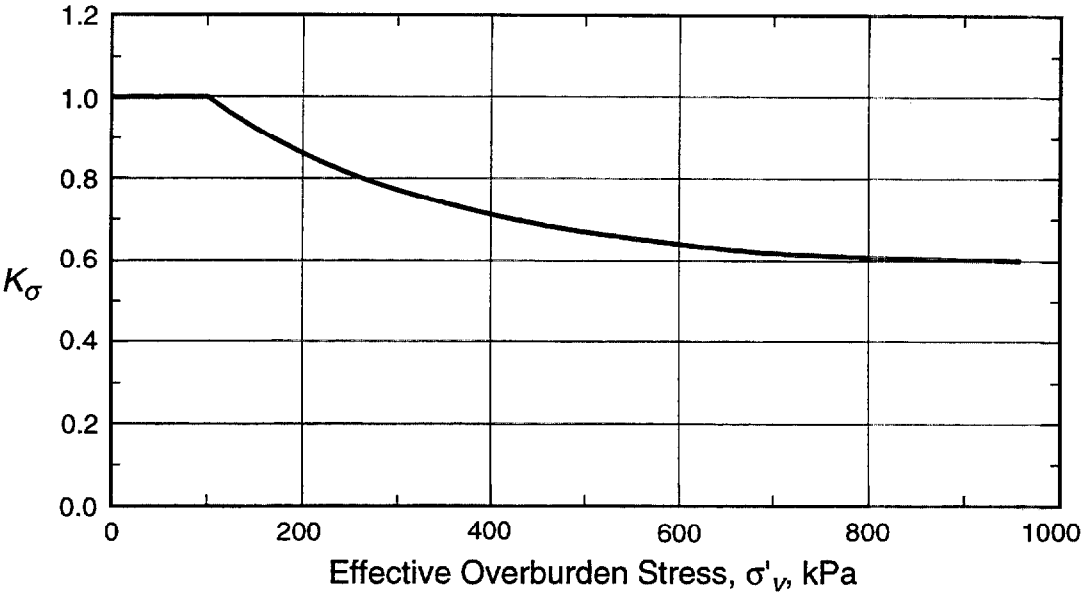

Fig. 4.18 - Minimum Values of K_σ Recommended by the 1996 NCEER Workshop (after Youd et al., 1997; Harder and Boulanger, 1997).

atmosphere, about 100 kPa, with CRR_7 from penetration tests in the field. They concluded that method of deposition, aging, stress history and density strongly influence K_σ. For practical liquefaction evaluation, Hynes and Olsen recommend K_σ be computed as (modified for σ'_v in kPa):

$$K_\sigma = \left(\frac{\sigma'_v}{100}\right)^{f-1} \tag{4.5}$$

where

$f = 0.8$	for loose soils,	(4.6a)
$f = 0.7$	for moderately dense soils, and	(4.6b)
$f = 0.6$	for dense or slightly overconsolidated soils.	(4.6c)

For very dense or highly overconsolidated soils, the value of f may be less than 0.6. Figure 4.19 presents the curves defined by Eqs. 4.5 and 4.6 along with the data reported by Hynes and Olsen. The K_σ recommendations from this study were adopted at the August 1998 MCEER workshop.

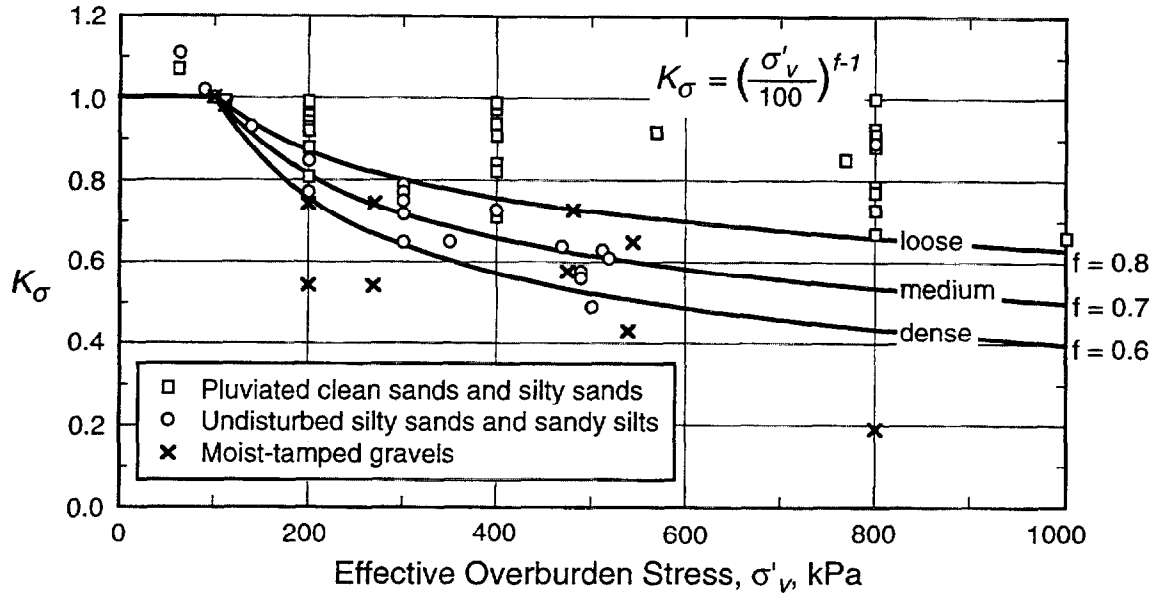

Fig. 4.19 - Recommended Values of K_σ Adopted by the 1998 MCEER Workshop (after Hynes and Olsen, 1998).

CHAPTER 5

APPLICATION OF THE PROCEDURE FOR EVALUATING LIQUEFACTION RESISTANCE

5.1 PROCEDURE SUMMARY

The procedure for evaluating liquefaction resistance outlined in the previous chapters is summarized in the following steps:

1. From available subsurface data, develop detailed profiles of shear wave velocity, soil type, fines content (particles less than 75 μm), and, if possible, soil density and penetration resistance.

2. Identify the depth of the ground water table, noting any seasonal fluctuations and artesian pressures.

3. Calculate the total and effective overburden stresses for each measurement depth at which seismic testing has been performed.

4. Correct the shear wave velocity measurements to the reference overburden stress of 100 kPa, as shown in Eq. 3.2.

5. Determine the limiting upper value of overburden stress-corrected shear wave velocity for liquefaction occurrence, V_{S1}^*, for each measurement depth using Eq. 4.1. If the fines content is unknown, assume 215 m/s for V_{S1}^*.

6. Determine the value of the correction factor C. The value of C can be assumed equal to 1, if the soil to be evaluated is uncemented, less than 10 000 years old, and lies below the ground water table when the seismic tests were conducted. If the soil is cemented, more than 10 000 years, or lies above the water table, the value of C may be estimated by the method described in Section 4.3.2. If the soil conditions are unknown and penetration data are not available, assume 0.6 for C.

7. Determine the design earthquake magnitude and the expected peak horizontal ground surface acceleration.

8. For each measurement depth below the water table, calculate the cyclic stress ratio, as shown in Eq. 3.1. The stress reduction coefficient is estimated using Fig. 2.1.

9. Plot values of V_{S1} and CSR, and the appropriate liquefaction resistance curves using Eqs. 2.13 and 4.3 with a = 0.022, b = 2.8, and n = -2.56. If the effective overburden stress is greater than 100 kPa, correct curves using Eqs. 4.5 and 4.6. Liquefaction is predicted at the site if the data points plot to the left of the respective liquefaction resistance curve. No liquefaction is predicted if the data points plot to the right of the respective curve.

A common way to quantify the potential or hazard for liquefaction is in terms of a factor of safety. The factor of safety, FS, against liquefaction can be defined by:

$$FS = \frac{CRR}{CSR} \tag{5.1}$$

Liquefaction is predicted to occur when FS is less than 1. When FS is greater than 1, liquefaction is predicted not to occur. The acceptable value of FS will depend on several factors including: (1) the acceptable level of risk for the project, (2) the extent and accuracy of seismic measurements, (3) the availability of other site information, and (4) the conservatism in determining the design earthquake magnitude and the expected peak ground acceleration.

Thus, the following step may be added to the nine-step procedure give above--

10. Calculate the value of FS for each measurement depth using Eq. 5.1.

5.2 CASE STUDIES

To illustrate the application of the procedure, two sites shaken by the 1989 Loma Prieta, California, earthquake (M_w = 7) are considered below. The two sites are Treasure Island Fire Station and Marina District School. These sites are discussed earlier to illustrate how values of V_{S1} and CSR are determined (see Section 3.2).

5.2.1 Treasure Island Fire Station

Figures 5.1 and 5.2 present the liquefaction evaluation for the 1989 earthquake and the crosshole test array B1-B4 at the Treasure Island Fire Station site. As discussed in Section 3.2, values of V_{S1} and *CSR* are calculated assuming densities of 1.76 Mg/m^3 above the water table and 1.92 Mg/m^3 below the water table. The geometric mean of the two peak values observed in the horizontal ground surface acceleration records for the fire station and the 1989 earthquake is 0.13 g. Profiles of soil type and fines content shown in Fig. 5.1 are based on information provided by de Alba et al. (1994) and de Alba and Faris (1996). The value of *C* is 1, since the soil to be evaluated at this site is uncemented, less than 10 000 years old, and lies below the ground water table.

For the measurement depth of 4.6 m, V_{S1} is 158 m/s and *CSR* is 0.131 (see calculations given in Eqs. 3.1 and 3.2). The average fines content is about 24 % (de Alba and Faris, 1996). The values of V_{S1}^*, *CRR*, and *FS* are calculated by:

$$V_{S1}^* = 215 - 0.5(FC-5) = 215 - 0.5(24-5) = 206 \text{ m/s} \tag{5.2}$$

and

$$\begin{aligned} CRR &= \left\{ a\left(\frac{CV_{S1}}{100}\right)^2 + b\left(\frac{1}{V_{S1}^* - CV_{S1}} - \frac{1}{V_{S1}^*}\right)\right\} MSF \\ &= \left\{ 0.022\left(\frac{158}{100}\right)^2 + 2.8\left(\frac{1}{206-158} - \frac{1}{206}\right)\right\}\left(\frac{7}{7.5}\right)^{-2.56} \\ &= 0.119 \end{aligned} \tag{5.3}$$

and

$$FS = \frac{CRR}{CSR} = \frac{0.119}{0.131} = 0.91 \tag{5.4}$$

Since the value of *FS* is less than 1, liquefaction is predicted.

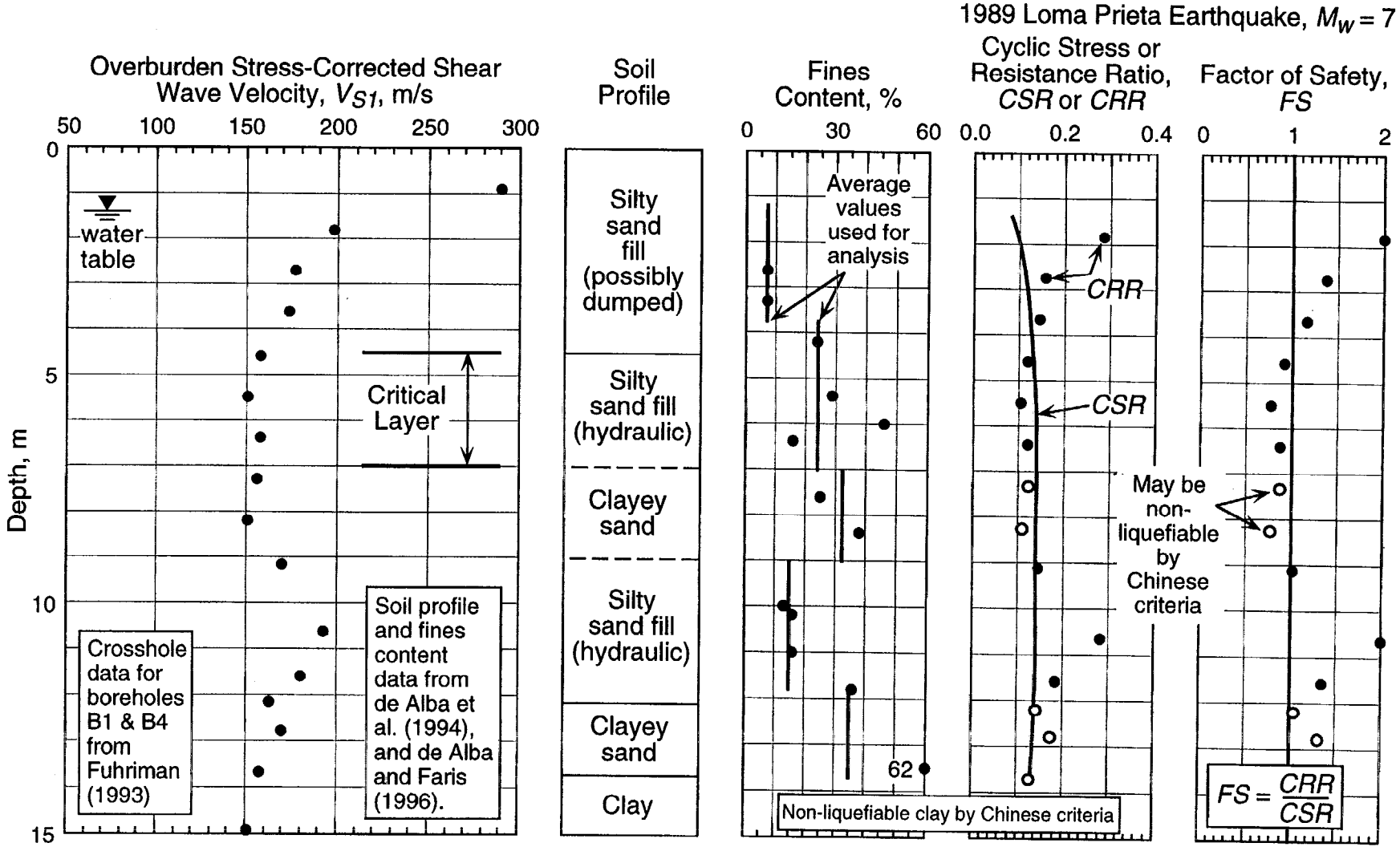

Fig. 5.1 - Application of the Recommended Procedure to the Treasure Island Fire Sation Site, Crosshole Test Array B1-B4 (Depth of 1.5 m to 14 m).

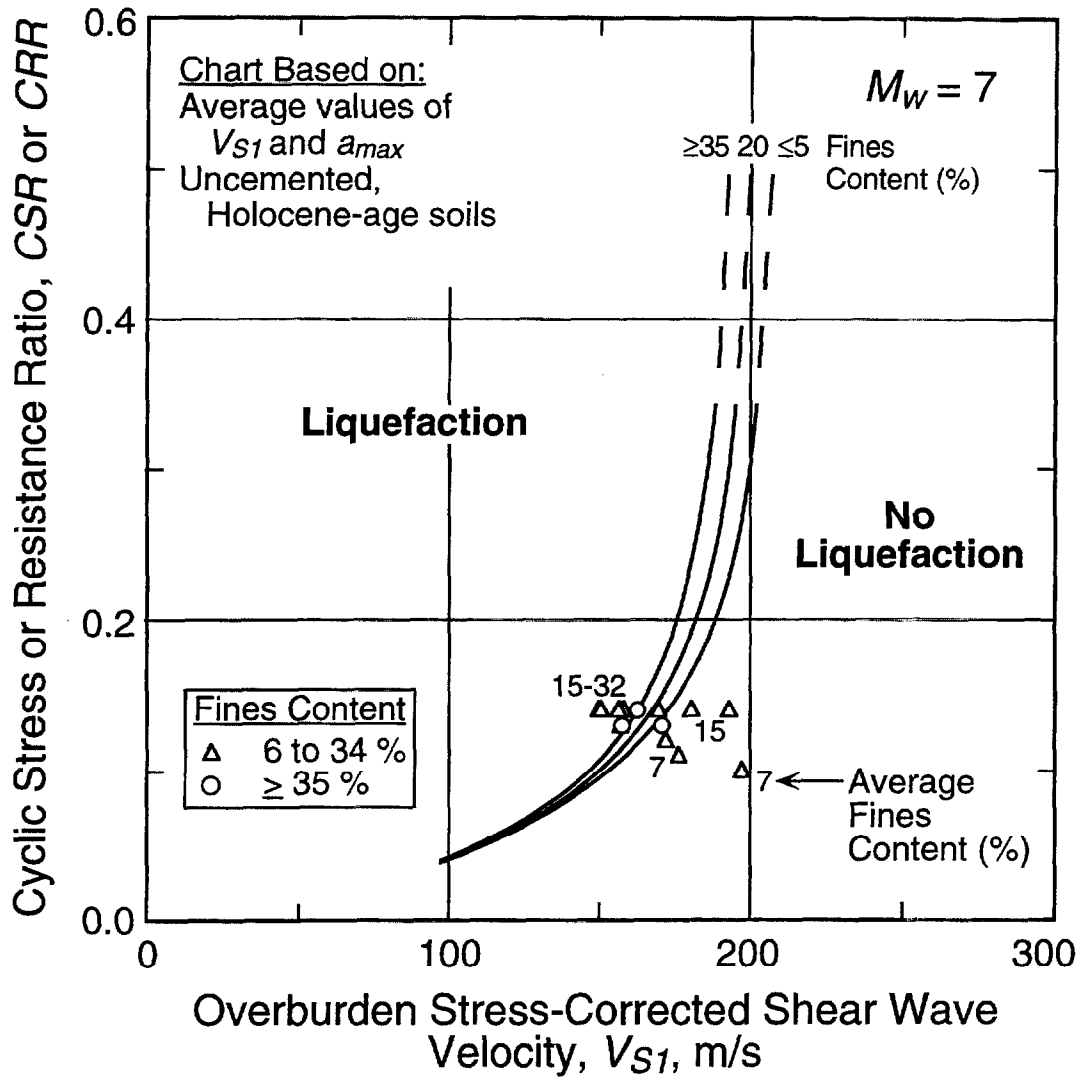

Fig. 5.2 - Recommended Liquefaction Assessment Chart for Magnitude 7 Earthquakes with Data for the 1989 Loma Prieta Earthquake and the Treasure Island Fire Station Site, Crosshole Test Array B1-B4 (Depths of 1.5 m to 14 m). Since no Surface Manifestations of Liquefaction Occurred at the Site During the Earthquake, the Data Shown are for a Non-liquefaction Case History.

Figure 5.1 shows the values of V_{S1}, *CSR*, *CRR*, and *FS* for crosshole test array B1-B4 at the measurement depths below the water table. Values of *FS* are less than 1 for the depths of 4 m to about 9 m. Between the depths of 4 m and 7 m, the sand contains non-plastic fines and is considered liquefiable by the Chinese criteria (see Section 1.1). Between the depths of 7 m and 9 m, the soil exhibits plastic characteristics and may be non-liquefiable by the Chinese criteria. Thus, the plotted values of *CRR* and *FS* for this clayey sand layer are shown as open circles. The layer most likely to liquefy, or the critical layer, lies between the depths of 4 m and 7 m.

Figures 5.3 and 5.4 present the liquefaction evaluation for the SASW test array. Locations of V_S measurements for the SASW test array are assumed at the center of the layer used in forward modeling of surface wave measurements. Values of *FS* are less than 1 between the depths of about 3.5 m and 11 m. The lowest values of *FS* in the non-plastic soil is 0.75 at a depth of 5.3 m. This *FS* value is similar to the lowest *FS* value of 0.77 determined from crosshole measurements in the critical layer.

Although no sand boils or ground cracks occurred at the fire station during the 1989 earthquake, the prediction of liquefaction agrees with the conclusion stated in Section 3.2.1 that liquefaction of an underlying sand cause the sudden drop in the acceleration time histories recorded at this site (de Alba et al., 1994). It is possible that the 4 m thick layer capping the site, predicted not to liquefy (see Figs. 5.1 and 5.3), prevented the formation of sand boils at the ground surface (Ishihara, 1985).

5.2.2 Marina District School

Figures 5.5 and 5.6 present the liquefaction evaluation for the Marina District School site and the 1989 Loma Prieta earthquake. Values of V_{S1} and *CSR* are calculated assuming densities of 1.76 Mg/m^3 above the water table and 1.92 Mg/m^3 below the water table, as described in Section 3.2.3. They are plotted in Fig. 5.5 at the depths midway between receiver locations. The profiles of soil type and fines content shown in Fig. 5.5 are based on information provided by Kayen et al. (1990). The upper 7.6 m of soil at the site consists of sand with 1 % to 8 % fines. Since the sand is uncemented, less than 10 000 years old, and lies below the ground water table, the value of *C* is 1.

Calculated values of *FS* are 0.42, 0.90, and 0.51 at the depths of 3 m, 4 m, and 6.7 m. The clean sand is underlain by a silty clay layer, which is non-liquefiable by the Chinese criteria (see Section 1.1). Having the lowest average value of *FS*, the sand fill just below the water table between the depths of 2.7 m and 4.4 m is identified as the critical layer that liquefied. A prediction of liquefaction agrees with the observed field behavior.

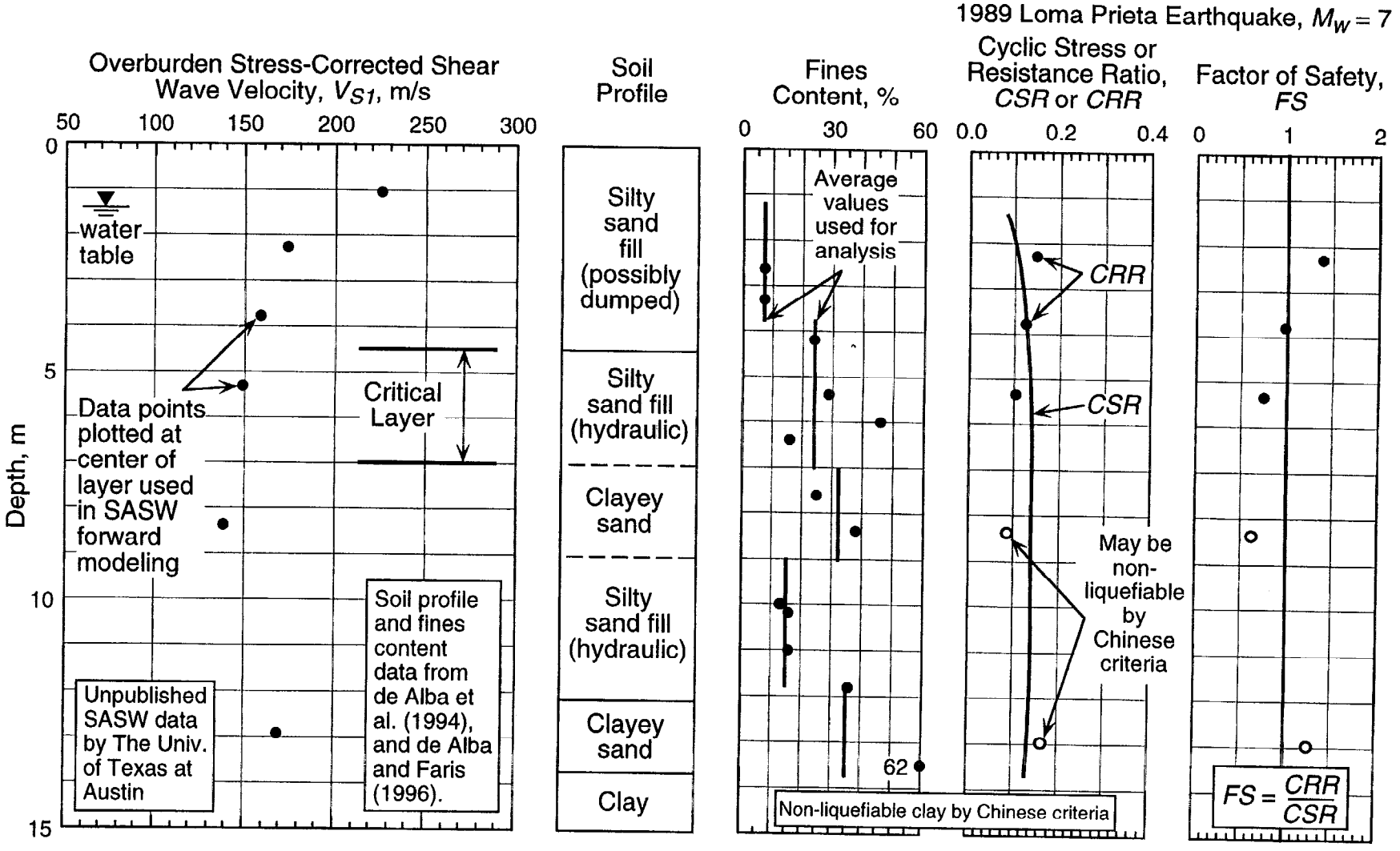

Fig. 5.3 - Application of the Recommended Procedure to the Treasure Island Fire Sation Site, SASW Test Array (Depths of 2 m to 13 m).

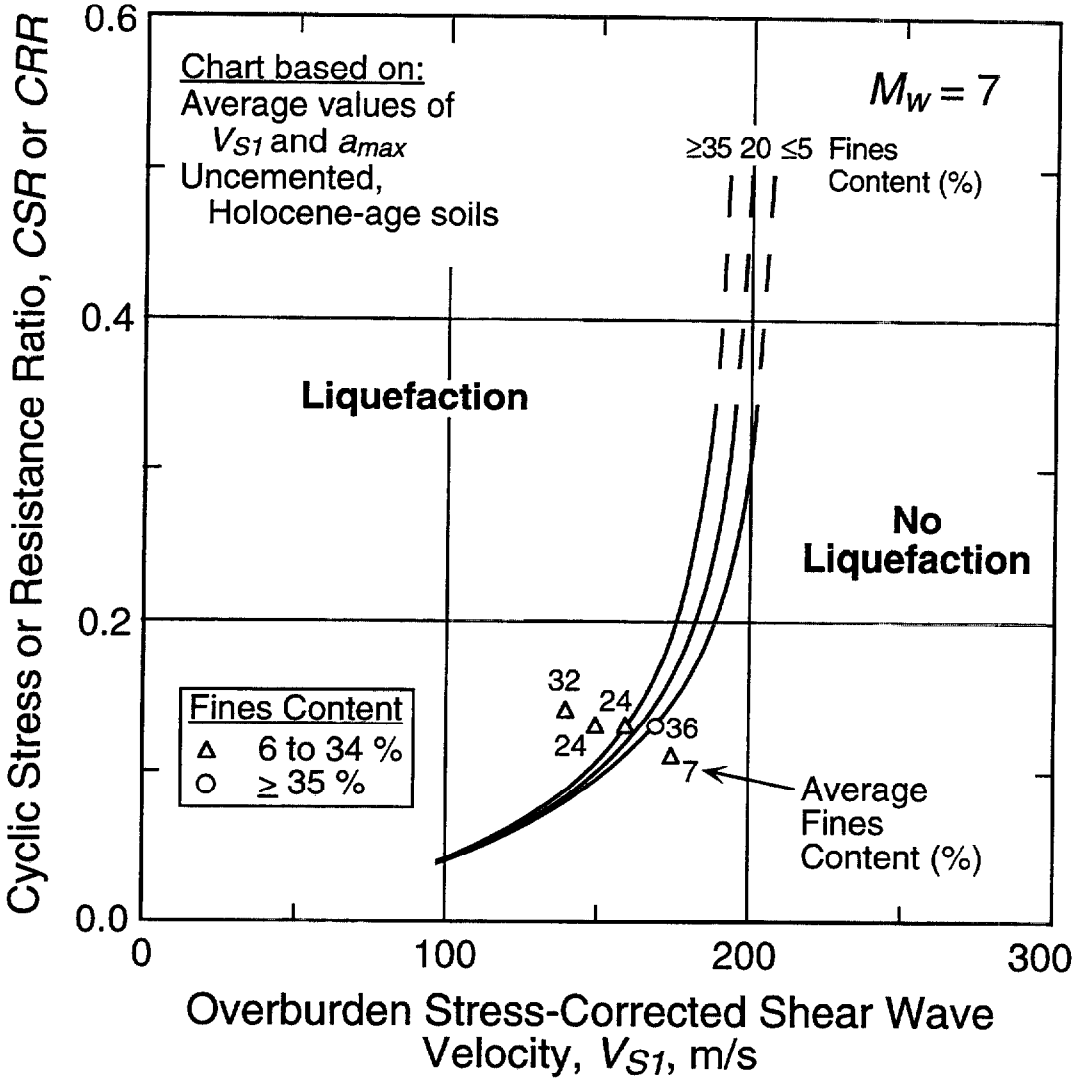

Fig. 5.4 - Recommended Liquefaction Assessment Chart for Magnitude 7 Earthquakes with Data for the 1989 Loma Prieta Earthquake and the Treasure Island Fire Station Site, SASW Test Array (Depths of 2 m to 13 m). Since no Surface Manifestations of Liquefaction Occurred at the Site During the Earthquake, the Data Shown are for a Non-liquefaction Case History.

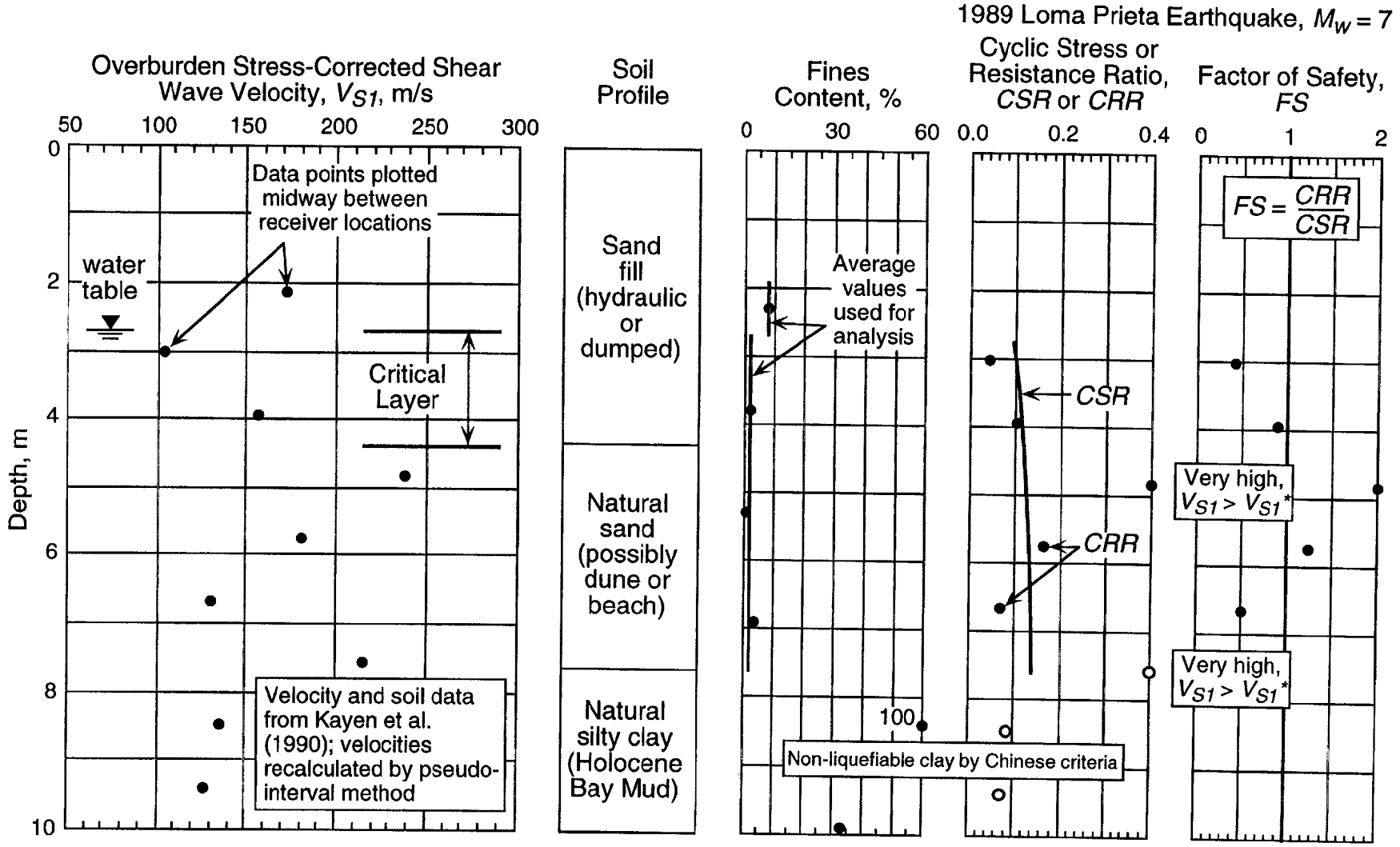

Fig. 5.5 - Application of the Recommended Procedure to the Marina District School Site (Depths of 3 m to 10 m).

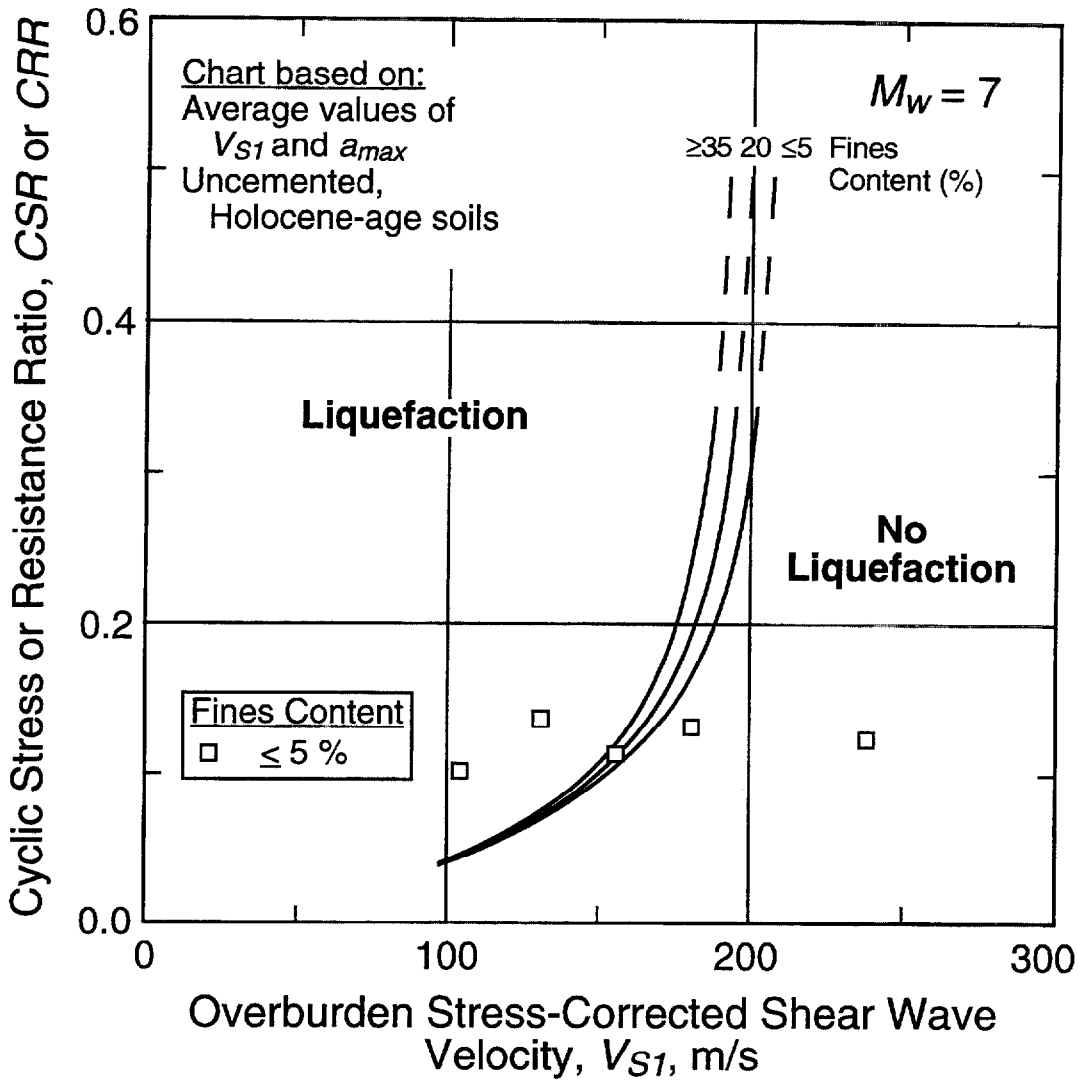

Fig. 5.6 - Recommended Liquefaction Assessment Chart for Magnitude 7 Earthquakes with Data for the 1989 Loma Prieta Earthquake and the Marina District School Site (Depths of 3 m to 7 m). Since Surface Manifestations of Liquefaction Occurred Near the Site During the Earthquake, the Data Shown are for a Liquefaction Case History.

CHAPTER 6

SUMMARY AND RECOMMENDATIONS

6.1 SUMMARY

Presented in this report are draft guidelines for evaluating liquefaction resistance through shear wave velocity, V_S, measurements. The guidelines were written in cooperation with industry, researchers and practitioners, and evolved from workshops held in 1996 and 1998. They include the development of a recommended procedure and guidance for its use.

The recommended procedure follows the general format of the simplified penetration-based procedure originally proposed by Seed and Idriss (1971). Cyclic stress ratios, *CSR*, are calculated using Eq. 2.1, with the average stress reduction coefficient estimated from Fig. 2.1. V_S measurements are corrected for overburden stress using Eq. 2.7. The ten main steps for applying the recommended procedure are summarized in Section 5.1.

Liquefaction resistance curves are based on a modified relationship between overburden stress-corrected shear wave velocity, V_{S1}, and cyclic stress ratio for constant average cyclic shear strain suggested by R. Dobry (personal communication to R. D. Andrus, 1996). The quadratic relationship proposed by Dobry is modified so that it is asymptotic to some limiting upper value of V_{S1}. This limit is related to the tendency of dense granular soils to exhibit dilative behavior at large strains, as well as the fact that dense soils expel dramatically less water during reconsolidation than loose soils. The modified relationship is given by Eq. 2.21. To determine the unknown parameters of Eq. 2.21, liquefaction and non-liquefaction case histories from 26 earthquakes and more than 70 measurement sites in soils ranging from clean fine sand to sandy gravel with cobbles to profiles including silty clay layers are analyzed. Penetration-V_S correlations are also considered.

Figures 4.1 through 4.6 present the recommended evaluation curves for uncemented, Holocene-age soils and different earthquake magnitudes. These curves are defined by Eqs. 2.13 and 2.21 with a = 0.022, b = 2.8, V_{S1}^* = 200 m/s to 215 m/s (depending on fines content), and n = -2.56. These values were selected such that the evaluation curves bounded over 95 %

of the case histories where liquefaction occurred. By constructing relationships between V_{S1} and penetration resistance from the recommended evaluation curves and plotting available *in situ* test data, it was shown that the V_{S1}-based evaluation curves are generally more conservative than the penetration-based evaluation curves. Corrections are suggested for cemented and aged soils, as well as high overburden stress conditions, in Sections 4.3.2 and 4.3.3.

Caution should be exercised when applying the procedure to sites where conditions are different from the database. The case history data are limited to relatively level ground sites with the following general characteristics: (1) uncemented soils of Holocene age; (2) average depths less than about 10 m; and (3) ground water table depths between 0.5 m and 6 m. All V_S measurements are from below the water table. About three-quarters of the case history data are for soils with fines content greater than 5 %. Almost half of the case histories are for earthquakes with magnitudes near 7.

Three concerns when using shear wave velocity as an indicator of liquefaction resistance are (1) its higher sensitivity (when compared with the penetration-based methods) to weak interparticle bonding, (2) the lack of a physical sample for identifying non-liquefiable clayey soils, and (3) not detecting thin liquefiable strata because the test interval is too large. The preferred practice is to drill sufficient boreholes and conduct sufficient other *in situ* tests to detect thin liquefiable strata, to identify non-liquefiable clay-rich soils, to identify silty soils above the ground water table that might have lower values of V_S should the water table rise, and to detect liquefiable weakly cemented soils.

6.2 FUTURE STUDIES

The following future studies are recommended:

1. Additional well-documented case histories with all types of soil that have and have not liquefied during earthquakes should be compiled, particularly from deeper deposits (depth > 8 m) and from denser soils (V_S > 200 m/s) shaken by stronger ground motions (a_{max} > 0.4 g), to further validate the recommended curves. Also, case histories from lower magnitude earthquakes (M_w < 7) may improve estimates of the magnitude scaling factor.

2. Laboratory and field studies should be conducted to further refine estimates of V_{S1}^*, the limiting value of V_{S1} for liquefaction occurrence. For example, careful laboratory studies may identify more clearly the influence of fines content and particle size on V_{S1}^*. Additional careful penetration-V_S correlation studies may also help refine the V_{S1}^* estimates.

3. Laboratory studies should also be conducted to evaluate the implied assumption observed in Fig. 4.9 that at low values of V_{S1} (say 100 m/s) liquefaction resistance is independent of fines content.

4. Additional work is needed to evaluate the significance of ignoring soil type and horizontal stress in the overburden correction.

5. Standard test procedures exist only for the crosshole test. Standard test methods should be developed for the other *in situ* seismic tests.

REFERENCES

Abdel-Haq, A., and Hryciw, R. D. (1998). "Ground Settlement in Simi Valley Following the Northridge Earthquake," *Journal of Geotechnical and Geoenvironmental Engineering*, ASCE, Vol. 124, No. 1, pp. 80-89.

Ambraseys, N. N. (1988). "Engineering Seismology," *Earthquake Engineering and Structural Dynamics*, Vol. 17, p. 1-105.

American Society of Testing and Materials, ASTM, D-4428M-91. "Standard Test Methods for Crosshole Seismic Testing," *Annual Book of ASTM Standards*, Vol. 4.08.

Andrus, R. D. (1994). "In Situ Characterization of Gravelly Soils That Liquefied in the 1983 Borah Peak Earthquake," *Ph.D. Dissertation*, The University of Texas at Austin, 533 p.

Andrus, R. D., and Stokoe, K. H., II (1997). "Liquefaction Resistance Based on Shear Wave Velocity," *NCEER Workshop on Evaluation of Liquefaction Resistance of Soils*, Technical Report NCEER-97-0022, T. L. Youd and I. M. Idriss, Eds., held 4-5 January 1996, Salt Lake City, UT, National Center for Earthquake Engineering Research, Buffalo, NY, pp. 89-128.

Andrus, R. D., Stokoe, K. H., II, Bay, J. A., and Chung, R. M. (1998a). "Delineation of Densified Sand at Treasure Island by SASW Testing," *Geotechnical Site Characterization*, P. K. Robertson and P. W. Mayne, Eds., A. A. Balkema, Rotterdam, Netherlands, pp. 459-464.

Andrus, R. D., Stokoe, K. H., II, Chung, R. M., and Bay, J. A. (1998b). "Liquefaction Evaluation of Densified Sand at Approach to Pier 1 on Treasure Island, California, Using SASW Method," *NISTIR 6230*, National Institute of Standards and Technology, Gaithersburg, MD, 75 p.

Andrus, R. D., Stokoe, K. H., II, Bay, J. A., and Youd, T. L. (1992). "In Situ V_S of Gravelly Soils Which Liquefied," *Proceedings, Tenth World Conference on Earthquake Engineering*, held 19-24 July 1992, Mardrid, Spain, A. A. Balkema, Rotterdam, Netherlands, pp. 1447-1452.

Andrus, R. D., and Youd, T. L. (1987). "Subsurface Investigation of a Liquefaction-Induced Lateral Spread, Thousand Springs Valley, Idaho," *Geotechnical Laboratory Miscellaneous Paper GL-87-8*, U.S. Army Engineer Waterways Experiment Station, Vicksburg, MS, 131 p.

Arango, I. (1996). "Magnitude Scaling Factors for Soil Liquefaction Evaluations," *Journal of Geotechnical Engineering*, ASCE, Vol. 122, No. 11, pp. 929-936.

Arulanandan, K., Yogachandran, C., Meegoda, N. J., Ying, L., and Zhauji, S. (1986). "Comparison of the SPT, CPT, SV and Electrical Methods of Evaluating Earthquake Induced Liquefaction Susceptibility in Ying Kou City During the Haicheng Earthquake," *Use of In Situ Tests in Geotechnical Engineering*, Geotechnical Special Publication No. 6, S. P. Clemence, Ed., ASCE, pp. 389-415.

Barrow, B. L. (1983). "Field Investigation of Liquefaction Sites in Northern California," *Geotechnical Engineering Thesis GT83-1*, The University of Texas at Austin, 213 p.

Bennett, M. J., Youd, T. L., Harp, E. L., and Wieczorek, G. F. (1981). "Subsurface Investigation of Liquefaction, Imperial Valley Earthquake, California, October 15, 1979," *Open-File Report 81-502*, U.S. Geological Survey, Menlo Park, CA, 83 p.

Bennett, M. J., McLaughlin, P. V., Sarmiento, J. S., and Youd, T. L. (1984). "Geotechnical Investigation of Liquefaction Sites, Imperial Valley, California," *Open-File Report 84-252*, U.S. Geological Survey, Menlo Park, CA, 103 p.

Bennett, M. J., and Tinsley, J. C. (1995). "Geotechnical Data from Surface and Subsurface Samples Outside of and within Liquefaction-Related Ground Failures Caused by the October 17, 1989, Loma Prieta Earthquake, Santa Cruz and Monterey Counties, California," *Open-File Report 95-663*, U.S. Geological Survey, Menlo Park, CA.

Bierschwale, J. G., and Stokoe, K. H., II (1984). "Analytical Evaluation of Liquefaction Potential of Sands Subjected to the 1981 Westmorland Earthquake," *Geotechnical Engineering Report GR-84-15*, The University of Texas at Austin, 231 p.

Boulanger, R. W., Idriss, I. M., and Mejia, L. H. (1995). "Investigation and Evaluation of Liquefaction Related Ground Displacements at Moss Landing During the 1989 Loma Prieta Earthquake," *Report No. UCD/CGM-95/02*, University of California at Davis.

Boulanger, R. W., Mejia, L. H., and Idriss, I. M. (1997). "Liquefaction at Moss Landing During Loma Prieta Earthquake," *Journal of Geotechnical and Geoenviromental Engineering*, ASCE, Vol. 123, No. 5, pp. 453-467.

Brady, A. G., and Shakal, A. F. (1994). "Strong-Motion Recordings," *The Loma Prieta, California, Earthquake of October 17, 1989--Strong Ground Motion*, U.S. Geological Survey Professional Paper 1551-A, R. D. Borcherdt, Ed., U.S. Gov. Printing Office, Washington, D.C., pp. A9-A38.

de Alba, P., Baldwin, K., Janoo, V., Roe, G., and Celikkol, B. (1984). "Elastic-Wave Velocities and Liquefaction Potential," *Geotechnical Testing Journal*, ASTM, Vol. 7, No. 2, pp. 77-87.

de Alba, P., Benoît, J., Pass, D. G., Carter, J. J., Youd, T. L., and Shakal, A. F. (1994). "Deep Instrumentation Array at the Treasure Island Naval Station," *The Loma Prieta, California, Earthquake of October 17, 1989--Strong Ground Motion*, U.S. Geological Survey Professional Paper 1551-A, R. D. Borcherdt, Ed., U.S. Gov. Printing Office, Washington, D.C., pp. A155-A168.

de Alba, P., and Faris, J. R. (1996). "Workshop on Future Research Deep Instrumentation Array, Treasure Island NGES, July 27, 1996: Report to the Workshop Current State of Site Characterization and Instrumentation," University of New Hampshire at Durham, 45 p.

Dobry, R. (1989). "Some Basic Aspects of Soil Liquefaction during Earthquakes," *Earthquake Hazards and the Design of Constructed Facilities in the Eastern United States*, K. H. Jacob and C. J. Turkstra, Eds., New York Academy of Sciences, Vol. 558, pp. 172-182.

Dobry, R., and Ladd, R. S. (1980). Discussion to "Soil Liquefaction and Cyclic Mobility Evaluation for Level Ground During Earthquakes," by. H. B. Seed and "Liquefaction Potential: Science versus Practice," by R. B. Peck, *Journal of the Geotechnical Engineering Division*, ASCE, Vol. 106, GT. 6, pp. 720-724.

Dobry, R., Ladd, R. S., Yokel, F. Y., Chung, R. M., Powell, D. (1982). "Prediction of Pore Water Pressure Buildup and Liquefaction of Sands During Earthquakes by the Cyclic Strain Method," *NBS Building Science Series 138*, National Bureau of Standards, Gaithersburg, MD, 152 p.

Dobry, R., Stokoe, K. H., II, Ladd, R. S., and Youd, T. L. (1981). "Liquefaction Susceptibility from S-Wave Velocity," *Proceedings, In Situ Tests to Evaluate Liquefaction Susceptibility*, ASCE National Convention, held 27 October 1981, St. Louis, MO.

Dobry, R., Baziar, M. H., O'Rourke, T. D., Roth, B. L., and Youd, T. L. (1992). "Liquefaction and Ground Failure in the Imperial Valley, Southern California During the 1979, 1981 and 1987 Earthquakes," *Case Studies of Liquefaction and Lifeline Performance During Past Earthquakes*, Technical Report NCEER-92-0002, T. O'Rourke and M. Hamada, Eds., National Center for Earthquake Engineering Research, Buffalo, NY, Vol. 2.

Drnevich, V. P., and Richart, F. E., Jr. (1970). "Dynamic Prestraining of Dry Sand," *Journal of the Soil Mechanics and Foundations Division*, ASCE, Vol. 96, No. SM2, pp. 453-469.

EPRI (1992). *Lotung Large-Scale Seismic Test Strong Motion Records,* EPRI NP-7496L, Electric Power Research Institute, Palo Alto, CA, Vols. 1-7.

Finn, W. D. L., and Bhatia, S. K. (1981). "Prediction of Seismic Pore-water Pressures," *Proceedings, Tenth International Conference on Soil Mechanics and Foundation Engineering*, Vol. 3, A. A. Balkema Publishers, Rotterdam, Netherlands, pp. 201-206.

Frankel, A., Mueller, C., Barnhard, T., Perkins, D., Leyendecker, E., Dickman, N., Hanson, S., and Hopper, M. (1996). "National Seismic-Hazard Maps: Documentation," *Open-File Report 96-532*, U.S. Geological Survey, Denver, CO, 110 p.

Frankel, A., Mueller, C., Barnhard, T., Perkins, D., Leyendecker, E., Dickman, N., Hanson, S., and Hopper, M. (1997). "Seismic-Hazard Maps for the Contiguous United States," *Open-File Report 97-131*, U.S. Geological Survey, Denver, CO, 12 maps.

Fuhriman, M. D. (1993). "Crosshole Seismic Tests at Two Northern California Sites Affected by the 1989 Loma Prieta Earthquake," *M.S. Thesis*, The University of Texas at Austin, 516 p.

Geomatrix Consultants (1990). "Results of Field Exploration and Laboratory Testing Program for Perimeter Dike Stability Evaluation Naval Station Treasure Island San Francisco, California," Project No. 1539.05, report prepared for U.S. Navy, Naval Facilities Engineering Command, Western Division, San Bruno, CA, Vol. 2.

Gibbs, J. F., Fumal, T. E., Boore, D. M., and Joyner, W. B. (1992). "Seismic Velocities and Geologic Logs from Borehole Measurements at Seven Strong-Motion Stations that Recorded the Loma Prieta Earthquake," *Open-File Report 92-287*, U.S. Geological Survey, Menlo Park, CA, 139 p.

Golesorkhi, R. (1989). "Factors Influencing the Computational Determination of Earthquake-Induced Shear Stresses in Sandy Soils," *Ph.D. Dissertation*, University of California at Berkeley, 369 p.

Hanshin Expressway Public Corporation (1998). "The Hanshin Expressway Geological Database, Volume for Seismic Damage Reconstruction of Route No. 3, the Kobe Line, and Route No. 5, the Harbor Line," 224 p. (in Japanese).

Hamada, M., Isoyama, R., and Wakamatsu, K. (1995). *The 1995 Hyogoken-Nanbu (Kobe) Earthquake: Liquefaction, Ground Displacement and Soil Condition in Hanshin Area*, Waseda University, Tokyo, Japan, 194 p.

Harder, L. F., Jr., and Boulanger, R. (1997). "Application of K_σ and K_α Correction Factors," *NCEER Workshop on Evaluation of Liquefaction Resistance of Soils*, Technical Report NCEER-97-0022, T. L. Youd and I. M. Idriss, Eds., held 4-5 January 1996, Salt Lake City, UT, National Center for Earthquake Engineering Research, Buffalo, NY, pp. 167-190.

Hardin, B. O., and Drnevich, V. P. (1972). "Shear Modulus and Damping in Soils: Design Equations and Curves," *Journal of the Soil Mechanics and Foundations Division*, ASCE, Vol. 98, SM7, pp. 667-692.

Heaton, T. H., Tajima, F., and Mori, A. W. (1982). "Estimating Ground Motions Using Recorded Accelerograms," Report by Dames and Moore to Exxon Production Res. Co., Houston Texas.

Holzer, T. L., Ed. (1998). "Map Showing Locations of Ground-Failures and Damage to Facilities on Treasure Island Attributed to the 1989 Loma Prieta Earthquake," *The Loma Prieta, California Earthquake of October 17, 1989--Liquefaction*, U.S. Geological Survey Professional Paper 1551-B, U.S. Gov. Printing Office, Washington, D.C., B1-B8.

Hryciw, R. D. (1991). "Post Loma Prieta Earthquake CPT, DMT and Shear Wave Velocity Investigations of Liquefaction Sites in Santa Cruz and on Treasure Island," Final Report to the U.S. Geological Survey, Award No. 14-08-0001-G1865, University of Michigan at Ann Arbor, 68 p.

Hryciw, R. D., Rollins, K. M., Homolka, M., Shewbridge, S. E., and McHood, M. (1991). "Soil Amplification at Treasure Island During the Loma Prieta Earthquake," *Proceedings, Second International Conference on Recent Advances in Geotechnical Earthquake Engineering and Soil Dynamics*, S. Prakash, Ed., held 11-15 March 1991, St. Louis, MO, University of Missouri at Rolla, Vol. II, pp. 1679-1685.

Hryciw, R. D., Shewbridge, S. E., Kropp, A., and Homolka, M. (1998). "Postearthquake Investigation at Liquefaction Sites in Santa Cruz and on Treasure Island," *The Loma Prieta, California Earthquake of October 17, 1989--Liquefaction*, U.S. Geological Survey Professional Paper 1551-B, T. L. Holzer, Ed., U.S. Gov. Printing Office, Washington, D.C., pp. B165-B180.

Hynes, M. E. (1988). "Pore Pressure Generation Characteristics of Gravel Under Undrainded Cyclic Loading," *Ph.D. Dissertation*, University of California, Berkeley.

Hynes, M. E., and Olsen, R. S. (1998). "Influence of Confining Stress on Liquefaction Resistance," *Proceedings, International Workshop on the Physics and Mechanics of Soil Liquefaction*, held 10-11 September 1998, Baltimore, MD, A. A. Balkema, Rotterdam, Netherlands.

Iai, S., Morita, T., Kameoka, T., Matsunaga, Y., and Abiko, K. (1995). "Response of a Dense Sand Deposit During 1993 Kushiro-Oki Earthquake," *Soils and Foundations*, Japanese Society of Soil Mechanics and Foundation Engineering, Vol. 35, No. 1, pp. 115-131.

Idriss, I. M. (1990). "Response of Soft Soil Sites During Earthquakes," *H. Bolton Seed Memorial Symposium*, BiTech Publishers, Vancouver, B.C., Vol. 2, pp. 273-289.

Idriss, I. M. (1991). "Earthquake Ground Motions at Soft Soil Sites," *Proceedings, Second International Conference on Recent Advances in Geotechnical Earthquake Engineering and Soil Dynamics*, S. Prakash, Ed., held 11-15 March 1991, St. Louis, MO, University of Missouri at Rolla, Vol. III, pp. 2265-2272.

Idriss, I. M. (1998). "Evaluation of Liquefaction Potential, Consequences and Mitigation--An Update," Presentation notes for Geotechnical Society Meeting, held 17 February 1998, Vancouver, Canada.

Idriss, I. M. (1999). "An Update of the Seed-Idriss Simplified Procedure for Evaluating Liquefaction Potential," Presentation notes for Transportation Research Board Workshop on New Approaches to Liquefaction Analysis, held 10 January 1999, Washington, D.C.

Inatomi, T., Zen, K., Toyama, S., Uwabe, T., Iai, S. Sugano, T., Terauchi, K., Yokota, H., Fujimoto, K., Tanaka, S., Yamazaki, H., Koizumi, T., Nagao, T., Nozu, A., Miyata, M., Ichii, K., Morita, T., Minami, K., Oikawa, K., Matsunaga, Y., Ishii, M., Sugiyama, M., Takasaki, N., Kobayashi, N., and Okashita, K. (1997). "Damage to Port and Port-related Facilities by the 1995 Hyogoken-Nanbu Earthquake," *Technical Note No. 857*, Port and Harbour Research Institute, Yokosuka, Japan, 1762 p.

Ishihara, K. (1985). "Stability of Natural Deposits During Earthquakes," *Proceedings, Eleventh International Conference on Soil Mechanics and Foundation Engineering*, A. A. Balkema Publishers, Rotterdam, Netherlands, pp. 321-376.

Ishihara, K., Shimizu, K., and Yamada, Y. (1981). "Pore Water Pressures Measured in Sand Deposits During an Earthquake," *Soils and Foundations*, Japanese Society of Soil Mechanics and Foundation Engineering, Vol. 21, No. 4, pp. 85-100.

Ishihara, K., Anazawa, Y., and Kuwano, J. (1987). "Pore Water Pressures and Ground Motions Monitored During the 1985 Chiba-Ibaragi Earthquake," *Soils and Foundations*, Japanese Society of Soil Mechanics and Foundation Engineering, Vol. 27, No. 3, pp. 13-30.

Ishihara, K., Muroi, T., and Towhata, I. (1989). "In-situ Pore Water Pressures and Ground Motions During the 1987 Chiba-Toho-Oki Earthquake," *Soils and Foundations*, Japanese Society of Soil Mechanics and Foundation Engineering, Vol. 29, No. 4, pp. 75-90.

Ishihara, K., Karube, T., and Goto, Y. (1997). "Summary of the Degree of Movement of Improved Masado Reclaimed Land," *Proceedings, 24th JSCE Earthquake Engineering Symposium*, Japan Society of Civil Engineering, held 24-26 July 1997, Kobe, Japan, Vol. 1, pp. 461-464 (in Japanese).

Ishihara, K., Kokusho, T., Yasuda, S., Goto, Y., Yoshida, N., Hatanaka, M., and Ito, K. (1998). "Dynamic Properties of Masado Fill in Kobe Port Island Improved through Soil Compaction Method," Summary of Final Report by Geotechnical Research Collaboration Committee on the Hanshin-Awaji Earthquake, Obayashi Corporation, Tokyo, Japan.

Jamiolkowski, M., and Lo Presti, D. C. F. (1990). "Correlation Between Liquefaction Resistance and Shear Wave Velocity," *Soils and Foundations*, Japanese Society of Soil Mechanics and Foundation Engineering, Vol. 32, No. 2, pp. 145-148.

Kayabali, K. (1996). "Soil Liquefaction Evaluation Using Shear Wave Velocity," *Engineering Geology*, Elsevier Publisher, New York, NY, Vol. 44, No. 4, pp. 121-127.

Kayen, R. E., Liu, H. -P., Fumal, T. E., Westerland, R. E., Warrick, R. E., Gibbs, J. F., and Lee, H. J. (1990). "Engineering and Seismic Properties of the Soil Column at Winfield Scott School, San Francisco," *Effects of the Loma Prieta Earthquake on the Marina District San Francisco, California*, Open-file Report 90-253, U.S. Geological Survey, Menlo Park, CA, pp. 112-129.

Kayen, R. E., Mitchell, J. K., Seed, R. B., Lodge, A., Nishio, S., and Coutinho, R. (1992). "Evaluation of SPT-, CPT-, and Shear Wave-Based Methods for Liquefaction Potential Assessment Using Loma Prieta Data," *Proceedings, Fourth Japan-U.S. Workshop on Earthquake Resistant Design of Lifeline Facilities and Countermeasures for Soil Liquefaction*, Technical Report NCEER-92-0019, M. Hamada and T. D. O'Rourke, Eds., held 27-29 May 1992, Honolulu, Hawaii, National Center for Earthquake Engineering Research, Buffalo, NY, Vol. 1, pp. 177-204.

Kimura, M. (1996). "Damage Statistics," *Soils and Foundations, Special Issue on Geotechnical Aspects of the January 17, 1995 Hyogoken-Nambu Earthquake*, Japanese Geotechnical Society, pp. 1-5.

Kokusho, T., Tanaka, Y., Kudo, K., and Kawai, T. (1995a). "Liquefaction Case Study of Volcanic Gravel Layer during 1993 Hokkaido-Nansei-Oki Earthquake," *Third International Conference on Recent Advances in Geotechnical Earthquake Engineering and Soil Dynamics*, S. Prakash, Ed., held 2-7 March 1995, St. Louis, MO, University of Missouri at Rolla, Vol. I, pp. 235-242.

Kokusho, T., Yoshida, Y., and Tanaka, Y. (1995b). "Shear Wave Velocity in Gravelly Soils with Different Particle Gradings," *Static and Dynamic Properties of Gravelly Soils*, Geotechnical Special Publication No. 56, M. D. Evans and R. J. Fragaszy, Eds., ASCE, pp. 92-106.

Kokusho, T., Tanaka, Y., Kawai, T., Kudo, K., Suzuki, K., Tohda, S., and Abe, S. (1995c). "Case Study of Rock Debris Avalanche Gravel Liquefied During 1993 Hokkaido-Nansei-Oki Earthquake," *Soils and Foundations*, Japanese Geotechnical, Vol. 35, No. 3, pp. 83-95.

Lee, N. J. (1993). "Experimental Study of Body Wave Velocities in Sand Under Anisotripic Conditions," *Ph.D. Dissertation*, The University of Texas at Austin, 503 p.

Lee, S. H. (1986). "Investigation of Low-Amplitude Shear Wave Velocity in Anisotripic Material," *Ph.D. Dissertation*, The University of Texas at Austin, 395 p.

Liao, S. S. C., and Whitman, R. V. (1986). "Overburden Correction Factors for SPT in Sands," *Journal of Geotechnical Engineering*, ASCE, Vol. 112, No. 3, pp. 373-377.

Lodge, A. L. (1994). "Shear Wave Velocity Measurements for Subsurface Characterization," *Ph.D. Dissertation*, University of California at Berkeley.

Marcuson, W. F., III, and Bieganousky, W. A. (1977). "SPT and Relative Density in Coarse Sands," *Journal of Geotechnical Engineering Division*, ASCE, Vol. 103, No. 11, pp. 1295-1309.

Martin, G. R., Finn, W. D. L., and Seed, H. B. (1975). "Fundamentals of Liquefaction Under Cyclic Loading," *Journal of the Geotechnical Engineering Division*, ASCE, Vol. 101, No. GT5, pp. 423-483.

Mitchell, J. K., Lodge, A. L., Coutinho, R. Q., Kayen, R. E., Seed, R. B., Nishio, S., and Stokoe, K. H., II (1994). "Insitu Test Results from Four Loma Prieta Earthquake Liquefaction Sites: SPT, CPT, DMT, and Shear Wave Velocity," *Report No. UCB/EERC-94/04*, Earthquake Engineering Research Center, University of California at Berkeley, 171 p.

National Research Council (1985). *Liquefaction of Soils During Earthquakes*, National Academy Press, Washington, D. C., 240 p.

Ohta, Y., and Goto, N. (1978). "Physical Background of the Statistically Obtained S-Wave Velocity Equation in Terms of Soil Indexes," *Butsuri-Tanko (Geophysical Exploration)*, Vol. 31, No. 1, pp. 8-17 (in Japanese; translated by Y. Yamamoto).

Olsen, R. S. (1997). "Cyclic Liquefaction Based on the Cone Penetrometer Test," *NCEER Workshop on Evaluation of Liquefaction Resistance of Soils*, Technical Report NCEER-97-0022, T. L. Youd and I. M. Idriss, Eds., held 4-5 January 1996, Salt Lake City, UT, National Center for Earthquake Engineering Research, Buffalo, NY, pp. 225-276.

Park, T., and Silver, M. L. (1975). "Dynamic Soil Properties Required to Predict the Dynamic Behavior of Elevated Transportation Structures," *Report DOT-TST-75-44*, U.S. Department of Transportation, Washington, D.C.

Pease, J. W., and O'Rourke, T. D. (1995). "Liquefaction Hazards in the San Francisco Bay Region: Site Investigation, Modeling, and Hazard Assessment at Areas Most Seriously Affected by the 1989 Loma Prieta Earthquake," Report to the U.S. Geological Survey, Cornell University, Ithaca, NY, 176 p.

Pillai, V. S., and Byrne, P. M. (1994). "Effect of Overburden Pressure on Liquefaction Resistance of Sand," *Canadian Geotechnical Journal*, Vol. 31, pp. 53-60.

Power, M. S., Egan, J. A., Shewbridge, S. E., deBecker, J., and Faris, J. R. (1998). "Analysis of Liquefaction-Induced Damage on Treasure Island," *The Loma Prieta, California Earthquake of October 17, 1989--Liquefaction*, U.S. Geological Survey Professional Paper 1551-B, T. L. Holzer, Ed., U.S. Gov. Printing Office, Washington, D.C., pp. B87-B119.

Poulos, S. J., Castro, G., and France, J. W. (1985). "Liquefaction Evaluation Procedure," *Journal of Geotechnical Engineering*, ASCE, Vol. 111, No. 6, pp. 772-792.

Pyke, R. M., Seed, H. B., and Chan, C. K. (1975). "Settlement of Sands Under Multi-Directional Shaking," *Journal of the Geotechnical Engineering Division*, ASCE, Vol. 101, No. GT4, pp. 379-398.

Rashidian, M. (1995). "Undrained Shearing Behavior of Gravelly Sands and Its Relation with Shear Wave Velocity," *Thesis*, Geotechnical Engineering Laboratory, Department of Civil Engineering, University of Tokyo, Japan, 343 p.

Redpath, B. B. (1991). "Seismic Velocity Logging in the San Francisco Bay Area," Report to the Electric Power Research Institute, Palo Alto, CA, 34 p.

Robertson, P. K., Woeller, D. J., and Finn, W. D. L. (1992). "Seismic Cone Penetration Test for Evaluating Liquefaction Potential Under Cyclic Loading," *Canadian Geotechnical Journal*, Vol. 29, pp. 686-695.

Robertson, P. K., and Wride, C. E. (1997). "Cyclic Liquefaction and its Evaluation Based on the SPT and CPT," *NCEER Workshop on Evaluation of Liquefaction Resistance of Soils*, Technical Report NCEER-97-0022, T. L. Youd and I. M. Idriss, Eds., held 4-5 January 1996, Salt Lake City, UT, National Center for Earthquake Engineering Research, Buffalo, NY, pp. 41-87.

Robertson, P. K., and Wride, C. E. (1998). "Evaluating Cyclic Liquefaction Potential Using the Cone Penetration Test," *Canadian Geotechnical Journal*, Vol. 35, No. 3, pp. 442-459.

Roesler, S. K. (1979). "Anisotropic Shear Modulus Due to Stress Anisotropy," *Journal of the Geotechnical Engineering Division*, ASCE, Vol. 105, No. GT7, pp. 871-880.

Rollins, K. M., Evans, M. D., Diehl, N. B., and Daily, W. D., III (1998a). "Shear Modulus and Damping Relationships for Gravels," *Journal of Geotechnical and Geoenvironmental Engineering*, ASCE, Vol. 124, No. 5, pp. 396-405.

Rollins, K. M., Diehl, N. B., and Weaver, T. J. (1998b). "Implications of V_S-BPT $(N_1)_{60}$ Correlations for Liquefaction Assessment in Gravels," *Geotechnical Earthquake Engineering and Soil Dynamics III*, Geotechnical Special Publication No. 75, P. Dakoulas, M. Yegian, and B. Holtz, Eds., ASCE, Vol. I, pp. 506-517.

Roy, D., Campanella, R. G., Byrne, P. M., and Hughes, J. M. O. (1996). "Strain Level and Uncertainty of Liquefaction Related Index Tests," *Uncertainty in the Geologic Environment: From Theory to Practice*, Geotechnical Special Publication No. 58, C. D. Shackelford, P. P. Nelson, and M. J. S. Roth, Eds., ASCE, Vol. 2, pp. 1149-1162.

Sato, K., Kokusho, T., Matsumoto, M., and Yamada, E. (1996). "Nonlinear Seismic Response and Soil Property During Strong Motion," *Soils and Foundations, Special Issue on Geotechnical Aspects of the January 17, 1995 Hyogoken-Nambu Earthquake*, Japanese Geotechnical Society, pp. 41-52.

Seed, H. B. (1979). "Soil Liquefaction and Cyclic Mobility Evaluation for Level Ground during Earthquakes," *Journal of the Geotechnical Engineering Division*, ASCE, Vol. 105, GT2, pp. 201-255.

Seed, H. B. (1983). "Earthquake-Resistant Design of Earth Dams," *Proceedings, Symposium on Seismic Design of Embankments and Caverns*, held 6-10 May 1983, Philadelphia, PA, ASCE, pp. 41-64.

Seed, H. B., and Idriss, I. M. (1971). "Simplified Procedure for Evaluating Soil Liquefaction Potential," *Journal of the Soil Mechanics and Foundations Division*, ASCE, Vol. 97, SM9, pp. 1249-1273.

Seed, H. B., and Idriss, I. M. (1982). *Ground Motions and Soil Liquefaction During Earthquakes*, Earthquake Engineering Research Institute, Berkeley, CA, 134 p.

Seed, H. B., Idriss, I. M., and Arango, I. (1983). "Evaluation of Liquefaction Potential Using Field Performance Data," *Journal of Geotechnical Engineering*, ASCE, Vol. 109, No. 3, pp. 458-482.

Seed, H. B., Tokimatsu, K., Harder, L. F., and Chung, R. M. (1985). "Influence of SPT Procedures in Soil Liquefaction Resistance Evaluations," *Journal of Geotechnical Engineering*, ASCE, Vol. 111, No. 12, pp. 1425-1445.

Seed, H. B., Wong, R. T., Idriss, I. M., and Tokimatsu, K. (1986). "Moduli and Damping Factors for Dynamic Analysis of Cohesionless Soils," *Journal of Geotechnical Engineering*, ASCE, Vol. 112, No. 11, pp. 1016-1032.

Seed, R. B., and Harder, L. F., Jr. (1990). "SPT-Based Analysis of Cyclic Pore Pressure Generation and Undrained Residual Strength," *Proceedings, H. Bolton Seed Memorial Symposium*, J. M Duncan, Ed., BiTech Publishers, Vancouver, B.C., Vol. 2, pp. 351-376.

Shen, C. K., Li, X. S., and Wang, Z. (1991). "Pore Pressure Response During 1986 Lotung Earthquakes," *Proceedings, Second International Conference on Recent Advances in Geotechnical Earthquake Engineering and Soil Dynamics*, S. Prakash, Ed., held 11-15 March 1991, St. Louis, MO, University of Missouri at Rolla, Vol. I, pp. 557-563.

Shibata, T., Oka, F., and Ozawa, Y. (1996). "Characteristics of Ground Deformation Due to Liquefaction," *Soils and Foundations, Special Issue on Geotechnical Aspects of the January 17, 1995 Hyogoken-Nambu Earthquake*, Japanese Geotechnical Society, pp. 65-79.

Silver, M. L., and Seed, H. B. (1971). "Volume Changes in Sands During Cyclic Loading," *Journal of the Soil Mechanics and Foundations Division*, ASCE, Vol. 97, No. SM9, pp. 1171-1182.

Stokoe, K. H., II, Andrus, R. D., Bay, J. A., Fuhriman, M. D., Lee, N. J., and Yang, Y. (1992). "SASW and Crosshole Seismic Test Results from Sites that Did and Did not Liquefy During the 1989 Loma Prieta, California Earthquake," Geotechnical Engineering Center, Department of Civil Engineering, The University of Texas at Austin.

Stokoe, K. H., II, Lee, S. H. H., and Knox, D. P. (1985). "Shear Moduli Measurements Under True Triaxial Stresses," *Proceedings, Advances in the Art of Testing Soil Under Cyclic Conditions*, ASCE, pp. 166-185.

Stokoe, K. H., II, and Nazarian, S. (1985). "Use of Rayleigh Waves in Liquefaction Studies," *Measurement and Use of Shear Wave Velocity for Evaluating Dynamic Soil Properties*, R. D. Woods, Ed., ASCE, pp. 1-17.

Stokoe, K. H., II, Nazarian, S., Rix, G. J., Sanchez-Salinero, I., Sheu, J.-C., and Mok, Y. J. (1988a). "In Situ Seismic Testing of Hard-to-Sample Soils by Surface Wave Method," *Earthquake Engineering and Soil Dynamics II--Recent Advances in Ground-Motion Evaluation*, Geotechnical Special Publication No. 20, J. L. Von Thun, Ed., ASCE, pp. 264-289.

Stokoe, K. H., II, Andrus, R. D., Rix, G. J., Sanchez-Salinero, I., Sheu, J. C., and Mok, Y. J. (1988b). "Field Investigation of Gravelly Soils Which Did and Did Not Liquefy During the 1983 Borah Peak, Idaho, Earthquake," *Geotechnical Engineering Report GR 87-1*, The University of Texas at Austin, 206 p.

Stokoe, K. H., II, Roesset, J. M., Bierschwale, J. G., and Aouad, M. (1988c). "Liquefaction Potential of Sands from Shear Wave Velocity," *Proceedings, Ninth World Conference on Earthquake Engineering*, Tokyo, Japan, Vol. III, pp. 213-218.

Sykora, D. W. (1987a). "Examination of Existing Shear Wave Velocity and Shear Modulus Correlations in Soils," *Geotechnical Laboratory Miscellaneous Paper GL-87-22*, U.S. Army Engineer Waterways Experiment Station, Vicksburg, MS.

Sykora, D. W. (1987b). "Creation of a Data Base of Seismic Shear Wave Velocities for Correlation Analysis," *Geotechnical Laboratory Miscellaneous Paper GL-87-26*, U.S. Army Engineer Waterways Experiment Station, Vicksburg, MS.

Sykora, D. W., and Stokoe, K. H., II (1982), "Seismic Investigation of Three Heber Road Sites After October 15, 1979 Imperial Valley Earthquake," *Geotechnical Engineering Report GR82-24*, The University of Texas at Austin, 76 p.

Teachavorasinskun, S., Tatsuoka, F., and Lo Presti, D. C. F. (1994). "Effects of the Cyclic Prestaining on Dilatancy Characteristics and Liquefaction Strength of Sand," *Pre-failure Deformation of Geomaterials*, S. Shibuya, T. Mitachi, and S. Miura, Eds., A. A. Balkema, Rotterdam, Netherlands, pp. 75-80.

Tokimatsu, K., Kuwayama, S., and Tamura, S. (1991a). "Liquefaction Potential Evaluation Based on Rayleigh Wave Investigation and Its Comparison with Field Behavior," *Proceedings, Second International Conference on Recent Advances in Geotechnical Earthquake Engineering and Soil Dynamics*, S. Prakash, Ed., held 11-15 March 1991, St. Louis, MO, University of Missouri at Rolla, Vol. I, pp. 357-364.

Tokimatsu, K., Kuwayma, S., Abe, A., Nomura, S., and Tamura, S. (1991b). "Considerations to Damage Patterns in the Marina District During the Loma Prieta Earthquake Based on Rayleigh Wave Investigation," *Proceedings, Second International Conference on Recent Advances in Geotechnical Earthquake Engineering and Soil Dynamics*, S. Prakash, Ed., held 11-15 March 1991, St. Louis, MO, University of Missouri at Rolla, Vol. II, pp. 1649-1654.

Tokimatsu, K., and Uchida, A. (1990). "Correlation Between Liquefaction Resistance and Shear Wave Velocity," *Soils and Foundations*, Japanese Society of Soil Mechanics and Foundation Engineering, Vol. 30, No. 2, pp. 33-42.

United States Bureau of Reclamation, USBR (1989). "Seismic Design and Analysis," *Design Standards No. 13 - Embankment Dams*, USBR, Denver, CO, Chapter 13.

Vaid, Y. P., Chern, J. C., and Tumi, H. (1985). "Confining Pressure, Grain Angularity, and Liquefaction," *Journal of Geotechnical Engineering*, ASCE, Vol. 111, No. 10, pp. 1229-1235.

Vaid, Y. P., and Thomas, J. (1994). "Liquefaction and Postliquefaction Behavior of Sand," *Journal of Geotechnical Engineering*, ASCE, Vol. 121, No. 2, pp. 163-173.

Woods, R. D., Ed. (1994). *Geophysical Characterization of Sites*, A. A. Balkema, Rotterdam, Netherlands.

Yoshimi, Y., Tokimatsu, K., Kaneko, O., and Makihara, Y. (1984). "Undrained Cyclic Shear Strength of Dense Niigata Sand," *Soils and Foundations*, Japanese Society of Soil Mechanics and Foundation Engineering, Vol. 24, No. 4, pp. 131-145.

Yoshimi, Y., Tokimatsu, K., and Hosaka, Y. (1989). "Evaluation of Liquefaction Resistance of Clean Sands Based on High-Quality Undisturbed Samples," *Soils and Foundations*, Japanese Society of Soil Mechanics and Foundation Engineering, Vol. 29, No. 1, pp. 93-104.

Youd, T. L. (1972). "Compaction of Sands by Repeated Shear Straining," *Journal of the Soil Mechanics and Foundations Division*, ASCE, Vol. 98, No. SM7, pp. 709-725.

Youd, T. L., and Noble, S. K. (1997). "Liquefaction Criteria Based on Statistical and Probabilistic Analyses," *NCEER Workshop on Evaluation of Liquefaction Resistance of Soils*, Technical Report NCEER-97-0022, T. L. Youd and I. M. Idriss, Eds., held 4-5 January 1996, Salt Lake City, UT, National Center for Earthquake Engineering Research, Buffalo, NY, pp. 201-215.

Youd, T. L., and Bennett, M. J. (1983). "Liquefaction Sites, Imperial Valley, California," *Journal of Geotechnical Engineering*, ASCE, Vol. 109, No. 3, pp. 440-457.

Youd, T. L., Harp, E. L., Keefer, D. K., and Wilson, R. C. (1985). "The Borah Peak, Idaho Earthquake of October 28, 1983 - Liquefaction," *Earthquake Spectra*, Earthquake Engineering Research Institute, El Cerrito, CA, Vol. 2, No. 1, pp. 71-89.

Youd, T. L., and Holzer, T. L. (1994). "Piezometer Performance at Wildlife Liquefaction Site, California," *Journal of Geotechnical Engineering*, ASCE, Vol. 120, No. 6, pp. 975-995.

Youd, T. L., and Hoose, S. N. (1978). "Historic Ground Failures in Northern California Triggered by Earthquakes," *U.S. Geological Survey Professional Paper 993*, U.S. Government Printing Office, Washington, D.C., 177 p.

Youd, T. L., and Idriss, I. M., eds. (1997). *NCEER Workshop on Evaluation of Liquefaction Resistance of Soils*, Technical Report NCEER-97-0022, held 4-5 January 1996, Salt Lake City, UT, National Center for Earthquake Engineering Research, Buffalo, NY, 276 p.

Youd, T. L., Idriss, I. M., Andrus, R. D., Arango, I., Castro, G., Christian, J. T., Dobry, R., Finn, W. D. L., Harder, L. F., Jr., Hynes, M. E., Ishihara, K., Koester, J. P., Liao, S. S. C., Marcuson, W. F., III, Martin, G. R., Mitchell, J. K., Moriwaki, Y., Power, M. S., Robertson, P. K., Seed, R. B., and Stokoe, K. H., II (1997). "Summary Report," *NCEER Workshop on Evaluation of Liquefaction Resistance of Soils*, Technical Report NCEER-97-0022, T. L. Youd and I. M. Idriss, Eds., held 4-5 January 1996, Salt Lake City, UT, National Center for Earthquake Engineering Research, Buffalo, NY, pp. 1-40.

Yu, P., and Richart, F. E., Jr. (1984). "Stress Ratio Effects on Shear Modulus of Dry Sands," *Journal of Geotechnical Engineering*, ASCE, Vol. 110, No. 3, pp. 331-345.

APPENDIX A

SYMBOLS AND NOTATION

The following symbols and notation are used in this report:

A	=	parameter that depends on the soil structure;
a	=	parameter related to the slope of the CRR-V_{S1} curve;
a_{max}	=	peak horizontal ground surface acceleration;
B_1, B_2	=	parameters relating V_{S1} and penetration resistance;
b	=	parameter related to the slope of the CRR-V_{S1} curve;
C	=	cementation, aging, and negative pore-water pressures correction factor;
CPT	=	Cone Penetration Test;
CRR	=	average cyclic resistance ratio;
CRR_{tx}	=	CRR for cyclic triaxial tests;
CRR_l	=	CRR corrected for high overburden stress;
$CRR_{7.5}$	=	CRR for magnitude 7.5 earthquakes;
CSR	=	cyclic stress ratio;
DA	=	double-amplitude axial strain;
D_r	=	relative density;
D_{50}	=	median grain size by mass;
exp	=	the constant e raised to the power of a given number;
F_1, F_2	=	age and soil type factors for correlating V_S and N_j;
FC	=	fines content (particles smaller than 75 μm);
f	=	high overburden stress exponent;
$f(e_{min})$	=	function of minimum void ratio;
$f(\gamma_{av})$	=	function of average peak cyclic shear strain;
G	=	shear modulus;
G_{max}	=	small-strain shear modulus;
G_N	=	G_{max} corrected for confining stress and void ratio;
$(G)_{\gamma_{av}}$	=	secant shear modulus at γ_{av};
g	=	acceleration of gravity;
K_o	=	coefficient of lateral earth pressure at rest;
K_σ	=	high overburden stress correction factor;

ln	=	natural logarithm function;
MSF	=	magnitude scaling factor;
M_w	=	earthquake moment magnitude;
m	=	stress exponent;
N_j	=	SPT blow count in Japanese practice;
N_{60}	=	SPT energy-corrected blow count;
$(N_1)_{60}$	=	SPT energy- and overburden stress-corrected blow count;
n	=	magnitude scaling factor exponent;
P_a	=	reference overburden stress (= 100 kPa);
P_L	=	probability of liquefaction occurrence
r_c	=	factor to account for effects of multidirectional shaking;
r_d	=	shear stress reduction coefficient;
SASW	=	Spectral-Analysis-of-Surface-Waves;
SCPT	=	Seismic Cone Penetration Test;
sin	=	sine function;
SPT	=	Standard Penetration Test;
S_{res}	=	residual standard deviation;
V_S	=	small-strain shear wave velocity;
V_{S1}	=	overburden stress-corrected V_S;
V^*_{S1}	=	limiting upper value of V_{S1} for liquefaction occurrence;
V_{S1m}	=	mean stress-corrected V_S;
z	=	depth;
$\alpha(z)$	=	function of depth;
$\beta(z)$	=	function of depth;
γ_{av}	=	average peak cyclic shear strain;
ρ	=	mass density of soil;
σ_d	=	cyclic deviator stress in cyclic triaxial tests;
σ'_h	=	initial effective horizontal confining stress;
σ'_m	=	mean effective confining stress;
σ'_o	=	initial effective confining stress in cyclic triaxial tests;
σ_v	=	total vertical (or overburden) stress;
σ'_v	=	initial effective vertical (or overburden) stress;
τ_{av}	=	average cyclic equivalent uniform shear stress generated by earthquake; and
τ_{max}	=	maximum cyclic shear stress generated by earthquake.

APPENDIX B

GLOSSARY OF TERMS

The following definitions apply to this report:

Case History	An earthquake and a test array.
Critical Layer	The layer of non-plastic soil below the ground water table where corrected values of shear wave velocity and penetration are the least, and where cyclic stress ratios are the greatest.
Liquefaction Occurrence	Surface manifestations of excess pore-water pressure at depth, such as sand boils, ground cracks and fissures, and ground settlement.
Moment Magnitude	An earthquake magnitude scale defined in terms of energy.
Overburden Stress-Corrected Shear Wave Velocity	Shear wave velocity measurement corrected to a reference vertical (or overburden) stress of 100 kPa.
Peak Horizontal Ground Surface Acceleration	The peak value in a horizontal ground surface acceleration record that would occur at the site in the absence of liquefaction or excess pore-water pressures.
Shear Wave Velocity	The velocity of a propagating shear wave within a material with either the direction of wave propagation or the direction of particle motion in the vertical direction.
Shear Wave	A body wave with the direction of particle motion transverse to the direction of wave propagation.

Test Array	The two boreholes used for crosshole measurements, the borehole and source used for downhole measurements, the cone sounding and source used for seismic cone measurements, the borehole used for suspension logging measurements, or the line of receivers used for Spectral-Analysis-of-Surface-Waves (SASW) measurements.

APPENDIX C

SUMMARY OF CASE HISTORY DATA

Table C.1 presents a summary of case history data described in Chapter 3, and used in Chapter 4 to establish the recommended liquefaction resistance curves. This database has been expanded and modified from the database presented by Andrus and Stokoe (1997). Most of the modifications are minor with the intent to have the data conform to the draft guidelines presented in this document. The major modifications are based on new information or correction of an error in calculations. Some case histories included in the earlier database by Andrus and Stokoe have been omitted due to one of the three following reasons: (1) The reported average downhole V_S measurement is for a depth interval much greater than the identified critical layer. (2) The critical layer is likely older than 10 000 years and contains carbonate. (3) The location of the critical layer or field behavior is uncertain. References for the case history data are given in Table 3.1.

Table C.1 - Summary Information for *Vs* -Based Liquefaction and Non-Liquefaction Case Histories.

						----General Characteristics of Critical Layer----						----Average Value for Critical Layer ----								
Site	Test Type	Mw	Suf. Liq. Eff.? 1 = Y 0 = N	Water Table Depth	amax. avg.	Top of Layer Depth	Thick-ness	Soil Type	Average Fines Content	Deposit Type	Age	No. of Values in Average	Depth	Vert. Stress	Eff. Vert. Stress	rd	Vs	Vs1	CSR	CSR 7.5
				m	g	m	m		%				m	kPa	kPa		m/s	m/s		
1906 SAN FRANCISCO, CALIFORNIA EARTHQUAKE																				
Coyote Creek, S-R1	Xhole	7.7	1	2.4	0.36	3.5	2.5	sand & gravel	<5	AF	H	3	4.6	83.3	61.9	0.97	136	153	0.30	0.32
Coyote Creek, R1-R2	Xhole	7.7	1	2.4	0.36	3.5	2.5	sand & gravel	<5	AF	H	2	4.2	75.2	58.0	0.97	154	177	0.29	0.31
Coyote Creek, R1-R3	Xhole	7.7	1	2.4	0.36	3.5	2.5	sand & gravel	<5	AF	H	2	4.2	75.2	58.0	0.97	161	185	0.29	0.31
Coyote Creek, R2-R3	Xhole	7.7	1	2.4	0.36	3.5	2.5	sand & gravel	<5	AF	H	3	4.6	83.3	61.9	0.97	169	191	0.30	0.32
Salinas River North, S-R1	Xhole	7.7	0	6.1	0.32	9.1	2.3	sandy silt (ML to SM)	44	A	H	3	9.9	177.2	139.8	0.90	177	163	0.24	0.25
Salinas River North, R1-R2	Xhole	7.7	0	6.1	0.32	9.1	2.3	sandy silt (ML to SM)	44	A	H	3	9.9	177.2	139.8	0.90	195	179	0.24	0.25
Salinas River North, R1-R3	Xhole	7.7	0	6.1	0.32	9.1	2.3	sandy silt (ML to SM)	44	A	H	3	9.9	177.2	139.8	0.90	200	184	0.24	0.25
Salinas River North, R2-R3	Xhole	7.7	0	6.1	0.32	9.1	2.3	sandy silt (ML to SM)	44	A	H	3	9.9	177.2	139.8	0.90	199	183	0.24	0.25
Salinas River South, S-R1	Xhole	7.7	1	6.1	0.32	6.6	5.3	sand & silty sand (SP to SM)	14	A	H	2	8.0	141.2	122.6	0.93	131	124	0.22	0.24
Salinas River South, R1-R2	Xhole	7.7	1	6.1	0.32	6.6	5.3	sand & silty sand (SP to SM)	14	A	H	2	8.0	141.2	122.6	0.93	149	141	0.22	0.24
Salinas River South, R1-R3	Xhole	7.7	1	6.1	0.32	6.6	5.3	sand & silty sand (SP to SM)	14	A	H	2	8.0	141.2	122.6	0.93	158	151	0.22	0.24
Salinas River South, R2-R3	Xhole	7.7	1	6.1	0.32	6.6	5.3	sand & silty sand (SP to SM)	14	A	H	2	8.0	141.2	122.6	0.93	168	159	0.22	0.24
1957 DALY CITY, CALIFORNIA EARTHQUAKE																				
Marina District, No. 2	SASW	5.3	0	2.9	0.11	2.9	7.1	sand to silty sand (SP-SM)	~8	FH	R	1	6.4	117.0	82.2	0.94	120	129	0.09	0.04
Marina District, No. 3	SASW	5.3	0	2.9	0.11	2.9	7.1	sand to silty sand (SP to SM)	~12	FH	R	1	6.4	117.0	82.2	0.94	105	113	0.09	0.04
Marina District, No. 4	SASW	5.3	0	2.9	0.11	2.9	2.1	sand (SP)	<5	FH	R	1	3.9	69.9	59.6	0.98	120	137	0.08	0.03
Marina District, No. 5	SASW	5.3	0	5.9	0.11	5.9	4.1	sand (SP)	<5	Dune?	H?	1	7.9	140.6	120.5	0.93	220	211	0.08	0.03
Marina District, school	Dhole	5.3	0	2.7	0.11	2.7	1.6	sand (SP)	2	FU	R	2	3.5	62.3	54.1	0.98	112	130	0.08	0.03
1964 NIIGATA, JAPAN EARTHQUAKE																				
Niigata, Railway Station	?	7.5	1	2.0	0.16	2.0	2.7	sand	<5	?	?	2	3.2	56.7	45.2	0.98	131	160	0.13	0.13
Niigata, Site A1	SASW	7.5	0	5.0	0.16	5.0	2.5	sand	<5	?	?	1	6.2	109.9	97.7	0.95	162	164	0.12	0.12
Niigata, Site C1	SASW	7.5	1	1.2	0.16	1.6	6.5	sand	<5	?	?	2	4.5	82.8	50.7	0.97	112	136	0.15	0.15
Niigata, Site C2	SASW	7.5	1	1.2	0.16	1.2	4.8	sand	<5	?	?	1	4.0	73.4	46.5	0.97	118	147	0.15	0.15
1975 HAICHENG, PRC EARTHQUAKE																				
Chemical Fibre	Dhole	7.3	1	1.5	0.12	6.0	5.5	sand to silty clay	61	?	?	3	8.6	159.7	90.3	0.92	147	151	0.13	0.12
Construction Building	Dhole	7.3	1	1.5	0.12	3.0	6.5	clayey silt to silty clay	83	?	?	2	6.8	124.8	73.6	0.95	103	111	0.13	0.12
Fisheries & Shipbuilding	Dhole	7.3	1	0.5	0.12	2.5	4.0	silty sand to clayey silt	90	?	?	4	4.4	81.7	43.7	0.97	101	124	0.14	0.13
Glass Fiber	Dhole	7.3	1	0.8	0.12	2.7	3.8	sandy silt to clayey silt	42	?	?	3	4.8	89.8	50.3	0.97	98	117	0.13	0.13
Middle School	Dhole	7.3	0	1.0	0.12	5.0	6.0	clayey silt to silty clay	92	?	?	2	10.2	191.6	100.9	0.90	143	143	0.13	0.12
Paper Mill	Dhole	7.3	1	1.0	0.12	2.5	2.5	clayey silt to silty clay	72	?	?	1	3.0	54.7	35.2	0.98	122	158	0.12	0.11

Test Type

Xhole = crosshole seismic test
Dhole = downhole seismic test
SCPT = Seismic Cone Penetration Test
SASW = Spectral-Analysis-of-Surface-Waves test
Susp. = suspension logger test

Deposit Type

F = fill
FH = fill, hydraulic
FD = fill, dumped
FU = fill, uncompacted
FI = fill, improved
A = Alluvial
AF = Alluvial, fluvial
VDF = volcanic debris flow

Age

R = Recent (< 500 years)
H = Holocene (< 10 000 years)

$CSR\ 7.5 = CSR/(M_w/7.5)^{-2.56}$
? = unknown

Table C.1 - Summary Information for *Vs* -Based Liquefaction and Non-Liquefaction Case Histories.

						----General Characteristics of Critical Layer----						----Average Value for Critical Layer ----								
			Suf.	Water		Top of			Average			No. of Values			Eff.					
	Test		Liq.	Table	amax.	Layer	Thick-	Soil	Fines	Deposit		in		Vert.	Vert.					CSR
Site	Type	Mw	Eff.?	Depth	avg.	Depth	ness	Type	Content	Type	Age	Average	Depth	Stress	Stress	rd	Vs	Vs1	CSR	7.5
			1 = Y																	
			0 = N	m	g	m	m		%				m	kPa	kPa		m/s	m/s		
1979 IMPERIAL VALLEY EARTHQUAKE																				
Heber Road Channel Fill, R1-R2	Xhole	6.5	1	1.8	0.50	2.0	2.7	silty sand (SM)	22	AF	R	4	3.5	63.2	46.8	0.98	131	159	0.42	0.29
Heber Road Channel Fill, S-R1	Xhole	6.5	1	1.8	0.50	2.0	2.7	silty sand (SM)	22	AF	R	4	3.5	63.2	46.8	0.98	133	161	0.42	0.29
Heber Road Point Bar, R1-R2	Xhole	6.5	0	1.8	0.50	1.8	2.4	sand w/silt (SP-SM)	10	AF	R	4	3.4	60.3	45.4	0.98	164	201	0.42	0.29
Heber Road Point Bar, S-R1	Xhole	6.5	0	1.8	0.50	1.8	2.4	sand w/silt (SP-SM)	10	AF	R	4	3.4	60.3	45.4	0.98	173	211	0.42	0.29
Kornbloom	SASW	6.5	0	2.4	0.12	2.5	3.5	sandy silt (ML)	75	AF	R	5	4.2	75.1	58.1	0.97	105	120	0.10	0.07
McKim	SASW	6.5	1	1.5	0.51	1.5	3.5	silty sand (SM)	20	AF	R	4	3.0	54.1	39.7	0.98	126	160	0.43	0.30
Radio Tower	SASW	6.5	1	2.0	0.21	2.7	3.4	silty sand to sandy silt (SM to ML)	35	AF	H?	5	4.4	79.2	55.8	0.97	90	104	0.19	0.13
Vail Canal	SASW	6.5	0	2.7	0.12	2.7	2.8	sand w/ silt to silty sand (SP-SM to SM)	13	AF	R	4	4.0	70.4	58.4	0.98	101	116	0.09	0.06
Wildlife	SASW	6.5	0	1.5	0.13	2.5	4.3	silty sand to sandy silt (SM to ML)	27	AF	R	5	4.7	86.7	55.3	0.97	114	133	0.13	0.09
Wildlife, 1	Xhole	6.5	0	1.5	0.13	2.5	4.3	silty sand to sandy silt (SM to ML)	27	AF	R	4	4.6	83.8	53.9	0.97	127	148	0.13	0.09
Wildlife, 2	Xhole	6.5	0	1.5	0.13	2.5	4.3	silty sand to sandy silt (SM to ML)	27	AF	R	4	4.6	83.8	53.9	0.97	124	146	0.13	0.09
1980 MID-CHIBA, JAPAN EARTHQUAKE																				
Owi Island No. 1, layer 1	dhole	5.9	0	1.3	0.08	4.5	3.3	silty sand	20	FH	R	1	6.1	111.4	65.3	0.96	155	173	0.08	0.04
Owi Island No. 1, layer 2	dhole	5.9	0	1.3	0.08	13.0	3.6	silty sand	35	A	H	1	14.8	255.8	124.5	0.77	195	185	0.08	0.04
1981 WESTMORLAND, CALIFORNIA EARTHQUAKE																				
Heber Road Channel Fill, R1-R2	Xhole	5.9	0	1.8	0.02	2.0	2.7	silty sand (SM)	22	AF	R	4	3.5	63.2	46.8	0.98	131	159	0.02	0.01
Heber Road Channel Fill, S-R1	Xhole	5.9	0	1.8	0.02	2.0	2.7	silty sand (SM)	22	AF	R	4	3.5	63.2	46.8	0.98	133	161	0.02	0.01
Heber Road Point Bar, R1-R2	Xhole	5.9	0	1.8	0.02	1.8	2.4	sand w/silt (SP-SM)	10	AF	R	4	3.4	60.3	45.4	0.98	164	201	0.02	0.01
Heber Road Point Bar, S-R1	Xhole	5.9	0	1.8	0.02	1.8	2.4	sand w/silt (SP-SM)	10	AF	R	4	3.4	60.3	45.4	0.98	173	211	0.02	0.01
Kornbloom	SASW	5.9	1	2.4	0.36	2.5	3.5	sandy silt (ML)	75	AF	R	5	4.2	75.1	58.1	0.97	105	120	0.29	0.16
McKim	SASW	5.9	0	1.5	0.06	1.5	3.5	silty sand (SM)	20	AF	R	4	3.0	54.1	39.7	0.98	126	160	0.05	0.03
Radio Tower	SASW	5.9	1	2.0	0.20	2.7	3.4	silty sand to sandy silt (SM to ML)	35	AF	H?	5	4.4	79.2	55.8	0.97	90	104	0.18	0.10
Vail Canal	SASW	5.9	1	2.7	0.30	2.7	2.8	sand w/ silt to silty sand (SP-SM to SM)	13	AF	R	4	4.0	70.4	58.4	0.98	101	116	0.23	0.12
Wildlife	SASW	5.9	1	1.5	0.27	2.5	4.3	silty sand to sandy silt (SM to ML)	27	AF	R	5	4.7	86.7	55.3	0.97	114	133	0.26	0.14
Wildlife, 1	Xhole	5.9	1	1.5	0.27	2.5	4.3	silty sand to sandy silt (SM to ML)	27	AF	R	4	4.6	83.8	53.9	0.97	127	148	0.26	0.14
Wildlife, 2	Xhole	5.9	1	1.5	0.27	2.5	4.3	silty sand to sandy silt (SM to ML)	27	AF	R	4	4.6	83.8	53.9	0.97	124	146	0.26	0.14

Test Type
Xhole = crosshole seismic test
Dhole = downhole seismic test
SCPT = Seismic Cone Penetration Test
SASW = Spectral-Analysis-of-Surface-Waves test
Susp. = suspension logger test

Deposit Type
F = fill
FH = fill, hydraulic
FD = fill, dumped
FU = fill, uncompacted
FI = fill, improved
A = Alluvial
AF = Alluvial, fluvial
VDF = volcanic debris flow

Age
R = Recent (< 500 years)
H = Holocene (< 10 000 years)

$CSR_{7.5} = CSR/(M_w/7.5)^{-2.56}$
? = unknown

Table C.1 - Summary Information for *Vs* -Based Liquefaction and Non-Liquefaction Case Histories.

						----General Characteristics of Critical Layer----						----Average Value for Critical Layer ----								
Site	Test Type	Mw	Suf. Liq. Eff.? 1 = Y 0 = N	Water Table Depth	amax. avg.	Top of Layer Depth	Thick-ness	Soil Type	Average Fines Content	Deposit Type	Age	No. of Values in Average	Depth	Vert. Stress	Eff. Vert. Stress	rd	Vs	Vs1	CSR	CSR 7.5
				m	g	m	m		%				m	kPa	kPa		m/s	m/s		
1983 BORAH PEAK, IDAHO EARTHQUAKE																				
Andersen Bar, SA-1	SASW	6.9	1	0.8	0.29	0.8	2.4	sandy gravel (GP-GW)	<5	AF	R	3	1.9	39.0	27.8	0.99	105	145	0.25	0.20
Andersen Bar, X1-X2	Xhole	6.9	1	0.8	0.29	0.8	2.4	sandy gravel (GP-GW)	<5	AF	R	8	2.0	40.6	28.7	0.99	106	146	0.26	0.21
Goddard Ranch, SA-2	SASW	6.9	1	1.2	0.30	1.2	2.0	sandy gravel (GP)	<5	AF	H	2	2.4	49.7	37.3	0.97	122	157	0.25	0.20
Goddard Ranch, SA-4	SASW	6.9	1	1.2	0.30	1.2	2.0	sandy gravel (GP)	<5	AF	H	2	2.4	49.8	37.4	0.97	105	136	0.25	0.20
Mackay Dam, Toe	SASW	6.9	0	2.3	0.23	2.3	2.7	silty sandy gravel (GW to GM)	6	?	H	2	2.8	57.2	52.3	0.98	270	318	0.16	0.13
North Gravel Bar, Bar Site	SASW	6.9	0	1.0	0.46	1.8	1.2	sandy gravel	~<5	A	H?	2	2.4	51.0	36.0	0.99	206	266	0.41	0.33
North Gravel Bar, Terrace	SASW	6.9	0	3.0	0.46	3.0	1.3	sandy gravel	~<5	A	H?	2	3.7	75.2	69.2	0.98	274	301	0.32	0.26
Pence Ranch, SA-1	SASW	6.9	1	1.7	0.36	1.8	1.9	gravelly sand to sandy gravel	<5	AF	H	4	2.8	57.3	46.2	0.98	103	125	0.28	0.23
Pence Ranch, SA-2	SASW	6.9	1	1.5	0.36	1.5	2.8	gravelly sand to sandy gravel	<5	AF	H	3	3.1	60.3	44.7	0.98	94	115	0.30	0.25
Pence Ranch, SA-3	SASW	6.9	1	1.4	0.36	1.4	1.8	gravelly sand to sandy gravel	<5	AF	H	3	2.4	45.8	36.8	0.98	102	131	0.28	0.23
Pence Ranch, SA-4	SASW	6.9	1	1.8	0.36	1.8	2.8	gravelly sand to sandy gravel	<5	AF	H	2	3.1	62.1	49.4	0.98	109	131	0.28	0.23
Pence Ranch, SA-5	SASW	6.9	1	1.5	0.36	1.5	1.9	gravelly sand to sandy gravel	<5	AF	H	2	3.0	60.5	45.6	0.98	123	151	0.29	0.24
Pence Ranch, SA-A	SASW	6.9	1	2.0	0.36	2.0	1.7	gravelly sand to sandy gravel	<5	AF	H	1	2.8	57.5	46.3	0.98	134	164	0.28	0.23
Pence Ranch, SA-B	SASW	6.9	1	1.5	0.36	1.5	1.7	gravelly sand to sandy gravel	<5	AF	H	2	2.1	38.8	32.9	0.99	128	170	0.27	0.21
Pence Ranch, SA-C	SASW	6.9	1	1.5	0.36	1.5	1.9	gravelly sand to sandy gravel	<5	AF	H	2	2.1	38.4	32.4	0.99	107	142	0.27	0.21
Pence Ranch, SA-D	SASW	6.9	1	1.5	0.36	1.5	1.7	gravelly sand to sandy gravel	<5	AF	H	2	2.1	39.4	33.8	0.99	131	173	0.26	0.21
Pence Ranch, SA-E	SASW	6.9	1	1.7	0.36	1.7	1.5	gravelly sand to sandy gravel	<5	AF	H	2	2.3	43.3	38.3	0.99	122	155	0.26	0.21
Pence Ranch, XD-XE	Xhole	6.9	1	1.5	0.36	2.8	1.0	gravelly sand to sandy gravel	<5	AF	H	3	3.4	64.7	46.8	0.98	146	176	0.32	0.26
1985 CHIBA-IBAARAGI, JAPAN EARTHQUAKE																				
Owl Island No. 1, layer 1	Dhole	6.0	0	1.3	0.05	4.5	3.3	silty sand	20	FH	R	1	6.1	111.4	65.3	0.96	155	173	0.05	0.03
Owl Island No. 1, layer 2	Dhole	6.0	0	1.3	0.05	13.0	3.6	silty sand	35	A	H	1	14.8	255.8	124.5	0.77	195	185	0.05	0.03
10/26/85 TAIWAN EARTHQUAKE (EVENT LSST2)																				
Lotung LSST, L2-L5/L6	Xhole	5.3	0	0.5	0.05	3.7	5.2	silty sand to sandy silt (SM-ML)	50	A	H	3	6.1	114.1	45.4	0.96	137	167	0.08	0.03
Lotung LSST, L2-L7	Xhole	5.3	0	0.5	0.05	3.7	5.2	silty sand to sandy silt (SM-ML)	50	A	H	3	6.1	114.1	45.4	0.96	127	155	0.08	0.03
Lotung LSST, L8-L3	Xhole	5.3	0	0.5	0.05	4.1	4.8	silty sand to sandy silt (SM-ML)	50	A	H	3	6.1	114.1	45.4	0.96	156	191	0.08	0.03
Lotung LSST, L8-L4	Xhole	5.3	0	0.5	0.05	3.0	5.9	silty sand to sandy silt (SM-ML)	50	A	H	4	5.3	99.8	40.4	0.96	142	179	0.08	0.03

Test Type
Xhole = crosshole seismic test
Dhole = downhole seismic test
SCPT = Seismic Cone Penetration Test
SASW = Spectral-Analysis-of-Surface-Waves test
Susp. = suspension logger test

Deposit Type
F = fill
FH = fill, hydraulic
FD = fill, dumped
FU = fill, uncompacted
FI = fill, improved
A = Alluvial
AF = Alluvial, fluvial
VDF = volcanic debris flow

Age
R = Recent (< 500 years)
H = Holocene (< 10 000 years)

CSR 7.5 = $CSR/(M_w/7.5)^{-2.56}$
? = unknown

Table C.1 - Summary Information for *Vs* -Based Liquefaction and Non-Liquefaction Case Histories.

						----General Characteristics of Critical Layer----						----Average Value for Critical Layer ----								
Site	Test Type	Mw	Suf. Liq. Eff.? 1 = Y 0 = N	Water Table Depth	amax. avg.	Top of Layer Depth	Thick-ness	Soil Type	Average Fines Content	Deposit Type	Age	No. of Values in Average	Depth	Vert. Stress	Eff. Vert. Stress	rd	Vs	Vs1	CSR	CSR 7.5
				m	g	m	m		%				m	kPa	kPa		m/s	m/s		
11/7/85 TAIWAN EARTHQUAKE (EVENT LSST 3)																				
Lotung LSST, L2-L5/L6	Xhole	5.5	0	0.5	0.02	3.7	5.2	silty sand to sandy silt (SM-ML)	50	A	H	3	6.1	114.1	45.4	0.96	137	167	0.03	0.01
Lotung LSST, L2-L7	Xhole	5.5	0	0.5	0.02	3.7	5.2	silty sand to sandy silt (SM-ML)	50	A	H	3	6.1	114.1	45.4	0.96	127	155	0.03	0.01
Lotung LSST, L8-L3	Xhole	5.5	0	0.5	0.02	4.1	4.8	silty sand to sandy silt (SM-ML)	50	A	H	3	6.1	114.1	45.4	0.96	156	191	0.03	0.01
Lotung LSST, L8-L4	Xhole	5.5	0	0.5	0.02	3.0	5.9	silty sand to sandy silt (SM-ML)	50	A	H	4	5.3	99.8	40.4	0.96	142	179	0.03	0.01
1/16/86 TAIWAN EARTHQUAKE (EVENT LSST 4)																				
Lotung LSST, L2-L5/L6	Xhole	6.6	0	0.5	0.22	3.7	5.2	silty sand to sandy silt (SM-ML)	50	A	H	3	6.1	114.1	45.4	0.96	137	167	0.34	0.25
Lotung LSST, L2-L7	Xhole	6.6	0	0.5	0.22	3.7	5.2	silty sand to sandy silt (SM-ML)	50	A	H	3	6.1	114.1	45.4	0.96	127	155	0.34	0.25
Lotung LSST, L8-L3	Xhole	6.6	0	0.5	0.22	4.1	4.8	silty sand to sandy silt (SM-ML)	50	A	H	3	6.1	114.1	45.4	0.96	156	191	0.34	0.25
Lotung LSST, L8-L4	Xhole	6.6	0	0.5	0.22	3.0	5.9	silty sand to sandy silt (SM-ML)	50	A	H	4	5.3	99.8	40.4	0.96	142	179	0.34	0.24
4/8/86 TAIWAN EARTHQUAKE (EVENT LSST 6)																				
Lotung LSST, L2-L5/L6	Xhole	5.4	0	0.5	0.04	3.7	5.2	silty sand to sandy silt (SM-ML)	50	A	H	3	6.1	114.1	45.4	0.96	137	167	0.06	0.03
Lotung LSST, L2-L7	Xhole	5.4	0	0.5	0.04	3.7	5.2	silty sand to sandy silt (SM-ML)	50	A	H	3	6.1	114.1	45.4	0.96	127	155	0.06	0.03
Lotung LSST, L8-L3	Xhole	5.4	0	0.5	0.04	4.1	4.8	silty sand to sandy silt (SM-ML)	50	A	H	3	6.1	114.1	45.4	0.96	156	191	0.06	0.03
Lotung LSST, L8-L4	Xhole	5.4	0	0.5	0.04	3.0	5.9	silty sand to sandy silt (SM-ML)	50	A	H	4	5.3	99.8	40.4	0.96	142	179	0.06	0.03
5/20/86 TAIWAN EARTHQUAKE (EVENT LSST 7)																				
Lotung LSST, L2-L5/L6	Xhole	6.6	0	0.5	0.18	3.7	5.2	silty sand to sandy silt (SM-ML)	50	A	H	3	6.1	114.1	45.4	0.96	137	167	0.28	0.20
Lotung LSST, L2-L7	Xhole	6.6	0	0.5	0.18	3.7	5.2	silty sand to sandy silt (SM-ML)	50	A	H	3	6.1	114.1	45.4	0.96	127	155	0.28	0.20
Lotung LSST, L8-L3	Xhole	6.6	0	0.5	0.18	4.1	4.8	silty sand to sandy silt (SM-ML)	50	A	H	3	6.1	114.1	45.4	0.96	156	191	0.28	0.20
Lotung LSST, L8-L4	Xhole	6.6	0	0.5	0.18	3.0	5.9	silty sand to sandy silt (SM-ML)	50	A	H	4	5.3	99.8	40.4	0.96	142	179	0.27	0.20
5/20/86 TAIWAN EARTHQUAKE (EVENT LSST 8)																				
Lotung LSST, L2-L5/L6	Xhole	6.2	0	0.5	0.04	3.7	5.2	silty sand to sandy silt (SM-ML)	50	A	H	3	6.1	114.1	45.4	0.96	137	167	0.06	0.04
Lotung LSST, L2-L7	Xhole	6.2	0	0.5	0.04	3.7	5.2	silty sand to sandy silt (SM-ML)	50	A	H	3	6.1	114.1	45.4	0.96	127	155	0.06	0.04
Lotung LSST, L8-L3	Xhole	6.2	0	0.5	0.04	4.1	4.8	silty sand to sandy silt (SM-ML)	50	A	H	3	6.1	114.1	45.4	0.96	156	191	0.06	0.04
Lotung LSST, L8-L4	Xhole	6.2	0	0.5	0.04	3.0	5.9	silty sand to sandy silt (SM-ML)	50	A	H	4	5.3	99.8	40.4	0.96	142	179	0.06	0.04

Test Type
Xhole = crosshole seismic test
Dhole = downhole seismic test
SCPT = Seismic Cone Penetration Test
SASW = Spectral-Analysis-of-Surface-Waves test
Susp. = suspension logger test

Deposit Type
F = fill
FH = fill, hydraulic
FD = fill, dumped
FU = fill, uncompacted
FI = fill, improved
A = Alluvial
AF = Alluvial, fluvial
VDF = volcanic debris flow

Age
R = Recent (< 500 years)
H = Holocene (< 10 000 years)

CSR 7.5 = $CSR/(M_w/7.5)^{-2.56}$
? = unknown

Table C.1 - Summary Information for *Vs* -Based Liquefaction and Non-Liquefaction Case Histories.

						----General Characteristics of Critical Layer----						----Average Value for Critical Layer ----								
						Top						No. of								
			Suf.	Water		of			Average			Values			Eff.					
	Test		Liq.	Table	amax.	Layer	Thick-	Soil	Fines	Deposit		In		Vert.	Vert.					CSR
Site	Type	Mw	Eff.?	Depth	avg.	Depth	ness	Type	Content	Type	Age	Average	Depth	Stress	Stress	rd	Vs	Vs1	CSR	7.5
			1 = Y																	
			0 = N	m	g	m	m		%				m	kPa	kPa		m/s	m/s		
7/30/86 TAIWAN EARTHQUAKE (EVENT LSST 12)																				
Lotung LSST, L2-L5/L6	Xhole	6.2	0	0.5	0.18	3.7	5.2	silty sand to sandy silt (SM-ML)	50	A	H	3	6.1	114.1	45.4	0.96	137	167	0.28	0.17
Lotung LSST, L2-L7	Xhole	6.2	0	0.5	0.18	3.7	5.2	silty sand to sandy silt (SM-ML)	50	A	H	3	6.1	114.1	45.4	0.96	127	155	0.28	0.17
Lotung LSST, L8-L3	Xhole	6.2	0	0.5	0.18	4.1	4.8	silty sand to sandy silt (SM-ML)	50	A	H	3	6.1	114.1	45.4	0.96	156	191	0.28	0.17
Lotung LSST, L8-L4	Xhole	6.2	0	0.5	0.18	3.0	5.9	silty sand to sandy silt (SM-ML)	50	A	H	4	5.3	99.8	40.4	0.96	142	179	0.27	0.17
7/30/86 TAIWAN EARTHQUAKE (EVENT LSST 13)																				
Lotung LSST, L2-L5/L6	Xhole	6.2	0	0.5	0.05	3.7	5.2	silty sand to sandy silt (SM-ML)	50	A	H	3	6.1	114.1	45.4	0.96	137	167	0.08	0.05
Lotung LSST, L2-L7	Xhole	6.2	0	0.5	0.05	3.7	5.2	silty sand to sandy silt (SM-ML)	50	A	H	3	6.1	114.1	45.4	0.96	127	155	0.08	0.05
Lotung LSST, L8-L3	Xhole	6.2	0	0.5	0.05	4.1	4.8	silty sand to sandy silt (SM-ML)	50	A	H	3	6.1	114.1	45.4	0.96	156	191	0.08	0.05
Lotung LSST, L8-L4	Xhole	6.2	0	0.5	0.05	3.0	5.9	silty sand to sandy silt (SM-ML)	50	A	H	4	5.3	99.8	40.4	0.96	142	179	0.08	0.05
11/14/86 TAIWAN EARTHQUAKE (EVENT LSST 16)																				
Lotung LSST, L2-L5/L6	Xhole	7.6	0	0.5	0.16	3.7	5.2	silty sand to sandy silt (SM-ML)	50	A	H	3	6.1	114.1	45.4	0.96	137	167	0.25	0.26
Lotung LSST, L2-L7	Xhole	7.6	0	0.5	0.16	3.7	5.2	silty sand to sandy silt (SM-ML)	50	A	H	3	6.1	114.1	45.4	0.96	127	155	0.25	0.26
Lotung LSST, L8-L3	Xhole	7.6	0	0.5	0.16	4.1	4.8	silty sand to sandy silt (SM-ML)	50	A	H	3	6.1	114.1	45.4	0.96	156	191	0.25	0.26
Lotung LSST, L8-L4	Xhole	7.6	0	0.5	0.16	3.0	5.9	silty sand to sandy silt (SM-ML)	50	A	H	4	5.3	99.8	40.4	0.96	142	179	0.24	0.25
1987 CHIBA-TOHO-OKI, JAPAN EARTHQUAKE																				
Sunamachi, Tokyo Bay	Dhole	6.5	0	6.2	0.10	6.2	5.8	sand with silt to silty sand	15	FH	R	2	9.0	166.8	138.8	0.92	150	141	0.06	0.04
1987 ELMORE RANCH EARTHQUAKE																				
Heber Road Channel Fill, R1-R2	Xhole	5.9	0	1.8	0.03	2.0	2.7	silty sand (SM)	22	AF	R	4	3.5	63.2	46.8	0.98	131	159	0.03	0.01
Heber Road Channel Fill, S-R1	Xhole	5.9	0	1.8	0.03	2.0	2.7	silty sand (SM)	22	AF	R	4	3.5	63.2	46.8	0.98	133	161	0.03	0.01
Heber Road Point Bar, R1-R2	Xhole	5.9	0	1.8	0.03	1.8	2.4	sand w/silt (SP-SM)	10	AF	R	4	3.4	60.3	45.4	0.98	164	201	0.03	0.01
Heber Road Point Bar, S-R1	Xhole	5.9	0	1.8	0.03	1.8	2.4	sand w/silt (SP-SM)	10	AF	R	4	3.4	60.3	45.4	0.98	173	211	0.03	0.01
Kornbloom	SASW	5.9	0	2.4	0.24	2.5	3.5	sandy silt (ML)	75	AF	R	5	4.2	75.1	58.1	0.97	105	120	0.19	0.10
McKim	SASW	5.9	0	1.5	0.06	1.5	3.5	silty sand (SM)	20	AF	R	4	3.0	54.1	39.7	0.98	126	160	0.05	0.03
Radio Tower	SASW	5.9	0	2.0	0.11	2.7	3.4	silty sand to sandy silt (SM to ML)	35	AF	H?	5	4.4	79.2	55.8	0.97	90	104	0.10	0.05
Vail Canal	SASW	5.9	0	2.7	0.13	2.7	2.8	sand w/ silt to silty sand (SP-SM to SM)	13	AF	R	4	4.0	70.4	56.4	0.98	101	116	0.10	0.05
Wildlife	SASW	5.9	0	1.5	0.13	2.5	4.3	silty sand to sandy silt (SM to ML)	27	AF	R	5	4.7	86.7	55.3	0.97	114	133	0.13	0.07
Wildlife, 1	Xhole	5.9	0	1.5	0.13	2.5	4.3	silty sand to sandy silt (SM to ML)	27	AF	R	4	4.6	83.8	53.9	0.97	127	148	0.13	0.07
Wildlife, 2	Xhole	5.9	0	1.5	0.13	2.5	4.3	silty sand to sandy silt (SM to ML)	27	AF	R	4	4.6	83.8	53.9	0.97	124	146	0.13	0.07

Test Type
Xhole = crosshole seismic test
Dhole = downhole seismic test
SCPT = Seismic Cone Penetration Test
SASW = Spectral-Analysis-of-Surface-Waves test
Susp. = suspension logger test

Deposit Type
F = fill
FH = fill, hydraulic
FD = fill, dumped
FU = fill, uncompacted
FI = fill, improved
A = Alluvial
AF = Alluvial, fluvial
VDF = volcanic debris flow

Age
R = Recent (< 500 years)
H = Holocene (< 10 000 years)

$CSR\ 7.5 = CSR/(M_w/7.5)^{-2.56}$
? = unknown

Table C.1 - Summary Information for *Vs* -Based Liquefaction and Non-Liquefaction Case Histories.

						----General Characteristics of Critical Layer----						----Average Value for Critical Layer ----								
Site	Test Type	Mw	Suf. Liq. Eff.? 1 = Y 0 = N	Water Table Depth m	amax. avg. g	Top of Layer Depth m	Thick-ness m	Soil Type	Average Fines Content %	Deposit Type	Age	No. of Values in Average	Depth m	Vert. Stress kPa	Eff. Vert. Stress kPa	rd	Vs m/s	Vs1 m/s	CSR	CSR 7.5
1987 SUPERSTITION HILLS, CALIFORNIA EARTHQUAKE																				
Heber Road Channel Fill, R1-R2	Xhole	6.5	0	1.8	0.18	2.0	2.7	silty sand (SM)	22	AF	R	4	3.5	63.2	46.8	0.98	131	159	0.15	0.11
Heber Road Channel Fill, S-R1	Xhole	6.5	0	1.8	0.18	2.0	2.7	silty sand (SM)	22	AF	R	4	3.5	63.2	46.8	0.98	133	161	0.15	0.11
Heber Road Point Bar, R1-R2	Xhole	6.5	0	1.8	0.18	1.8	2.4	sand w/silt (SP-SM)	10	AF	R	4	3.4	60.3	45.4	0.98	164	201	0.15	0.10
Heber Road Point Bar, S-R1	Xhole	6.5	0	1.8	0.18	1.8	2.4	sand w/silt (SP-SM)	10	AF	R	4	3.4	60.3	45.4	0.98	173	211	0.15	0.10
Kornbloom	SASW	6.5	0	2.4	0.21	2.5	3.5	sandy silt (ML)	75	AF	R	5	4.2	75.1	58.1	0.97	105	120	0.17	0.12
McKim	SASW	6.5	0	1.5	0.19	1.5	3.5	silty sand (SM)	20	AF	R	4	3.0	54.1	39.7	0.98	126	160	0.16	0.11
Radio Tower	SASW	6.5	0	2.0	0.20	2.7	3.4	silty sand to sandy silt (SM to ML)	35	AF	H?	5	4.4	79.2	55.8	0.97	90	104	0.18	0.12
Vail Canal	SASW	6.5	0	2.7	0.20	2.7	2.8	sand w/ silt to silty sand (SP-SM to SM)	13	AF	R	4	4.0	70.4	58.4	0.98	101	116	0.15	0.10
Wildlife	SASW	6.5	1	1.5	0.20	2.5	4.3	silty sand to sandy silt (SM to ML)	27	AF	R	5	4.7	86.7	55.3	0.97	114	133	0.20	0.14
Wildlife, 1	Xhole	6.5	1	1.5	0.20	2.5	4.3	silty sand to sandy silt (SM to ML)	27	AF	R	4	4.6	83.8	53.9	0.97	127	148	0.19	0.13
Wildlife, 2	Xhole	6.5	1	1.5	0.20	2.5	4.3	silty sand to sandy silt (SM to ML)	27	AF	R	4	4.6	83.8	53.9	0.97	124	146	0.19	0.13
1989 LOMA PRIETA, CALIFORNIA EARTHQUAKE																				
Bay Farm Island, Dike	SASW	7.0	0	3.6	0.27	3.6	2.8	sand with fines (SP-SM)	10	R	R	1	5.2	91.9	77.0	0.96	204	219	0.20	0.16
Bay Farm Island, Dike S-R1	Xhole	7.0	0	3.6	0.27	3.6	2.8	sand with fines (SP-SM)	10	R	R	5	4.9	87.1	75.2	0.97	193	207	0.20	0.16
Bay Farm Island, Dike R1-R2	Xhole	7.0	0	3.6	0.27	3.6	2.8	sand with fines (SP-SM)	10	R	R	4	4.9	81.4	72.4	0.97	205	222	0.19	0.16
Bay Farm Island, Loop	SASW	7.0	1	3.5	0.27	3.5	1.7	sand with fines	<12	RH	R	1	3.8	66.7	61.4	0.98	125	142	0.18	0.15
Bay Farm Island, Loop S-R1	Xhole	7.0	1	3.5	0.27	3.5	1.7	sand with fines	<12	RH	R	3	4.3	75.6	68.2	0.98	98	107	0.19	0.16
Bay Farm Island, Loop R1-R2	Xhole	7.0	1	3.5	0.27	3.5	1.7	sand with fines	<12	RH	R	3	4.3	75.6	68.2	0.98	113	124	0.19	0.16
Coyote Creek, S-R1	Xhole	7.0	0	2.4	0.18	3.5	2.5	sand & gravel	<5	AF	H	3	4.6	83.3	61.9	0.97	136	153	0.15	0.13
Coyote Creek, R1-R2	Xhole	7.0	0	2.4	0.18	3.5	2.5	sand & gravel	<5	AF	H	2	4.2	75.2	58.0	0.97	154	177	0.15	0.12
Coyote Creek, R1-R3	Xhole	7.0	0	2.4	0.18	3.5	2.5	sand & gravel	<5	AF	H	2	4.2	75.2	58.0	0.97	161	185	0.15	0.12
Coyote Creek, R2-R3	Xhole	7.0	0	2.4	0.18	3.5	2.5	sand & gravel	<5	AF	H	3	4.6	83.3	61.9	0.97	169	191	0.15	0.13
Harbor Office, UC-12	SCPT	7.0	1	1.9	0.25	3.0	1.6	silty sand	15	?	H	2	4.1	74.3	52.6	0.97	150	176	0.22	0.19
Marina District, No. 2	SASW	7.0	1	2.9	0.15	2.9	7.1	sand to silty sand (SP-SM)	~8	RH	R	1	6.4	117.0	82.2	0.94	120	129	0.12	0.10
Marina District, No. 3	SASW	7.0	1	2.9	0.15	2.9	7.1	sand to silty sand (SP to SM)	~12	RH	R	1	6.4	117.0	82.2	0.94	105	113	0.12	0.10
Marina District, No. 4	SASW	7.0	1	2.9	0.15	2.9	2.1	sand (SP)	<5	RH	R	1	3.9	69.9	59.6	0.98	120	137	0.11	0.09
Marina District, No. 5	SASW	7.0	0	5.9	0.15	5.9	4.1	sand (SP)	<5	Dune?	H?	1	7.9	140.6	120.5	0.93	220	211	0.10	0.09
Marina District, school	Dhole	7.0	1	2.7	0.15	2.7	1.6	sand (SP)	2	FU	R	2	3.5	62.3	54.1	0.98	112	130	0.11	0.09
Port of Oakland, POO7-1	SCPT	7.0	1	3.0	0.24	5.0	4.0	sand (SP)	<5	RH	R	3	7.2	131.5	90.4	0.94	148	152	0.21	0.18
Port of Oakland, POO7-2	SASW	7.0	1	3.0	0.24	5.0	4.0	sand (SP)	<5	RH	R	2	6.4	115.7	82.9	0.95	157	165	0.21	0.17
Port of Oakland, POO7-2	SCPT	7.0	1	3.0	0.24	5.0	4.0	sand (SP)	<5	RH	R	3	7.2	131.8	90.7	0.94	151	155	0.21	0.18
Port of Oakland, POO7-2, S-R1	Xhole	7.0	1	3.0	0.24	5.0	4.0	sand (SP)	<5	RH	R	6	7.0	127.4	88.5	0.95	147	152	0.21	0.18
Port of Oakland, POO7-2, R1-R2	Xhole	7.0	1	3.0	0.24	5.0	4.0	sand (SP)	<5	RH	R	6	7.0	127.4	88.5	0.95	181	186	0.21	0.18

Test Type

Xhole = crosshole seismic test
Dhole = downhole seismic test
SCPT = Seismic Cone Penetration Test
SASW = Spectral-Analysis-of-Surface-Waves test
Susp. = suspension logger test

Deposit Type

F = fill
FH = fill, hydraulic
FD = fill, dumped
FU = fill, uncompacted
FI = fill, improved
A = Alluvial
AF = Alluvial, fluvial
VDF = volcanic debris flow

Age

R = Recent (< 500 years)
H = Holocene (< 10 000 years)

$CSR\ 7.5 = CSR/(M_w/7.5)^{-2.56}$
? = unknown

Table C.1 - Summary Information for *Vs* -Based Liquefaction and Non-Liquefaction Case Histories.

						----General Characteristics of Critical Layer----						----Average Value for Critical Layer ----								
						Top						No. of								
			Suf.	Water		of			Average			Values			Eff.					
	Test		Liq.	Table	amax.	Layer	Thick-	Soil	Fines	Deposit		In		Vert.	Vert.					CSR
Site	Type	Mw	Eff.?	Depth	avg.	Depth	ness	Type	Content	Type	Age	Average	Depth	Stress	Stress	rd	Vs	Vs1	CSR	7.5
			1 = Y																	
			0 = N	m	g	m	m		%				m	kPa	kPa		m/s	m/s		
Port of Oakland, POO7-3	SCPT	7.0	1	3.0	0.24	5.5	1.5	sand with silt (SP-SM)	10	FH	R	1	6.2	112.7	81.3	0.95	176	185	0.21	0.17
Port of Richmond, POR-2	SCPT	7.0	1	3.5	0.16	4.0	4.0	silt (ML)	57	FH	R	4	5.8	102.9	80.9	0.96	145	152	0.13	0.10
Port of Richmond, POR-2	SASW	7.0	1	3.5	0.16	4.0	4.0	silt (ML)	57	FH	R	2	5.3	93.6	76.4	0.97	117	125	0.12	0.10
Port of Richmond, POR-2, S-R1	Xhole	7.0	1	3.5	0.16	4.0	4.0	silt (ML)	57	FH	R	7	6.1	109.4	84.1	0.95	143	150	0.13	0.11
Port of Richmond, POR-2, R1-R2	Xhole	7.0	1	3.5	0.16	4.0	4.0	silt (ML)	57	FH	R	7	6.1	109.4	84.0	0.95	135	141	0.13	0.11
Port of Richmond, POR-3	SCPT	7.0	1	3.5	0.16	4.0	3.0	silt to silty sand (ML to SM)	>25	FH	R	3	5.2	93.4	76.3	0.96	110	118	0.13	0.11
Port of Richmond, POR-4	SCPT	7.0	1	3.5	0.16	3.8	3.2	silty sand (ML to SM)	>32	FH	R	3	5.2	93.4	76.3	0.96	128	137	0.12	0.10
Salinas River North, S-R1	Xhole	7.0	0	6.1	0.15	9.1	2.3	sandy silt (ML to SM)	44	A	H	3	9.9	177.2	139.8	0.90	177	163	0.11	0.09
Salinas River North, R1-R2	Xhole	7.0	0	6.1	0.15	9.1	2.3	sandy silt (ML to SM)	44	A	H	3	9.9	177.2	139.8	0.90	195	179	0.11	0.09
Salinas River North, R1-R3	Xhole	7.0	0	6.1	0.15	9.1	2.3	sandy silt (ML to SM)	44	A	H	3	9.9	177.2	139.8	0.90	200	184	0.11	0.09
Salinas River North, R2-R3	Xhole	7.0	0	6.1	0.15	9.1	2.3	sandy silt (ML to SM)	44	A	H	3	9.9	177.2	139.8	0.90	199	183	0.11	0.09
Salinas River South, S-R1	Xhole	7.0	0	6.1	0.15	6.6	5.3	sand & silty sand (SP to SM)	14	A	H	2	8.0	141.2	122.6	0.93	131	124	0.10	0.09
Salinas River South, R1-R2	Xhole	7.0	0	6.1	0.15	6.6	5.3	sand & silty sand (SP to SM)	14	A	H	2	8.0	141.2	122.6	0.93	149	141	0.10	0.09
Salinas River South, R1-R3	Xhole	7.0	0	6.1	0.15	6.6	5.3	sand & silty sand (SP to SM)	14	A	H	2	8.0	141.2	122.6	0.93	158	151	0.10	0.09
Salinas River South, R2-R3	Xhole	7.0	0	6.1	0.15	6.6	5.3	sand & silty sand (SP to SM)	14	A	H	2	8.0	141.2	122.6	0.93	168	159	0.10	0.09
Sandholdt Road, UC-4 Layer 1	SCPT	7.0	1	1.8	0.25	2.1	0.6	sand	2	?	H	1	2.5	44.3	37.4	0.99	91	116	0.19	0.16
Sandholdt Road, UC-4 Layer 2	SCPT	7.0	0	1.8	0.25	5.9	4.1	sand	4	?	H	4	8.0	148.0	87.2	0.94	209	216	0.26	0.22
Sandholdt Road, UC-6	SCPT	7.0	0	1.7	0.25	3.0	4.3	sand	1	?	H	5	4.7	85.5	56.4	0.97	171	199	0.24	0.20
Santa Cruz, SC02	SCPT	7.0	1	0.6	0.42	1.3	3.2	silty sand	~35?	A	H	11	2.9	53.6	31.2	0.98	122	164	0.45	0.38
Santa Cruz, SC03	SCPT	7.0	1	2.1	0.42	2.1	2.4	sand to silty sand	~12?	A	H	8	3.4	59.8	47.9	0.98	145	175	0.33	0.28
Santa Cruz, SC04	SCPT	7.0	0	1.8	0.42	1.8	2.1	silty sand	~35?	A	H	7	2.9	51.7	41.3	0.98	163	202	0.33	0.28
Santa Cruz, SC05	SCPT	7.0	0	2.8	0.42	3.0	1.8	silty sand to sandy silt	>35?	A	H	6	4.0	70.2	58.9	0.98	149	170	0.32	0.26
Santa Cruz, SC13	SCPT	7.0	0	1.8	0.42	2.0	1.3	silty sand	~35?	A	H	4	2.8	48.9	39.9	0.98	119	149	0.33	0.27
Santa Cruz, SC14	SCPT	7.0	1	1.2	0.42	1.5	1.5	sand	<5?	A	H	5	2.3	41.2	30.7	0.99	126	169	0.36	0.30
State Beach, UC-15	SCPT	7.0	1	1.8	0.25	1.8	2.8	sand	1	?	H	3	3.5	62.0	45.4	0.98	116	142	0.21	0.18
State Beach, UC-16	SCPT	7.0	1	2.3	0.25	2.3	7.1	sand	1	?	H	7	5.5	99.8	68.2	0.96	162	179	0.22	0.18
TI Fire Station, Redpath	Dhole	7.0	0	1.4	0.13	4.5	2.5	silty sand(SM)	24	FH	R	1	6.9	127.1	73.3	0.95	129	142	0.14	0.11
TI Fire Station, Gibbs et al.	Dhole	7.0	0	1.4	0.13	4.5	2.5	silty sand(SM)	24	FH	R	1	5.8	107.0	63.7	0.96	133	150	0.14	0.11
TI Fire Station, 1992	SASW	7.0	0	1.4	0.13	4.5	2.5	silty sand(SM)	24	FH	R	1	5.3	98.4	59.6	0.96	131	149	0.14	0.11
TI Fire Station	SCPT	7.0	0	1.4	0.13	4.5	2.5	silty sand(SM)	24	FH	R	1	5.3	98.4	59.6	0.96	133	152	0.13	0.11
TI Fire Station, B1-B4	Xhole	7.0	0	1.4	0.13	4.5	2.5	silty sand(SM)	24	FH	R	3	5.5	101.3	60.9	0.96	137	155	0.14	0.11
TI Fire Station, B2-B3	Xhole	7.0	0	1.4	0.13	4.5	2.5	silty sand(SM)	24	FH	R	8	5.5	101.3	60.9	0.96	129	146	0.14	0.11
TI Fire Station, B2-B4	Xhole	7.0	0	1.4	0.13	4.5	2.5	silty sand(SM)	24	FH	R	3	5.5	101.3	60.9	0.96	132	149	0.14	0.11
TI Fire Station, B4-B5	Xhole	7.0	0	1.4	0.13	4.5	2.5	silty sand(SM)	24	FH	R	3	5.5	101.3	60.9	0.96	131	148	0.14	0.11
TI Fire Station, Portable	Xhole	7.0	0	1.4	0.13	4.5	2.5	silty sand(SM)	24	FH	R	7	5.8	97.0	63.5	0.96	130	145	0.14	0.11
TI Perimeter, UM03	SCPT	7.0	0	1.5	0.14	6.5	5.2	sand to clayey silty sand	13	FH	R	17	9.1	174.7	99.8	0.92	173	173	0.15	0.12
TI Perimeter, UM05	SCPT	7.0	1	2.4	0.14	3.3	2.3	sand to silty sand	5	FH	R	8	4.6	83.7	62.5	0.97	151	169	0.12	0.10
TI Perimeter, UM06	SCPT	7.0	1	1.4	0.14	2.0	1.7	sand to silty sand	5	FH	R	5	2.9	53.4	38.7	0.98	123	157	0.12	0.10

Test Type
Xhole = crosshole seismic test
Dhole = downhole seismic test
SCPT = Seismic Cone Penetration Test
SASW = Spectral-Analysis-of-Surface-Waves test
Susp. = suspension logger test

Deposit Type
F = fill
FH = fill, hydraulic
FD = fill, dumped
FU = fill, uncompacted
FI = fill, improved
A = Alluvial
AF = Alluvial, fluvial
VDF = volcanic debris flow

Age
R = Recent (< 500 years)
H = Holocene (< 10 000 years)

CSR 7.5 = $CSR/(M_w/7.5)^{-2.56}$
? = unknown

Table C.1 - Summary Information for *Vs* -Based Liquefaction and Non-Liquefaction Case Histories.

						----General Characteristics of Critical Layer----						----Average Value for Critical Layer ----								
Site	Test Type	Mw	Suf. Liq. Eff.? 1 = Y 0 = N	Water Table Depth	amax. avg.	Top of Layer Depth	Thick-ness	Soil Type	Average Fines Content	Deposit Type	Age	No. of Values in Average	Depth	Vert. Stress	Eff. Vert. Stress	rd	Vs	Vs1	CSR	CSR 7.5
				m	g	m	m		%				m	kPa	kPa		m/s	m/s		
TI Perimeter, UM09	SCPT	7.0	1	2.7	0.14	2.7	3.8	sand to silty sand	14	FH	R	12	4.6	83.1	64.8	0.97	143	160	0.11	0.09
TI Approach to Pier, SA-5b	SASW	7.0	0	2.0	0.14	2.0	10.8	sand to sand with silt (SP to SP-SM)	5	FI	R	3	6.6	123.7	78.1	0.94	189	206	0.13	0.11
TI Approach to Pier, SA-6	SASW	7.0	0	2.0	0.14	2.0	10.8	sand to sand with silt (SP to SP-SM)	5	FI	R	5	5.8	104.0	67.1	0.95	187	211	0.13	0.11
TI Approach to Pier, SA-7	SASW	7.0	0	2.0	0.14	2.0	10.8	sand to sand with silt (SP to SP-SM)	5	FI	R	3	6.6	123.7	78.1	0.98	187	203	0.13	0.11
Bay Bridge Toll Plaza, S-R1	Xhole	7.0	1	3.0	0.24	5.0	2.5	sand to silty sand (SP-SM)	~9	FU	R	4	6.4	116.0	82.5	0.95	143	150	0.21	0.17
Bay Bridge Toll Plaza, R1-R2	Xhole	7.0	1	3.0	0.24	5.0	2.5	sand to silty sand (SP-SM)	~9	FU	R	4	6.4	116.0	82.5	0.95	144	151	0.21	0.17
Bay Bridge Toll Plaza, SFOBB-1	SCPT	7.0	1	3.0	0.24	5.0	2.5	sand to silty sand (SP-SM)	~9	FU	R	2	6.5	117.8	83.4	0.95	148	155	0.21	0.18
Bay Bridge Toll Plaza, SFOBB-2	SCPT	7.0	1	3.0	0.24	6.0	3.0	sand to silty sand (SP-SM)	~13	FU	R	4	7.5	98.9	92.4	0.94	148	151	0.22	0.18
1993 KUSHIRO-OKI, JAPAN EARTHQUAKE																				
Kushiro Port, No. 2	Susp.	8.3	1	0.9	0.41	2.7	3.0	sand with silt (SP-SM)	7	A	H	3	4.2	74.8	41.9	0.97	152	189	0.46	0.60
Kushiro Port, No. D	Susp.	8.3	1	1.9	0.41	1.9	6.8	sand	5	FU	R	2	4.5	82.3	56.6	0.97	135	161	0.35	0.46
1993 HOKKAIDO-NANSEI-OKI, JAPAN EARTHQUAKE																				
Pension House, BH-1	Dhole	8.3	1	1.0	0.19	1.0	2.5	sandy gravel	<5	VDF	H	2	2.0	40.4	30.4	0.99	74	99	0.16	0.20
Hakodate Port, No. 1	Susp.	8.3	1	1.2	0.15	2.7	7.0	silty sand to sand with silt (SM to SP-SM)	20	?	?	7	7.0	112.5	55.7	0.94	131	154	0.18	0.23
Hakodate Port, No. 2	Susp.	8.3	0	1.4	0.15	2.1	8.2	sand with silt (SP-SM)	8	?	?	8	6.5	107.7	57.8	0.95	143	166	0.17	0.22
Hakodate Port, No. 3	Susp.	8.3	1	1.4	0.15	1.5	11.5	silty sand (SM)	54	?	?	11	7.0	117.1	62.2	0.93	124	141	0.16	0.21
1994 NORTHRIDGE, CALIFORNIA EARTHQUAKE																				
Rory Lane, M-20	SCPT	6.7	1	3.4	0.51	3.4	4.9	silty sand	~10	A	?	3	5.6	100.6	78.4	0.97	160	170	0.40	0.30
Rory Lane, M-32	SCPT	6.7	1	3.4	0.51	3.4	3.3	silty sand	~10	A	?	2	5.4	97.0	76.7	0.96	152	161	0.40	0.30
Rory Lane, M-33	SCPT	6.7	1	3.4	0.51	3.4	2.1	silty sand	~10	A	?	1	4.4	78.6	67.9	0.97	129	142	0.37	0.28
1995 HYOGOKEN-NANBU, JAPAN EARTHQUAKE																				
Hanshin Expressway 5, 3	Susp.	6.9	1	2.1	0.50	2.1	3.2	gravelly silty sand (SP-SM to SM)	18	FD	R	1	5.6	96.6	62.8	0.96	160	180	0.48	0.39
Hanshin Expressway 5, 10	Susp.	6.9	1	1.8	0.58	3.5	3.5	silty sandy gravel (SM)	16	FD	R	4	5.5	100.8	64.6	0.96	112	126	0.56	0.45
Hanshin Expressway 5, 14	Susp.	6.9	1	4.3	0.63	4.5	4.1	silty sandy gravel	~12	FD	R	4	6.5	115.7	94.2	0.95	175	178	0.48	0.38
Hanshin Expressway 5, 25	Susp.	6.9	1	3.2	0.65	5.3	6.3	gravelly sitly sand to gravelly sand	9	FD	R	5	8.8	151.6	96.7	0.92	172	173	0.60	0.48
Hanshin Expressway 5, 29	Susp.	6.9	1	2.5	0.65	3.0	8.3	silty sand to sandy gravel with silt	12	?	?	3	7.2	123.1	77.8	0.94	167	179	0.60	0.48
KNK	Dhole	6.9	0	2.0	0.12	2.0	15.0	silt, sand, gravel	~10	?	H	2	6.6	128.5	83.4	0.94	139	147	0.10	0.08
Kobe-Nishinomiya EWY, 3	Susp.	6.9	0	3.7	0.63	4.4	6.1	gravelly sand-sandy gravel with silt	7	?	?	6	7.0	126.1	93.8	0.95	175	178	0.51	0.41
Kobe-Nishinomiya EWY, 17	Susp.	6.9	0	2.0	0.53	2.0	2.5	gravelly sand with silt	8	?	?	1	3.3	60.9	49.0	0.98	200	239	0.42	0.34
Kobe-Nishinomiya EWY, 23	Susp.	6.9	0	2.9	0.63	2.9	3.1	gravelly sand-sandy gravel with silt	11	?	?	1	4.0	71.5	60.8	0.98	130	147	0.47	0.38

Test Type
Xhole = crosshole seismic test
Dhole = downhole seismic test
SCPT = Seismic Cone Penetration Test
SASW = Spectral-Analysis-of-Surface-Waves test
Susp. = suspension logger test

Deposit Type
F = fill
FH = fill, hydraulic
FD = fill, dumped
FU = fill, uncompacted
FI = fill, improved
A = Alluvial
AF = Alluvial, fluvial
VDF = volcanic debris flow

Age
R = Recent (< 500 years)
H = Holocene (< 10 000 years)

$CSR\ 7.5 = CSR/(M_w/7.5)^{-2.56}$
? = unknown

Table C.1 - Summary Information for *Vs* -Based Liquefaction and Non-Liquefaction Case Histories.

						----General Characteristics of Critical Layer----						----Average Value for Critical Layer ----								
						Top						No. of								
			Suf.	Water		of			Average			Values			Eff.					
	Test		Liq.	Table	amax.	Layer	Thick-	Soil	Fines	Deposit		in		Vert.	Vert.					CSR
Site	Type	Mw	Eff.?	Depth	avg.	Depth	ness	Type	Content	Type	Age	Average	Depth	Stress	Stress	rd	Vs	Vs1	CSR	7.5
			1 = Y																	
			0 = N	m	g	m	m		%				m	kPa	kPa		m/s	m/s		
Kobe-Nishinomiya EWY, 28	Susp.	6.9	0	2.2	0.65	3.0	3.0	sand with gravel	2	?	?	1	6.0	110.7	74.0	0.96	160	173	0.60	0.48
Kobe Port, 7C	Dhole	6.9	1	4.4	0.55	7.5	15.0	sand to silty sand	10	FD	R	1	15.0	299.3	195.4	0.88	160	135	0.48	0.39
LPG Tank Yard, Kobe	Dhole	6.9	1	1.5	0.50	2.0	6.0	gravelly sand with silt	10	FD	R	1	4.0	79.3	54.6	0.98	110	129	0.46	0.37
Port Island, 1C	Dhole	6.9	1	3.0	0.50	4.0	12.2	gravelly sand to silty gravelly sand	13	FD	R	1	8.6	171.4	116.3	0.88	170	164	0.42	0.34
Port Island, 2C	Dhole	6.9	1	1.5	0.50	5.0	10.5	sand with silt	10	FD	R	1	11.5	232.3	134.4	0.87	200	186	0.49	0.40
Port Island, Common Factory	Dhole	6.9	0	3.2	0.50	3.2	11.8	gravelly sand with silt (SP-SM)	6	A	R	12	9.0	183.3	126.4	0.90	214	202	0.41	0.33
Port Island, Common Factory	Susp.	6.9	0	3.2	0.50	3.2	11.8	gravelly sand with silt (SP-SM)	6	A	R	22	9.2	188.6	129.3	0.90	193	183	0.41	0.33
Port Island, Dhole Array '91	Dhole	6.9	1	2.4	0.50	2.4	14.6	sandy gravel with silt	10	FD	R	2	7.2	140.5	93.0	0.92	190	201	0.40	0.32
Port Island, Dhole Array '95	Dhole	6.9	1	2.4	0.50	2.4	14.6	sandy gravel with silt	10	FD	R	2	7.8	152.8	99.4	0.93	165	165	0.45	0.36
SGK	Dhole	6.9	0	7.0	0.45	7.0	5.0	silt, sand, gravel	~10	F?	R?	1	8.5	151.6	136.9	0.93	190	176	0.30	0.24

Test Type
Xhole = crosshole seismic test
Dhole = downhole seismic test
SCPT = Seismic Cone Penetration Test
SASW = Spectral-Analysis-of-Surface-Waves test
Susp. = suspension logger test

Deposit Type
F = fill
FH = fill, hydraulic
FD = fill, dumped
FU = fill, uncompacted
FI = fill, improved
A = Alluvial
AF = Alluvial, fluvial
VDF = volcanic debris flow

Age
R = Recent (< 500 years)
H = Holocene (< 10 000 years)

CSR 7.5 = $CSR/(M_w/7.5)^{-2.56}$
? = unknown